Bernhard Putsche, BSc

Influence of potassium on the nucleation and growth of para-hexaphenyl on mica

Master Thesis

For obtaining the academic degree

Diplom-Ingenieur

Master Programme of
Technical Physics

Graz University of Technology

Supervisor:

Ao.Univ.-Prof.Dipl.Ing. Dr.techn. Adolf Winkler
Institute of Solid State Physics

Graz, June 2012

Bernhard Putsche BSc

Der Einfluss von Kalium auf die Nukleation und das Wachstum von para-Hexaphenyl auf Glimmer

Masterarbeit

zur Erlangung des akademischen Grades

Diplom-Ingenieur

der Studienrichtung Technische Physik

Technische Universität Graz

Betreuer:

Ao.Univ.-Prof.Dipl.Ing. Dr.techn. Adolf Winkler

Institut für Festkörperphysik

Graz, Juni 2012

Acknowledgement

First and foremost I offer my sincerest gratitude to my supervisor, Adolf Winkler, who has supported me throughout my thesis with his patience and knowledge whilst allowing me the room to work in my own way. I also want to thank my colleagues from the surface science group, W. Lukesch, L. Tümbek and C. Gleichweit, as well as all the members of the Institute of Solid State Physics of the Graz University of Technology. I am grateful to work in such a pleasant group. Additionally I have to acknowledge the Austrian Science Fund (FWF) for financial support.
Finally I want to say that I am deeply grateful to my parents, Julius and Regina, and my sister Ilona for their love, all the emotional support and for being there for me my whole life.

Abstract

Conjugated organic molecules, such as para-hexaphenyl (6P), are attractive candidates as active layer material for organic electronic devices. In order to fabricate such devices with high quality, the thin film layer growth of organic materials on a substrate has to be well understood. A model system to investigate the growth parameters is the growth of 6P on mica (001). 6P adsorbed on freshly cleaved mica forms needle-like islands of flat lying molecules on top of a wetting layer. Previous investigations have shown that surface modifications like sputtering lead to the formation of islands of standing molecules and dewetting. When mica is cleaved, the sample always splits along its potassium layer and a half monolayer of potassium remains on each face.
This master thesis describes the effects of an increased amount of potassium on thin film layer growth of 6P. Performing the measurements in ultra high vacuum ensured precisely controlled conditions for the experiments. 6P was evaporated by using a Knudsen cell and the amount of evaporated material was determined by a quartz microbalance. In order to increase the amount of potassium on the freshly cleaved mica a SAES Getter was used to evaporate potassium on the surface. Thermal desorption spectroscopy (TDS, in-situ) and atomic force microscopy (AFM, ex-situ) were the main analytical methods to describe the effects of the potassium on the growth of the 6P molecules. Auger electron spectroscopy (AES) was applied for chemical analysis of the mica sample before and after the potassium deposition.
It could be shown that adsorption of potassium on the freshly cleaved mica leads to changes of the layer growth of 6P on mica. Dewetting and the formation of islands of standing molecules were obtained by TDS and AFM measurements. Furthermore AES and TDS measurements revealed that a proper potassium coverage, after the first adsorption, leads to a stable potassium layer, which cannot be removed by heating the sample.

Kurzfassung

Konjugierte organische Moleküle wie zum Beispiel para-Hexaphenyl (6P), sind aufgrund ihrer halbleitenden Eigenschaften interessante Materialien für organische elektronische Bauteile. Um solche Bauteile in hoher Qualtität herstellen zu können, muss das Schichtwachstum von organischen Materialien im Detail verstanden werden. Als Modellsystem dienen hierbei para-Hexaphenyl auf Muskovit Glimmer. 6P formt auf einer frisch gespalteten Glimmer Oberfläche in erster Lage einen sogenannten wetting-layer, bestehend aus liegenden 6P Molekülen. Auf diesem wetting-layer bilden sich nadelförmige Inseln aus liegenden 6P Molekülen in der Multilage aus. Vorangegangene Untersuchungen haben gezeigt, dass Veränderungen an der Oberfläche, wie beispielsweise durch sputtern, zu einer Änderung im Schichtwachstum von 6P führen. Anstatt nadelförmige Inseln auf einer Monolage liegender 6P Moleküle zu bilden, entstehen Inseln aus aufrechtstehenden 6P Molekülen direkt auf der Glimmer Oberfläche.

Im Rahmen dieser Masterarbeit haben wir uns nun mit dem Einfluss von adsorbierten Kalium Schichten auf das Schichtwachstum von 6P beschäftigt. Alle Messungen wurden im Ultrahochvakuum durchgeführt um Wechselwirkungen mit dem Restgas zu minimieren. 6P wurde mittels einer Knudsen Zelle aufgedampft, wobei die aufgedampfte Menge mit einem Schwingquarz überwacht wurde. Zum Aufdampfen von Kalium auf die Glimmer Oberfläche wurde ein sogenannter SAES-Getter als Kalium Quelle verwendet. Mit Hilfe der Thermodesorptions-Spektroskopie (TDS, in-situ) und der Rasterkraftmikroskopie (AFM, ex-situ) kann das Schichtwachstum der 6P Moleküle auf der Glimmer Oberfläche untersucht werden. Zusätzlich kann mit Hilfe der Auger Elektronen Spektroskopie (AES) die chemische Zusammensetzung der Probenoberfläche vor und nach dem Kalium Bedampfen gemessen werden.

Es hat sich gezeigt, dass die Adsorption von Kalium tatsächlich zu einer Änderung des Schichtwachstums von 6P führt. Mit Hilfe von TDS und AFM war es möglich dewetting und die Adsorption von 6P in Form von Inseln, bestehend aus aufrechtstehenden Molekülen, nachzuweisen. Des Weiteren haben TDS und AES Messungen gezeigt, dass sich bei angemessener Kalium Bedeckung, nach der ersten Adsorption, eine stabile Kalium Schicht bildet, die beim Aufheizen der Probe nicht verdampft.

Contents

Introduction

Thin organic films have attracted enormous interest over the last years, because they are attractive candidates as active layer material for organic electronic devices [1]. Muscovite mica is a frequently used material for the epitaxial growth. Due to the layered structure, one can easily obtain smooth surfaces just by cleaving. Together with the oligomer para-hexaphenyl (6P), mica can be used as a model system to study thin film layer growth.

6P deposited on freshly cleaved mica forms needle-like islands that are composed of lying 6P molecules, on top of a wetting layer of lying 6P molecules. It is assumed that this particular behaviour is caused by lateral electric fields existing on the surface of freshly cleaved mica. Mica is a sheet like aluminosilicate, $KAl_2(Si_3, Al)O_{10}(OH)_2$, consisting of octahedral Al-O layers sandwiched between two tetrahedral Si-O layers [2]. One out of four Si^{4+} cations is replaced with an Al^{3+} ion. The resulting negative charge, due to the substitution, is compensated by a layer of K^+ cations in-between the tetrahedral layers. The weakest bonds in the crystal are those between potassium and oxygen so that cleavage takes place along a potassium layer [3] and half a layer of potassium remains on each face [2]. Between the K^+ ions and the negatively charged Al^{3+} substitutional sites dipoles are generated, that lead to dipole fields parallel to the surface [3, 4].

Previous investigations have shown that surface modifications, like carbon deposition or argon sputtering, lead to dewetting and the formation of islands of standing 6P molecules [5]. It was argued, that a surface modification destroys the dipoles and thus weakens the forces between the 6P molecules and the surface. The contribution here describes the effects of increased amounts of potassium on the thin film layer growth of

6P. It will be demonstrated that the evaporation of potassium under UHV conditions creates a potassium covered mica sample with a potassium layer that is stable up to 1000 K. On such a surface 6P indeed forms islands of standing molecules instead of needle-like islands composed of lying molecules.

Chapter 1

Theoretical Background

In this chapter the Theoretical Background is explained. In order to understand the main in-situ examination methods (thermal desorption spectroscopy TDS, Auger electron spectroscopy AES) the following physical principles are illustrated: Adsorption and desorption kinetics and Auger Electrons. The atomic force microscopy (AFM) is an ex-situ examination method to study the morphology of the surface. In the Experiments materials like mica, para-hexaphenyl and potassium are used. Thus the physical properties of these materials will be explained as well.

1.1 Adsorption

In a large number of investigations it is of great interest to add foreign species on a clean substrate. There exist different techniques to prepare surfaces with certain amounts of foreign species. In this thesis the adsorbates will be provided by physical vapor deposition. Depending on the strength of the interaction between the substrate and the adsorbate, the adsorption can be subdivided in two classes [6]:

- physisorption (weak interaction)
- chemisorption (strong interaction)

The terms are not well defined since the distinction was made according to the adsorption energy, with physisorption denoting the realm of lower adsorption energies

[7]. The conventionally accepted value to distinguish between chemisorption and physisorption is about 0.5 $eV/molecule$ (or $atom$) [6].

Physisorption: There is no direct chemical bond between substrate and particle, but the adsorbate is held by physical forces, like Van der Waals (VdW) forces, near the surface [8]. Due to the weak interaction, the physisorbed particles do not disturb the structural environment of the substrate. A typical example for physisorption is the adsorption of inert gases (like argon) on the substrate at low temperatures [6]. The VdW-forces originate in the ground state fluctuations of electronic charges of an atom, generating a dynamic dipole moment. The electric field, emerging from these fluctuations, induces a dipole moment in another atom and thus the particles attract each other, even in absence of chemical bonding. At small distances, the VdW-forces are balanced by the Pauli-repulsion. The potential that describes all this is the Lennard Jones potential [7].

Chemisorption: Indicates a strong chemical bonding between the adsorbate and the surface. These bonds can be either ionic or covalent. Through the strong interaction, between the adsorbate and the surface, changes of the chemical state of the adatom can occur. If the adsorbate is a molecule, the whole molecule or the single atoms (dissociative adsorption) can chemisorbs to the surface. The interaction between the adatoms and the substrate can also cause changes in the structure of the surface. These changes can range from relaxation of the interlayer spacing in the top layers to reconstruction of the atomic structure in the top layer. A typical example of chemisorption is the adsorption of reactive gases or metals atoms on metal or semiconductors [6].

Dissociative Adsorption: Both, the physisorption and chemisorption describe the bonding of the whole molecule to the surface, but there are molecules like H_2 and O_2 which dissociate and therefore bond as individual atoms (see [7], [9], [10]). A way to describe this effect can be seen in figure 1.1.

Consider a molecule AB approaching from $r = \infty$ to the surface. Figure 1.1 shows the potential energy curves for such a molecule, whereat curve (a) is the potential of the splintered molecule ($A+B$) chemisorbing to the surface as atom A and B and curve (b)

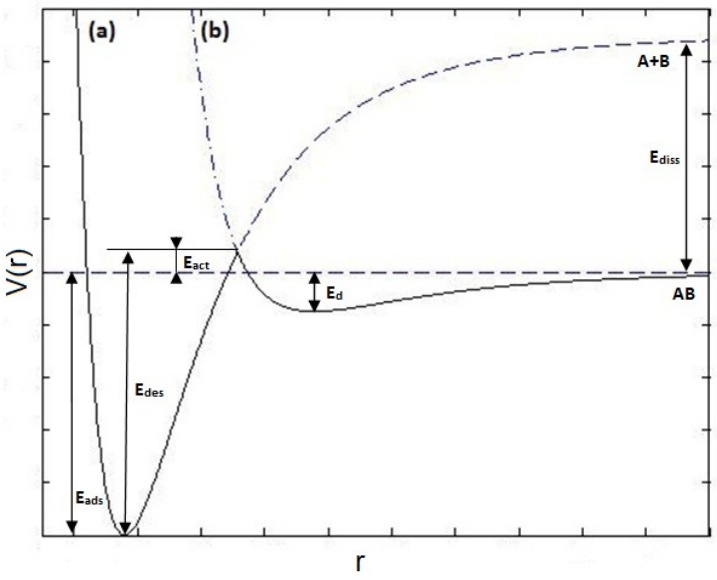

Figure 1.1: Schematic of the potential energy curves for a dissociative adsorption. (a) potential for the chemisorption of the atoms A+B. (b) potential for the physisorption of the molecule AB.

is the potential of the molecule (AB) physisorbed to the surface. The solid line, which is a combination of curve (a) and (b), is the effective potential V(r) of the molecule. At a point far away from the surface the splintered molecule (A+B) has a higher energy than the molecule (AB) (which is taken zero). The energy difference between these levels is the dissociation energy E_{diss}. The molecule approaches the surface along the physisorption curve (b). If the molecule has a sufficient energy it can directly go into the chemisorptive state. If, however, the energy is not sufficient the molecule goes into a transient physisorptive state, with the desorption energy E_d. From this transient state the molecule can either desorb into the gas phase, or change into the chemisorptive state and therefore dissociate. To do the latter, the molecule has to overcome the activation energy E_{act} at the cross section of curve (a) and (b). If the molecule goes from the physisorptive state into the chemisorptive state, the physisorption is called a precursor of the chemisorption.

This crossing point specifically defines the type of dissociative adsorption. If the cross section is above the zero line ($E_{act} > 0$) it is an activated dissociative adsorption. In this case the activation energy must be put into the system to go from the physisorptive state into the chemisorptive state. The necessary energy can be calculated by the following equation:

$$E_{act} = E_{des} - E_{ads} \tag{1.1}$$

with E_{des} the desorption energy of the dissociative adsorption and E_{ads} the adsorption energy of the chemisorption. When the cross section is underneath the zero energy line, the molecule has enough energy to overcome the crossing point and therefore no additional energy must be applied to the system to go into the chemisorptive state. This is called the non activated dissociative adsorption.

If atoms or molecules are adsorbed on the surface it is essential to describe the concentration of the adsorbate on the surface. The *coverage* Θ characterizes this concentration in orders of monolayer units [6]. One monolayer corresponds to one adsorbed atom or molecule per unit cell of the ideal non reconstructed substrate surface. Thus a monolayer is a relative value associated with a given surface.

1.1.1 Adsorption kinetics

In the previous section only the results of an adsorption process were discussed, but not the process itself. The latter should be discussed as a kinetic process, in which the adsorbate approaches to the surface. The phenomenon of adsorption is a result of this approach. The adsorption of atoms or molecules depends on external parameters, such as vapor pressure, temperature of substrate/vapor, the surface structure, etc. [6].

To describe the kinetic process, we consider a uniform solid surface exposed to an adsorbing gas. The number of particles (atoms or molecules) hitting the surface is given by the *impingement rate* I:

$$I = \frac{p}{\sqrt{2\pi m k_B T}} \tag{1.2}$$

with p the partial pressure of the adsorbing gas, m the mass of the particles, k_B the

Boltzmann constant and T the temperature.

Note that not all particles, hitting the surface, are adsorbed as well. The number of particles, sticking to the surface, depends on the *sticking coefficient* $S(\Theta)$. This value is defined by the ratio of the number of particles adsorbing (N_{ads}) and the number of particles impinging the surface (N_{imp}):

$$S(\Theta) = \frac{N_{ads}}{N_{imp}} \tag{1.3}$$

Thus, the adsorption rate r_{ads} is defined by the number of particles hitting the surface times the probability to actually stick on it:

$$r_{ads} = S(\Theta) \cdot I \tag{1.4}$$

The simplest model to describe the adsorption process is the Langmuir adsorption.

Langmuir Adsorption Model

It is assumed that every surface has a specific number of adsorption sites. These sites are all equivalent and each site can only be occupied by one particle. The adsorption is limited to one monolayer, which is achieved when all sites are occupied. Thus an incident particle only adsorbs on an empty adsorption site and scatters if the site is occupied. Therefore the sticking coefficient can be written as [6] [10]:

$$S(\Theta) = S_0 \cdot (1 - \Theta)^n \tag{1.5}$$

with S_0 the sticking probability at zero coverage, Θ the coverage and n the order of kinetics, a value to distinguish between the non dissociative Langmuir adsorption ($n = 1$) and the dissociative Langmuir adsorption ($n = 2$). If a molecule dissociates into n species, the exponent has the value n. That means if the molecule A_4 dissociates into 4 atoms the factor n is equal 4.

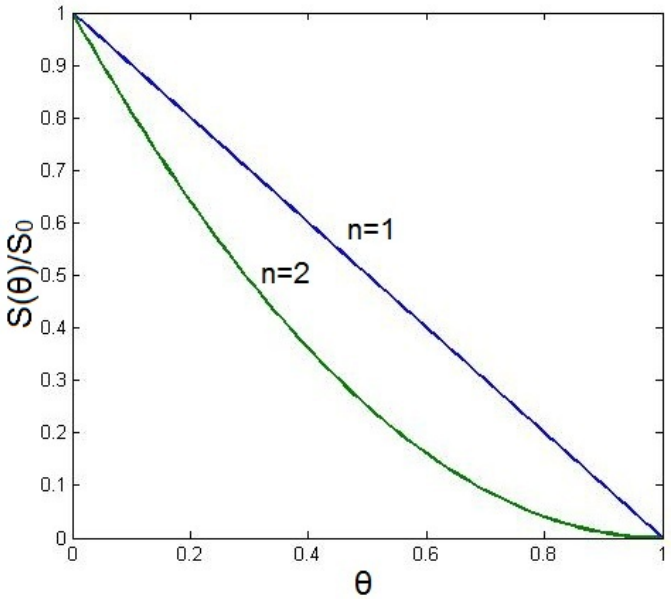

Figure 1.2: Sticking coefficient for non dissociative ($n = 1$) and dissociative ($n = 2$) Langmuir adsorption

The sticking coefficient as a function of the coverage depends on the kind of Langmuir adsorption. If the Langmuir adsorption is dissociative, a diatomic molecule (for example) will dissociate during the adsorption and occupy two instead of one adsorption sites. If, however, the adsorption is non dissociative, the molecule will only occupy one adsorption site. The effects on the sticking coefficient can be seen in figure 1.2, where the relative sticking coefficient $S(\Theta)/S_0$ changes with respect to the coverage Θ. The non dissociative case shows a linear decrease of the relative sticking coefficient, whereas the dissociative case shows fast drop of S/S_0 at the beginning of the adsorption. In the end, due to the definition of the Langmuir Adsorption, the sticking coefficients of both cases reach zero when a monolayer is formed.

Equation 1.5 is a good approximation for direct adsorption, but does not describe the precursor mediated adsorption. In this particular case it is possible that molecules do not chemisorb directly, but go into a transient state, the precursor state. This is possible for both, the dissociative and the non dissociative adsorption. When a molecule is in the precursor state, it is kept near the surface by the VdW-forces and can diffuse

around the surface to find a free site. Through the precursor state the molecules have a longer residence time near the surface and adsorb more likely.

To describe the behaviour of a precursor mediated adsorption it is necessary to define a few new variables. The initial sticking coefficient S_0 is substituted by S_p, which is the probability for trapping molecules from the gas phase into the precursor state. Since it is possible for molecules to ad- or desorb from the precursor state, the constants k_a and k_d are considered. k_a is the rate constant for adsorption from the precursor state into the final chemisorbed state and k_d is the rate for desorption from the precursor state into the gas phase. Thus the overall sticking coefficient can be written as [6]:

$$S(\Theta) = S_p \cdot \frac{(1+K)(1-\Theta)^n}{1+K(1-\Theta)^n} \tag{1.6}$$

with $K = k_a/k_d$ and n the order of the kinetics. Figure 1.3 shows a plot of equation 1.6 for the case of a dissociative adsorption ($n = 2$), with $K = 0,\ 10,\ 100,\ 1000$ and $S_p = 1$.

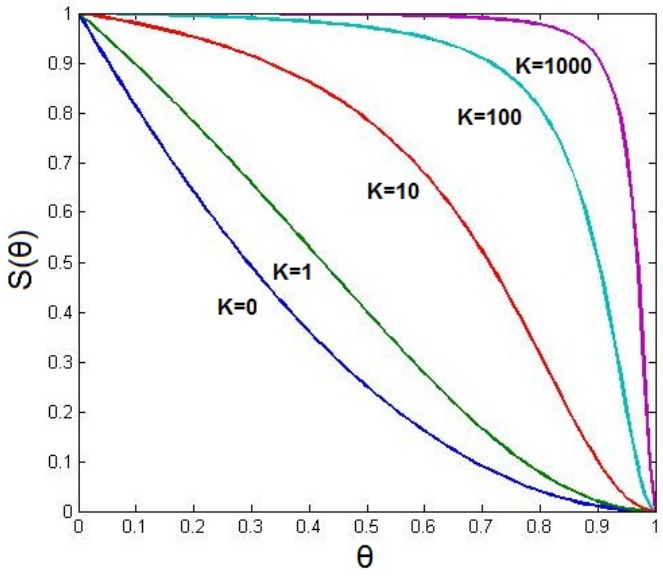

Figure 1.3: Sticking coefficient for precursor mediated dissociative Langmuir adsorption.

Figure 1.3 demonstrates that for low desorption rates from the precursor state ($K \rightarrow \infty$) $S(\Theta)$ approaches the value S_p (the highest probability for adsorption), whereas for a high desorption rate from the precursor state ($K \rightarrow 0$) the sticking coefficient approaches the Langmuir type kinetics (equation 1.5) [6].

1.2 Desorption

An adsorbate remains on a surface till it gains a sufficient amount of energy to desorb. Depending on the energy source, there are different types of desorption. If a particle (atom or molecule) gains enough energy from thermal vibrations, the desorption is called thermal desorption [6]. The kinetic process of thermal desorption can be described in terms of the desorption rate r_{des}, which is the number of particles desorbing from unit surface area per unit time. Considering that all adsorbed molecules or atoms occupy identical sites and do not interact with each other, the desorption rate can be expressed by the Polanyi-Wigner equation [11]:

$$r_{des} = -\frac{d\Theta}{dt} = \nu_n \cdot \Theta^n \cdot exp\left(-\frac{E_{des}}{k_B T}\right) \tag{1.7}$$

with E_{des} the activation energy for the desorption, T the surface temperature, Θ the coverage, n the order of kinetics and ν_n the pre-exponential factor.

The order of kinetics n describes the coverage dependence of the desorption rate. A zero order desorption ($n = 0$) takes place in the presence of a multilayer. In this case the maximum number of particles per surface unit is always available and therefore the desorption is coverage independent (Θ^0). If the last monolayer desorbs from the surface the desorption rate depends on the number of particles on the surface and thus is proportional to Θ^1. This is the so called first order of desorption ($n = 1$) [11]. The second order of desorption ($n = 2$) can be observed, if two species A and B have to recombine, before a molecule AB can desorb from the surface [12]. If, however, the adsorbate has formed circular islands, fractional orders of desorption (see [12], [13], [14]) are possible. The weakest bondings of such islands are at their edges, where adsorbate most likely desorbs. With the assumption that all islands have the same diameter, the circumference will be proportional to $\Theta^{1/2}$, leading to a fractional order of desorption,

with $n = 1/2$. [13].

The desorption energy is constant in the case of a multilayer desorption, whereas for a monolayer desorption the desorption energy may be coverage dependent [11]. The amount of energy, that is necessary for desorption, depends on the kind of adsorption (physisorption, chemisorption). In the case of chemisorption the particles can be activated or non activated adsorbed. This has consequences for the desorption energy [6]:

- In the case of a *non activated chemisorption* the desorption energy is simply the binding energy of the chemisorptive state, $E_{des} = E_{ads}$.
- In the case of an *activated chemisorption* the desorption energy is the binding energy for the chemisorption plus the activation energy for adsorption, $E_{des} = E_{ads} + E_{act}$.

The pre-exponential factor ν can be interpreted as the attempt frequency of the adsorbed particle to desorb. For small molecules and atoms a pre-exponential factor of $10^{13}\ Hz$ is a typical value [15]. For large molecules, however, this perception is not appropriate. The pre-exponential factor is in this case typically by many orders of magnitude larger than for atoms [11].

1.3 Thermal desorption spectroscopy (TDS)

The thermal desorption spectroscopy is one of the most frequently used techniques to gather information about the energetics and kinetics of adsorbed particles (see [6], [7], [16], [17]). To obtain the spectrum of desorbing particles, a sample with one or more different species of adsorbates is prepared. The sample is kept at a low temperature in order to maintain this situation. When the sample holder is placed in front of the mass spectrometer, the sample will be heated up. The heating process is controlled with a heating program, which guarantees constant heating rates. The desorbing particles are detected by the quadrupole mass spectrometer (QMS), which records the number of particles as a function of temperature (see figure 1.4). The recorded TD-spectrum contains some valuable information:

- The area underneath the desorption peak is proportional to the amount of particles desorbed from the surface.
- The shape of the TD-spectrum and the shift of the peak maximum with changing coverage gives information about the order of kinetics.

1.3.1 TDS analysis

The Polanyi-Wigner equation (1.7) describes desorption of the particles during the heating process. The temperature increases linear and can be described with the following heating ramp:

$$T(t) = T_0 + \beta t \tag{1.8}$$

where T is the temperature at a specific time t, T_0 is the starting temperature and β is the heating rate. Through the combination of equation 1.7 and 1.8, the desorption rate r_{des} can be written as a function of the temperature [6]:

$$r_{des} = -\frac{d\Theta}{dT} = \frac{\nu_n \cdot \Theta^n}{\beta} \cdot exp\left(-\frac{E_{des}}{k_B T}\right) \tag{1.9}$$

A TD-spectrum recored with the QMS can be described with this equation. Thus the desorption energy and the pre-exponential factor can be obtained from the Polanyi-Wigner equation and the data according to the TD-spectrum. Previously one has to determine the order of kinetics from the shape of the TD-spectrum. In figure 1.4 the shapes of the zero-, first- and second order of desorption are depicted. One can clearly see different shapes for different orders of kinetics [6, 11]:

- In the case of zero order of desorption (a) the desorption peaks of different coverages increase along the same leading edge. When the coverage goes to zero the desorption peak has a sharp cutoff at the trailing edge. The peak maxima shift to higher temperatures with increasing coverage. However, this peak shape is never observed for real situations, where always a less sharp trailing edge is detected, because the desorption of the last monolayer corresponds to a first order of desorption.
- For the first order kinetics (b), the peak has an asymmetric shape and the temperature for the peak maximum T_m is coverage independent.

- For the second order kinetics (c), the shape of the peak is nearly symmetric and the temperature of the peak maximum T_m decreases with increasing coverage Θ_0.

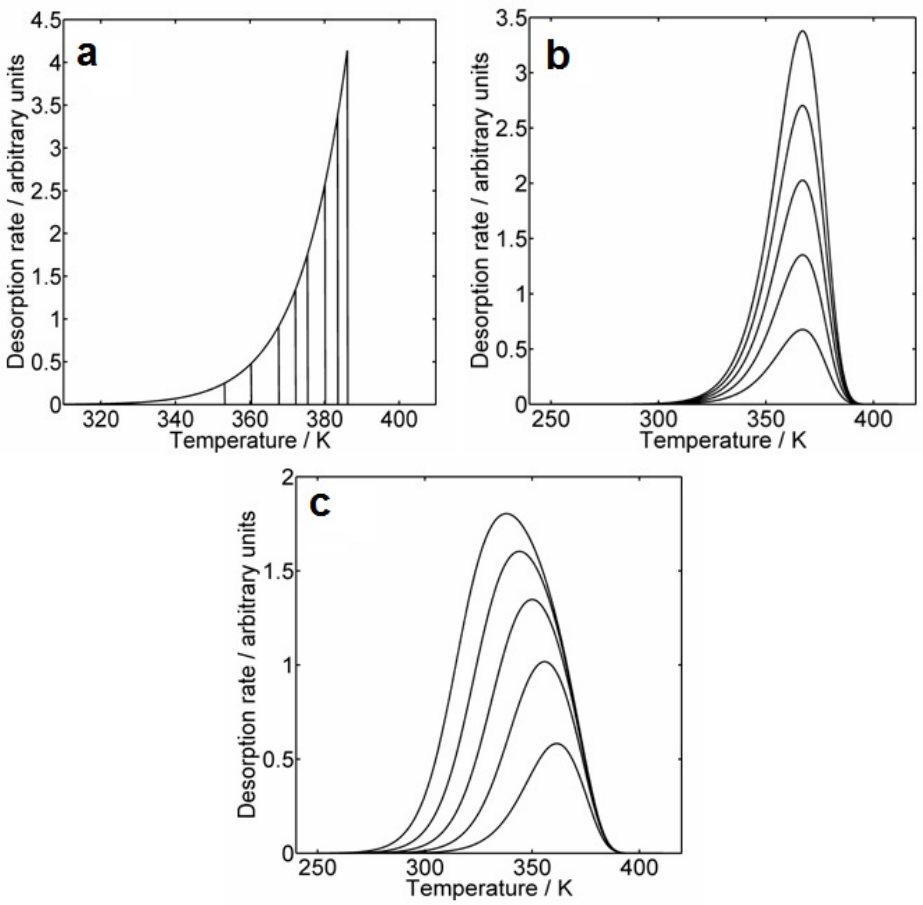

Figure 1.4: Thermal desorption spectra for zero order (a), first order (b) and second order (c) desorption kinetics for various initial coverages Θ_0. The pre-exponential factor and the desorption energy are assumed to be independent from the coverage Θ.

According to the shape, and therefore the order of desorption, there are different methods to calculate the desorption energy of the desorbed particles. Here only the calculation for zero and first order kinetics are explained:

In the case of the zero order desorption the TD-spectrum contains all the information. The Polanyi-Wigner equation only consists of the constant ν and the exponential

part. The desorption energy can be calculated by taking the logarithm of equation 1.9 for $n = 0$:

$$ln\left(r_{des}\right) = ln\left(\frac{\nu_0}{\beta}\right) - \frac{E_{des}}{k_B T} \tag{1.10}$$

This linear equation is used for the so-called Arrhenius plot. The equation is linear with respect to $(1/T)$. Plotting the left-hand side of this expression $[ln(r_{des})]$ versus $(1/T)$ yields a line with the slope (E_{des}/k_B) and the intercept $ln(\nu/\beta)$. Thus, the desorption energy and the pre-exponential factor can be evaluated with a linear fit of the logarithmic TD spectrum.

The characteristic feature of the first order desorption is the coverage independent temperature of the peak maximum T_m. According to Redhead [18] the desorption energy E_{des} can be calculated with the following equation:

$$E_{des} = k_B \cdot T_m \cdot \left[ln\left(\frac{\nu_1 T_m}{\beta}\right) - 3.64\right] \tag{1.11}$$

Equation 1.11 can be derived from equation 1.9 by assuming that for $n = 1$ the activation parameters E_{des} and ν_1 are independent from the coverage. At the temperature $T = T_m$ the peak has its maximum and therefore $\frac{dr_{des}}{dT} = 0|_{T_m}$ leads to equation 1.11.

1.4 Auger Electron Spectroscopy (AES)

AES is a commonly used technique to analyse surface compositions of different materials. It is possible to measure the chemical composition of the first few monolayers of a given surface with a sensitivity of the order of 0.1 atomic % and a spatial resolution of the order of 10 nm [19]. The surface composition of a sample can be determined from the energy of the Auger electrons in the spectrum of the secondary electrons emitted from the sample. To create a secondary electron spectrum, the sample is bombarded with an electron beam (generated by an electron gun) and the scattered electrons are detected with the analyser. The typical energies of Auger electrons are in the range of 5 to 2000 eV [6].

The surface sensitivity of this technique arises from the range of the Auger electrons ejected. When an electron passes through a solid it has inelastic collisions. The number of collisions that occur and hence the range of the electron in the solid is given by the inelastic mean free path (IMPF). The length of the IMPF depends strongly on the energy of the electron. Thus, for the typical energies of an AES, the IMPF for the Auger electrons are in the range of 5 to 20 $\AA$. Therefore Auger electrons originate from the first 3 to 10 atomic layers [19].

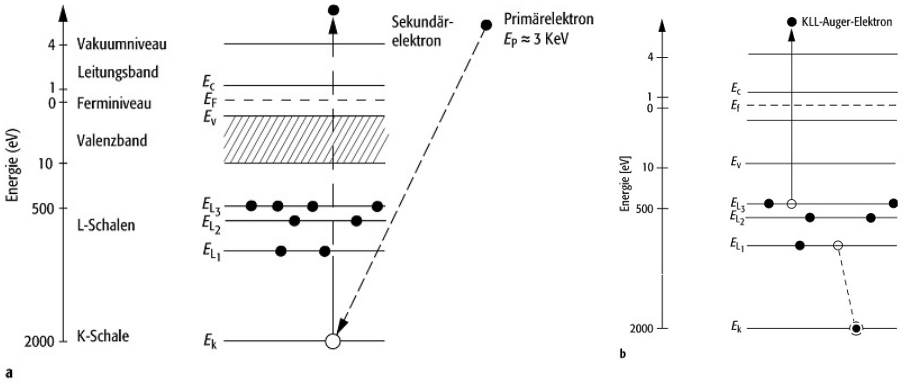

Figure 1.5: The schematics of the Auger process. (a) Illustrates the impingement of a primary electron and the creation of the core hole; (b) shows the actual Auger process and the ejection of an Auger electron.

AES uses the physical principle of the Auger process, which is illustrated in figure 1.5. The surface of the sample is irradiated with a beam of electrons to ionize a core level in the surface atoms (here in the K-shell). The excited atom can relax by either emitting an X-ray photon or an Auger electron [20]. In the case of the Auger process, the core level hole is filled up by an electron of an upper level (in the schematics it's the L_1-shell). Afterwards the ionized atom is in a highly excited state and will rapidly relax by emitting an Auger electron.

Since the Auger process is a three electron process, all elements except hydrogen and helium can be detected. For lighter elements the emission of an Auger electron is preferred, whereas for the heavier atoms the x-ray fluorescence is the favoured relax-

ation [20].

Energy of the Auger electrons: The kinetic energy $E_{KL_1L_{2,3}}$ of the emitted Auger electron (fig.1.5) can be calculated by the following equation [6]:

$$E_{KL_1L_{2,3}} = E_K - E_{L_1} - E_{L_{2,3}} - \phi \tag{1.12}$$

Where $E_K - E_{L_1}$ is the energy available, due to the excitation of the atom. $E_{L_{2,3}}$ is the binding energy of the $L_{2,3}$ electron and thus the energy necessary to lift this electron up to the Fermi level. ϕ is the work function of the material and the amount of energy that is needed to lift the electron from the Fermi into the vacuum level.

In the secondary electron spectrum the number of electrons, detected by the analyser, is recorded as a function of energy. Typically the Auger peaks in the secondary electron spectrum are relatively small compared to the background of true secondary electrons. Thus, for an Auger spectrum the signal is usually recorded in the derivative mode $dN(E)/dE$ to suppress the huge background.
Auger spectra for all elements can be found in a so-called Auger atlas [21]. Further information can be found in the corresponding literature [19, 20].

1.5 Atomic force microscopy

The atomic force microscope (AFM) is part of the family of scanning force microscopes [20]. Unlike scanning tunnel microscopy (STM), AFM is not restricted to conducting surfaces [22]. Thus, it is possible to gather three dimensional images of insulating sample surfaces. However, rough samples cannot be investigated [15].

An AFM consists of a small cantilever, with a sharp tip, attached normal to the cantilever. If the distance between the tip and the investigated surface is small, atomic-range forces can act between them [15]. The cantilever is attached to the motion system of the AFM, which consists of piezo crystals. With these crystals it is possible to move the tip on a picometer scale in x,y,z- direction across the surface [20]. The contraction and expansion of the crystal, due to the piezo electric effect, is used to move the tip.

When the cantilever is moved along the surface, while the tip is in interaction with the surface, the cantilever bends over and follows the surface-morphology, like it is shown in figure 1.6. The deflection of the cantilever is in the nanometre scale and is detected with a laser system. The system uses a laser, that is focused on the front end on the cantilever. Thus, the laser beam is reflected from the front end into a position sensitive detector (PSD). If a force is acting on the tip, the cantilever bends over. This leads to a change of the position of the laser reflection on the PSD.

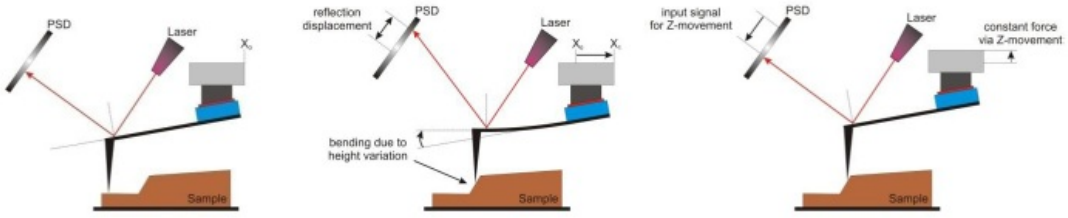

Figure 1.6: The schematics of the atomic force microscope. The distortion of the cantilever is detected with the PSD and can be addressed to the forces between tip and surface.

In our case, the obtained data is processed by the *Nanosurf easyScan 2 AFM system*, which compiles the data into a three dimensional picture of the sample surface. An explanation of the used AFM is given in the PhD thesis by Frank [22]; detailed information can be found in the manuals of the manufacturer [23, 24].

1.6 Mica

The substrate material used in the experiments is muscovite mica. This crystal has a monoclinic structure with the lattice constants $a = 5.1998$ Å, $b = 9.0266$ Å, $c = 20.1058$ Å and the angle $\beta = 95.782°$ [25]. The chemical composition of mica is:

$$KAl_2(AlSi_3)O_{10}(OH, F)_2 \tag{1.13}$$

(OH,F) means that either OH or F is on the site. The here used mica consists of

potassium, aluminium, silicon and oxygen in the following chemical composition:

$$KAl_2(Si_3, Al)O_{10}(OH)_2$$

The particles are arranged in a layered structure, like it is shown in figure 1.7. One sheet of layers (of all particles) has a thickness of 10 $\mathring{A}$ (from plane A to B). The sheet consists of octahedral Al-O layers sandwiched between two tetrahedral Si-O layers [2]. One out of four Si^{4+} cations is replaced with an Al^{3+} ion. The resulting negative charge, due to the substitution, is compensated by a layer of K^+ cations in-between the tetrahedral layers. The weakest bonds in the crystal are those between potassium and oxygen so that cleavage takes place along a potassium layer [3] and half a layer of potassium remains on each face [2].

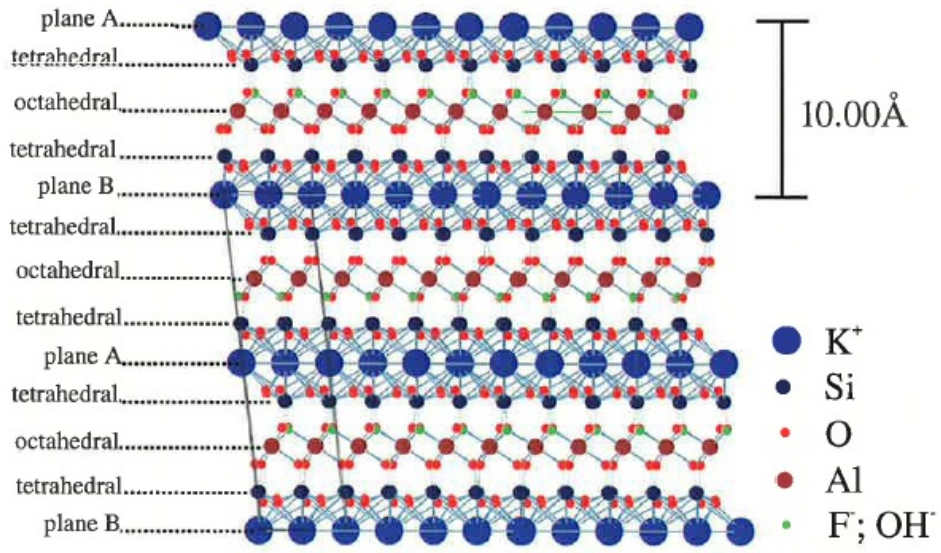

Figure 1.7: The crystallographic structure of muscovite mica.

Between the K^+ ions, remaining on the surface, and the negatively charged Al^{3+} substitutional sites dipoles are generated, that lead to dipole fields parallel to the surface [3, 4]. It is assumed that these electric fields, existing on the surface of freshly cleaved mica, cause the formation of a wetting layer and needle-like islands, composed of lying 6P molecules [2].

In addition mica shows an anisotropic behaviour in electrical and thermal conductivity. It was shown that mica has a rather low thermal conductivity normal to the (001) plane [26]. The temperature is measured on the back of the sample holder, which is also used to heat the mica sample. Thus the temperature of the mica surface always lags behind the measured temperature.

1.7 Para-hexaphenyl

Para-hexaphenyl is also called 6P, p-6P, PSP or para-sexiphenyl. In this master thesis only the names 6P or para-hexaphenyl will be used. Schematics of 6P can be seen in figure 1.8. It is an organic molecule that consists of six phenyl rings (aromatic hydrocarbons). In the gas phase the molecule has a rod like shape, in the condensed phase 6P forms a monoclinic structure. The lattice constants of this system are [27]:

$$a = 8.091 \text{ Å}, \;\; b = 5.568 \text{ Å}, \;\; c = 26.241 \text{ Å}$$

$$\alpha = \gamma = 90^\circ$$

$$\beta = 98.17^\circ$$

6P ($C_{36}H_{26}$) is an aromatic molecule, where the phenyl rings are arranged along one line in para-position (the substituents occupy the opposite ends). An individual 6P molecule shows a twist angle between neighbouring molecules of more than 40° [27], whereas in the crystalline state all phenyl rings arrange in one plane. However, the monocline crystal structure is classified as a layered herringbone structure, which contains two 6P molecules per unit cell [25, 27]. In the gas phase, however, 6P has a rod-like shape with the VdW-dimensions 2.85x0.35x0.67 nm^3 [28].

Para-hexaphenyl has a $\pi-$conjugation that is elongated over the whole molecule. These π electrons are responsible for the optical and electrical properties of 6P. Like many conjugated materials, 6P has a band gap and thus semiconducting properties [25].

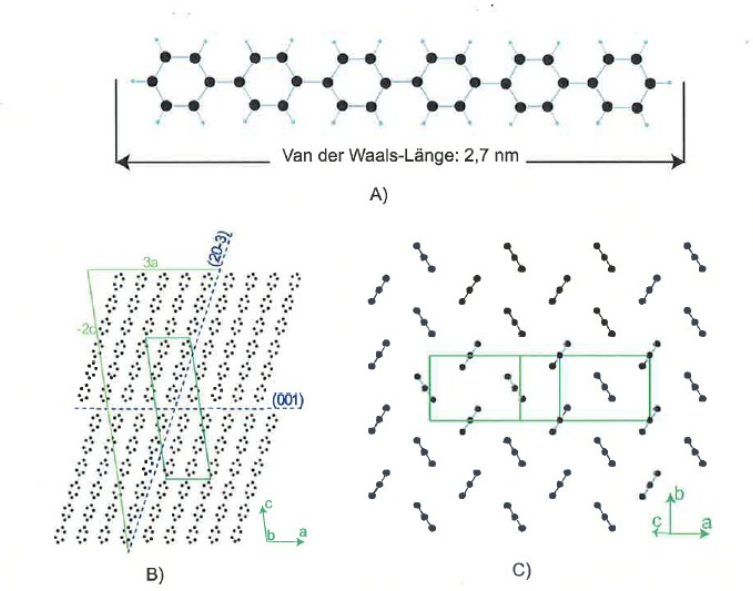

Figure 1.8: The hexaphenyl molecule with all the hydrogen atoms and the carbon rings can be seen in (A). The six carbon rings have a VdW length of 2.7 nm. The crystal structure of this molecule is monoclinic and consists of layers of lying molecules (B). When the 6P is observed along the long axis, one can see that it forms a herringbone structure (C).

1.8 Potassium

Potassium (K) has the atomic number 19 and belongs to the group of the alkali metals. The mass of one potassium atom is 39.098 amu, which leads to a mass of $m = 6.5 \cdot 10^{-23}$ g [29]. Since potassium only has one valance electron it is very reactive with water and oxygen, which is why UHV conditions are necessary. In the metallic form, potassium has a crystal structure with a body centred unit cell, which contains two atoms per cell [30]. The lattice constant of this unit cell is $a = 0.533$ nm and the density of metallic potassium at room temperaure is $\rho = 0.86 g/cm^3$ [29].

Due to the high reactivity of alkali metals, the deposition in UHV is a little bit more difficult. In the case of potassium a SAES Getter is used. In this deposition source the potassium is bonded to some material, therefore it cannot react with the residual gas, while the source is turned off. To evaporate potassium, the source is heated and when

a certain temperature is reached, the bondings of potassium and the getter material start to break up. Hence, potassium can evaporate through a small slit in the source into the chamber [6].

Chapter 2

Experimental Setup

In this chapter the main parts of the chamber shall be explained. The ultra high vacuum ensures precisely controlled conditions for the experiments. The evaporation of 6P molecules was realized by using a Knudsen cell, whereas the amount of evaporated material is controlled by a microbalance. Since potassium easily reacts with the residual gas, the deposition requires a SAES Getter. During the experiment the substrate can be cooled down to about 110 K and heated up electrically to about 1000 K. This doesn't only require a cooling system with liquid nitrogen, but also a precise heating program.

2.1 The vacuum chamber

The vacuum chamber and its attached instruments can be seen in figure 2.1. The chamber has two deposition sources for the evaporation of potassium and 6P. A quadrupole mass spectrometer (QMS) records the TDS spectra. On the backside of the chamber there is the Auger electron spectrometer (AES). The AES is used to measure the surface composition of the mica sample and to compare the amount of potassium on the potassium covered mica with the amount on freshly cleaved mica. The chamber also has an argon sputter gun, which is used to clean the sample surface. All instruments are aligned at the same height on a circle around the manipulator (fig. 2.2). The mica sheet is air cleaved and the sample is mounted on the sample holder, which is a one square centimeter big steel plate. On its back the heating wires and a Ni-NiCr thermocouple are attached. Four tantalum clamps on the sample holder press the mica sample

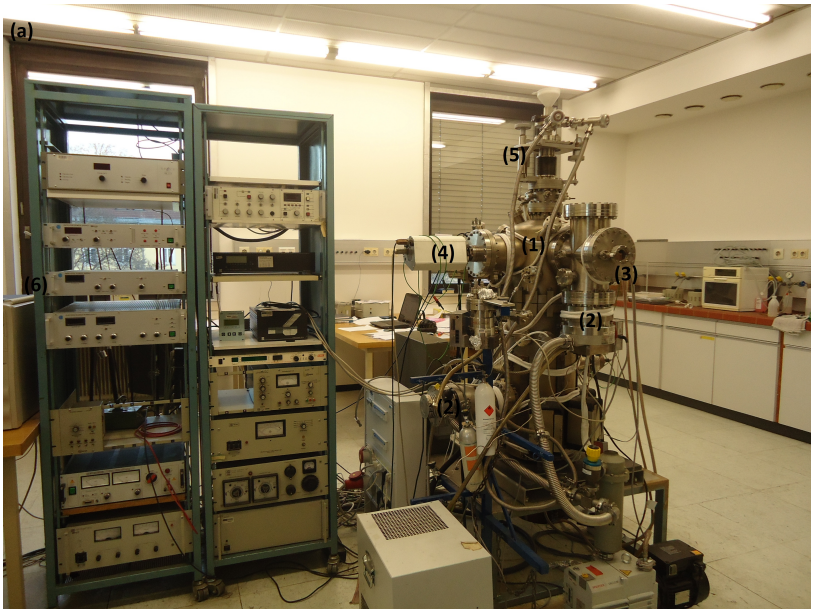

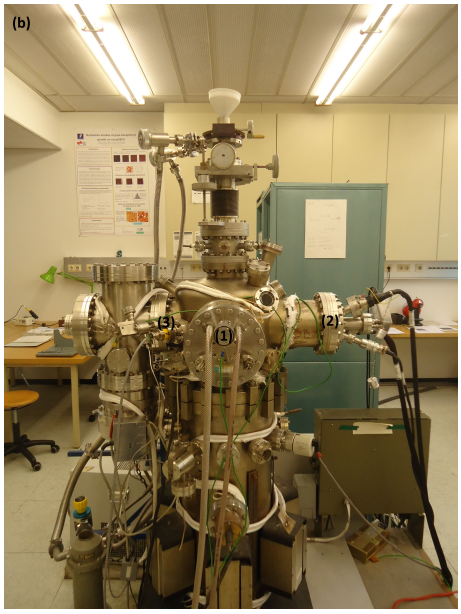

Figure 2.1: UHV setup (a) front view of the chamber and the attached instruments (1) Vacuum chamber (2) Turbomolecular pumps (3) Potassium evaporation source (4) Quadrupole mass spectrometer (5) Manipulator (6) Power supply AES (b) View from the right side of the chamber. (1) Knudsen cell (2) AE-spectrometer (3) Sputter gun

against the steel plate and hold it there. The sample holder then is mounted on the rotatable manipulator, which can place the mica in front of every instrument. Both, the sample holder and the manipulator can be seen in figure 2.2.

(a) The manipulator

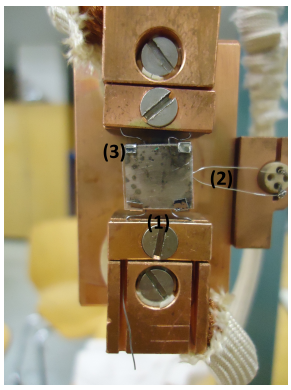

(b) The sample holder

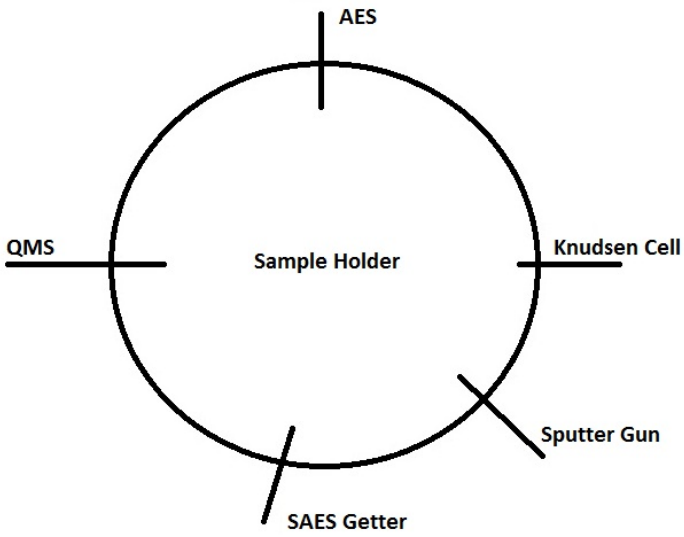

(c) Top view of the chamber

Figure 2.2: (a) With the manipulator it is possible to move the sample in x,y,z- direction and rotate it within the chamber (b) Sample holder: (1) heating wires (2) thermocouple (3) tantalum clamps (c) A schematic of the positions of all the instruments in the chamber

2.2 Ultra high vacuum

In surface science it is essential to run the experiments in ultra high vacuum (UHV). During the characterization of a solid surface on an atomic scale, it is necessary that the surface composition remains unchanged. This means that the experiments should be conducted in vacuum in order to minimize the reactions of the residual gas with the surface. In this thesis the main topic is the understanding of the thin film layer growth of 6P on freshly cleaved mica and on potassium covered mica. Thus, the UHV conditions are essential to guarantee on the one hand a clean mica surface during the adsorption of the different materials and on the other hand a low interaction between the evaporated materials with the residual gas. The concept of vacuum is normally understood in terms of molecular density n, mean free path λ, time constant to form a monolayer τ and impingement rate of the residual gas I (equation1.2) [6]:

$$n = \frac{p}{k_B T} \tag{2.1}$$

$$\lambda = \frac{k_B T}{\sqrt{2}\pi d^2 p} \tag{2.2}$$

$$\tau = \frac{n_0}{I} = \frac{n_0 \sqrt{2\pi m k_B T}}{p} \tag{2.3}$$

Here p is the pressure, k_B is the Boltzmann's constant, T is the temperature, d is the diameter of the gas particle, n_0 is the number of particles in a monolayer and m is the mass of the molecule.

Table 2.1 shows the change of these values with decreasing pressure. The values are calculated for nitrogen molecules at room temperature. By taking a closer look at the table one can see that in UHV the time constant to form a monolayer is rather high and the mean free path is much higher than the typical dimensions of a vacuum chamber. Hence the molecules will collide with the chamber walls many times before they hit each other.

Table 2.1: Molecular density n, impingement rate I, mean free path λ and the time constant to form a monolayer τ for nitrogen molecules at room temperature (293 K) [6].

$p/Torr$	n/cm^{-3}	$I/cm^{-2}s^{-1}$	λ	τ
760	$2 \cdot 10^{19}$	$3 \cdot 10^{23}$	70 nm	3 ns
1	$3 \cdot 10^{16}$	$4 \cdot 10^{20}$	50 μm	2 μs
10^{-3}	$3 \cdot 10^{13}$	$4 \cdot 10^{17}$	5 cm	2 ms
10^{-6}	$3 \cdot 10^{10}$	$4 \cdot 10^{14}$	50 m	2 s
10^{-9}	$3 \cdot 10^{7}$	$4 \cdot 10^{11}$	50 km	1 hour

The table is a good example why UHV conditions are needed to ensure precisely controlled conditions during the experiments. Due to the low pressure the interaction between the gas molecules is low, which ensures a low interaction with the residual gas during the evaporation. The high value of the time constant guarantees, that the surface of the substrate remains unchanged during the adsorption.

2.2.1 UHV pumping system

In figure 2.3 one can see the schematics of the UHV pumping system. It consists of two turbomolecular pumps (Pfeiffer TMU521, Leybold Turbovac 361) to achieve the UHV conditions and one rotary pump (Pfeiffer DUO20) as a backing pump. All gaskets in the chamber are made of copper. The pressure was measured with an extractor gauge system (Leybold IE514). By pumping the system without a bake-out one can reach pressures in the high 10^{-8} $Torr$ region. To reach lower pressures the system must be heated up to around 150 °C for one day. This bake-out enables pressures in the range of 10^{-10} $Torr$.

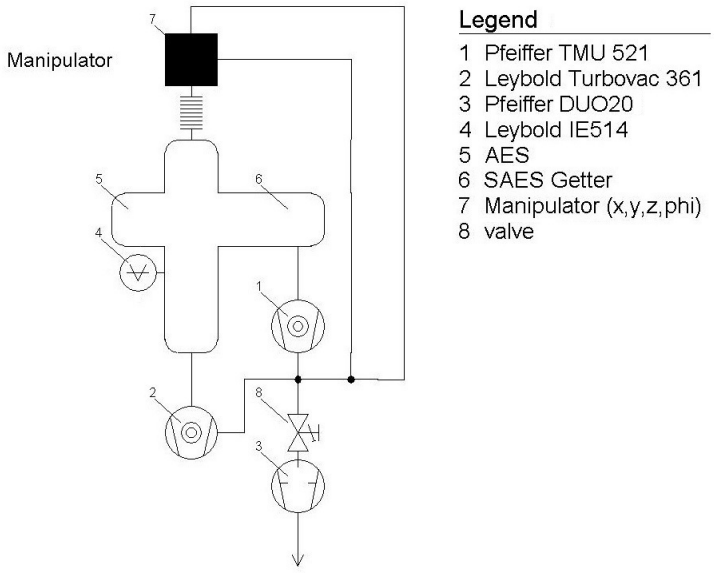

Figure 2.3: Schematics of the vacuum system

2.2.2 Cleaning the surface

As already mentioned above, the investigation of surfaces and the thin film layer growth of some materials on a surface implies the preparation of atomically clean surfaces. In general there exist several methods to clean a sample. For the experiments the mica surface was cleaned by heating, sputtering (both in-situ) and cleaving (ex-situ) [6, 7]:

- **Cleavage:** In the case of mica, it is a suitable technique because one can easily obtain a well defined single crystal surface after the cleavage [5]. This cleaning procedure was applied ex-situ, which means that all samples were air cleaved. To cleave the mica sample it is placed onto an adhesive tape to remove the top layers with this tape. As explained in chapter 1, the mica sample is a sheet silicate, with a potassium layer that links these sheets. The weakest bonds in the crystal are between potassium and oxygen so that cleavage takes place along a potassium layer. The air cleaved sample should be immediately mounted in ultra high vacuum in order to keep it clean.

- **Heating:** Another method to clean the surface is to heat it up to about 1000

K. During this so called flash adsorbed materials, like water and carbon, can desorb from the surface. Impurities in the sample bulk can redistribute and even segregate to the surface. In the case of mica the heating procedure was realized by electrically heating the sample holder. The temperature of the mica sample during the flash was controlled with a heating program.

- **Sputtering:** A second in-situ method to clean the surface was ion sputtering. The impurities on top of the substrate were removed by a bombardment of the sample surface with argon ions. The position of the sputter gun in the chamber can be seen in figure 2.1. If the gun was used, the mica sample was sputtered for ten minutes with an energy of 0.8 keV and a base pressure of $5 \cdot 10^{-6}$ $Torr$. The SPECS IQE 11/35 sputter gun used here, has a different solution for the position of the gas in let (compared to other sputter guns). The IQE 11/35 is mounted with a separate gas inlet flange which goes directly to the ionizer. Other sputter guns have the a gas inlet flange that is directly attached to the chamber.

Due to results of further experiments [5, 15] sputtering is in our case normally not the method of choice. The investigations have shown that sputtering the mica surface has an influence on the thin film layer growth of 6P. On freshly cleaved mica adsorbed 6P forms needle-like islands of flat lying molecules on top of a wetting layer. Sputtering changes the growth parameters in a way that the formation of islands of standing molecules and dewetting occurs. Hence sputtering will normally be avoided in this thesis, because the influences of increased amounts of surface-potassium on the thin film layer growth of 6P should be investigated.

2.3 Deposition sources

In order to deposit 6P or potassium on the surface of the mica sample two different sources are built in the chamber. 6P was evaporated by using a Knudsen cell (fig.2.4(a)) and a SAES Getter evaporation source (fig.2.4(b)) was used to evaporate potassium. To evaporate 6P the Knudsen cell must be heated up to temperatures between 250 and 270 °C (depending on the desired evaporation rate). The temperature is measured with a thermo-couple on the back of the Knudsen cell and the amount of evaporated material was determined by a quartz microbalance. A new microbalance oscillates

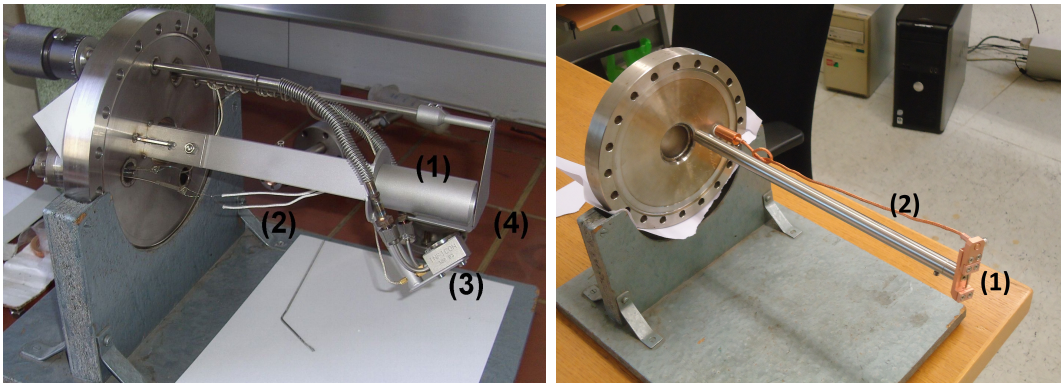

(a) (b)

Figure 2.4: (a) Knudsen cell to evaporate 6P. (1) Chamber with 6P powder (2) Heating wires (3) Quartz micro balance (4) Shutter, different positions enable evaporation only on the microbalance or sample, on both or none (b) SAES Getter to evaporate potassium. (1) SAES Getter (2) current supply

with a frequency of 6 MHz. When some material like 6P adsorbs on the device the frequency decreases with increasing amounts of the adsorbate. By measuring the frequency change the amount of adsorbate can be determined.

Alkali metals like potassium have properties that are inconvenient for the use as deposition material in UHV. Thus, commercially available deposition sources, called SAES Getters are used for the evaporation of these metals. In the source potassium is bonded to a porous material (getter). When the temperature of the source is increased to sufficiently high value, the bonding breaks and potassium can evaporate. Since the evaporation rate increases exponentially with the heating current, the current has to be increased slowly, especially when a new SAES Getter is turned on the first time. In order to have a good and constant evaporation one needs at least a heating current of around 6 A (the heating current changes to higher values for a nearly empty deposition source). Unfortunately there is no thermo-couple or quartz microbalance to control the evaporation of the potassium. To guarantee constant evaporation rates during the adsorption, the ísotropic concentration of potassium was always measured with the quadrupole mass spectrometer (see chapter 3.3.1).

2.4 Heating and cooling of the substrate

The heating and cooling of the mica sample is realized by controlling the temperature of the sample holder. In order to cool the system liquid nitrogen comes into use. Inside the manipulator (fig.2.2(a)) is a tube that is thermally conducted to the sample holder. By filling liquid nitrogen into this tube the whole manipulator and thus the sample holder are cooled down. This cooling system enables sample temperatures of about 110 K. In order to heat the system a voltage is applied on the heating wires of the sample holder (fig.2.2(b)), thus temperatures up to 1200 K can be reached. In our case the mica sample was never heated up to temperatures above 1000 K. In order to have an exact and constant heating rate the whole process is controlled by a computer program (self-made LabView program). The program can generate constant heating rates of 1 K/s or even lower, by measuring the actual temperature and applying the according voltage. These constant heating rates are especially important for the TD-spectrum.

By taking a closer look on the sample holder shown in figure 2.2(b), one can see that the measured temperature is in fact not the one of the mica sample but of the sample holder. Since mica is a thermal insulator this leads to slight problems in the temperature measurement, because the temperature measured on the sample holder is not the same as on the top of the surface. In order to correct the measured temperature to the true values of the mica surface one needs to do a temperature correction as explained in chapter A.1.

Chapter 3

Results and discussion

A cleaved mica surface always shows a well defined single crystal structure with half a monolayer of potassium on the surface. To study the effects of potassium on the adsorption of para-hexaphenyl, 6P was adsorbed on freshly cleaved mica and on potassium covered mica. In this chapter the preparation of the mica sample and the ad- and desorption of potassium and 6P will be explained.

3.1 Freshly cleaved mica sample

The mica sample was cleaved in air and immediately transferred into the vacuum chamber. The transfer has to be performed within minutes, otherwise the formation of a water layer will prevent the needle-like growth of 6P [31]. At first the freshly cleaved mica sample was investigated with AES, which provides information about the chemical composition of the surface. Figure 3.1 shows the AE-spectrum in the range of 50 - 550 eV. In this spectrum the expected elements of the sample can be seen [21]:

- Aluminum, Al: 68 eV; not measured
- Silicon, Si: 92 eV; measured: 85 eV
- Potassium, K: 252 eV; measured: 249 eV
- Carbon, C: 272 eV; measured: 267 eV (impurity)
- Oxygen, O: 510 eV; measured: 508 eV

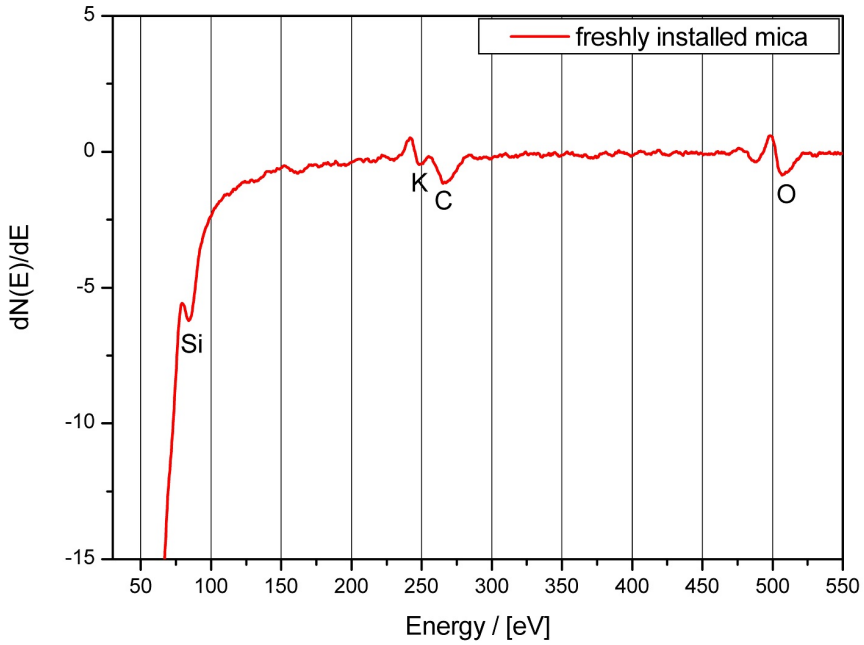

Figure 3.1: AE-spectrum of a freshly installed mica sample. The image shows the expected elements of mica (Si, K, and O) and some carbon on the surface. In this measurement the aluminum peak was not detected.

The carbon peak in the spectrum indicates that the surface was not clean; therefore different cleaning methods were tested. The effects of sputtering and heating have already been studied in the master thesis of Potocar [15]. Heating leads to an increased carbon peak, probably because carbon contributions in the bulk segregate to the surface. Sputtering changes the roughness of the surface. To see the effects of the temperature, the cleaved mica was heated up from 300 K to 900 K with a heating rate of 1 K/s. After the sample has cooled down to 300 K an AE-spectrum was recorded. To see the effects of sputtering, the sample was sputtered for 10 minutes with Ar^+-ions with an energy of 800 eV at a pressure of $5 \cdot 10^{-6}$ $Torr$. Subsequently, the sample was again investigated with AES. The results of these measurements can be seen in figure 3.2, where (a) is an overview of the chemical composition of the mica sample and (b) shows details of the potassium and carbon peak.

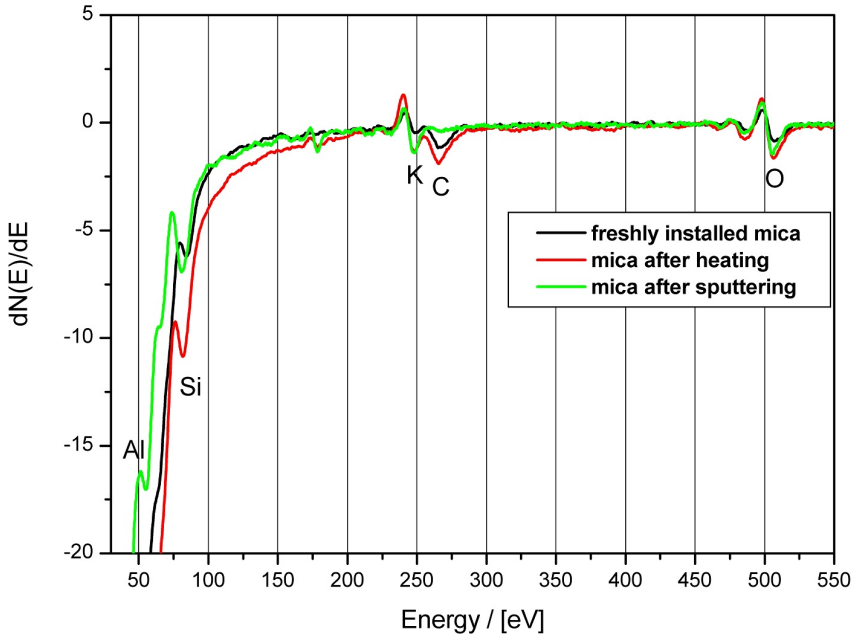

(a) Overview AE-spectrum of the mica surface

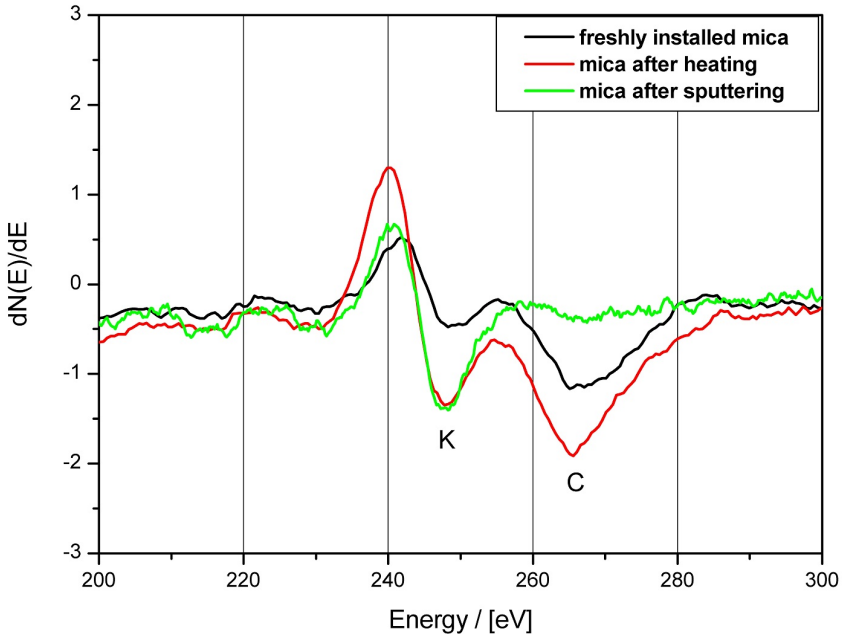

(b) Potassium and Carbon peak

Figure 3.2: (a) The AE spectra show an overview spectrum of the mica surface before and after the heating and sputtering process. After the sputter process one can also see the aluminum peak. (b) The AE-spectra show details of the changes of the potassium and carbon peak due to heating and sputtering.

Figure 3.2 shows what was mentioned above. The AE-spectrum recorded after the heating process shows a higher amount of carbon and potassium on the surface compared to the spectrum of the freshly installed mica. It is possible to remove the carbon by sputtering the surface but it also removes some of the potassium. The measurements demonstrate that sputtering would be a good method to clean the surface, but it influences the subsequent thin film layer growth of 6P [5, 15]. Since the effects of potassium on the layer growth of 6P should be investigated, sputtering must be avoided.

3.1.1 Preparation of the mica sample

It is important for the results of any experiment that the mica sample is well characterized before the measurement. Thus the following procedure was implemented:

- Cleaving the mica sample with an adhesive tape
- Installing the sample immediately in the ultra high vacuum
- Heating it up to 1000 K with a heating rate of 1 K/s
- Taking an AE-spectrum of the freshly cleaved sample

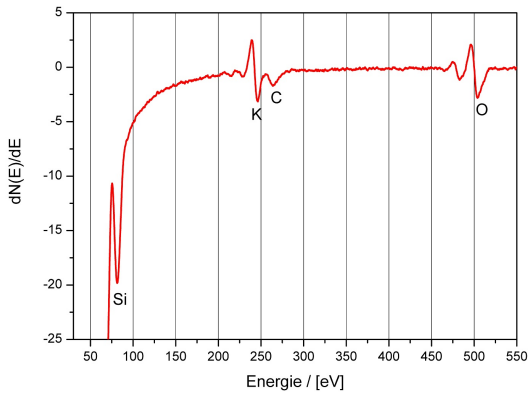

Figure 3.3: The AE-spectrum of a freshly cleaved mica surface after the described preparation.

An AE-spectrum of the freshly cleaved mica surface treated with this procedure can be seen in figure 3.3. In order to know the initial surface composition, such a spectrum was taken for every sample. Afterwards the sample is ready for the actual experiments.

3.2 Adsorption of 6P on freshly cleaved mica

In the last years several groups investigated the thin film layer growth of 6P on freshly cleaved mica [2, 5, 31, 32]. As already explained, 6P forms needle-like islands of flat lying molecules on top of a wetting layer. In order to study the influence of potassium on the thin film layer growth, first the growth of 6P on freshly cleaved mica has to be studied. Additionally, the results of the 6P adsorption on freshly cleaved mica shall be compared with corresponding literature [15, 25].

3.2.1 The Knudsen cell

The Knudsen cell is a perfect deposition source for physical vapor deposition. The cell itself is heated electrically (indirectly with heating wires), thus the 6P inside the cell vaporizes and passes through a small hole in the cell into the chamber and onto the sample surface. To control the vapor deposition the temperature of the Knudsen cell is measured on its back and the microbalance measures the amount of adsorbed material. Note that the amount is measured in terms of frequency change on the microbalance. A frequency change of 1 Hz on the microbalance corresponds approximately to a 1 $\mathring{A}$ thick film of 6P (see chapter A.3). Thus, the amount of deposited 6P is always written in terms of mean film thickness, as measured by the quartz microbalance.

First of all it had to be verified that it is possible to adsorb specific amounts of 6P by monitoring the frequency of the microbalance and the temperature of the Knudsen cell. In order to show this a 30 $\mathring{A}$ thick film of 6P was adsorbed on the surface. This was done three times, always with different temperatures of the Knudsen cell and hence different deposition rates. After each adsorption the sample was heated up to 1000 K and a TD-spectrum of 6P (mass 61) was recorded. The TD- spectra of all three measurements in figure 3.4 have the same shape and nearly the same size. Thus, monitoring the temperature and the frequency enables the adsorption of specific

amounts of 6P.

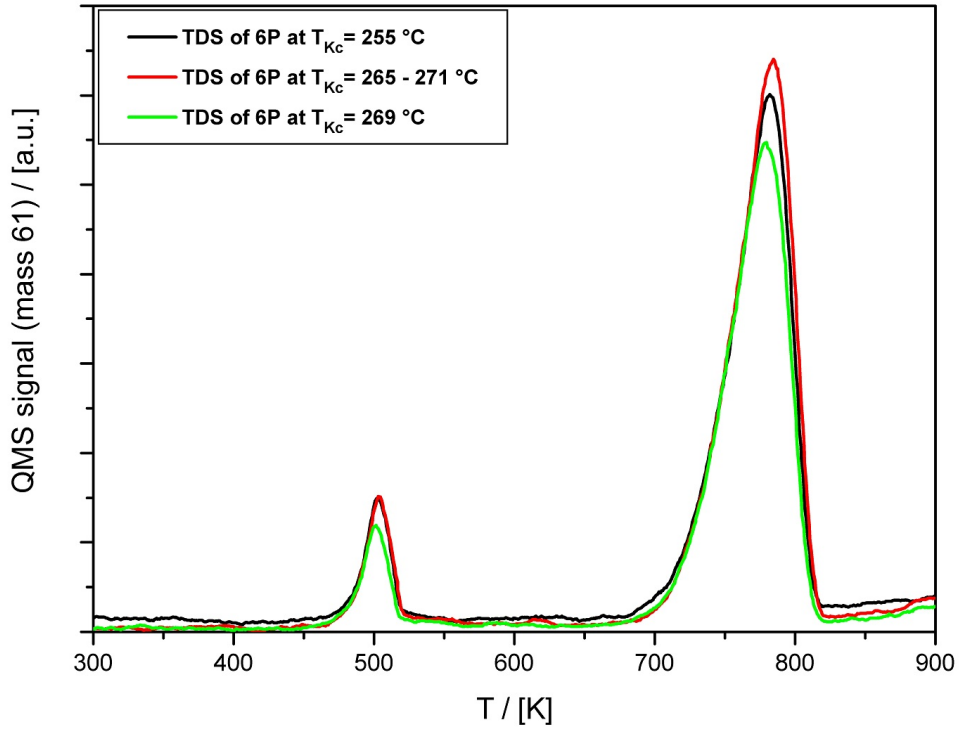

Figure 3.4: Three TD-spectra after the deposition of 30 $\AA$ 6P with different temperatures of the Knudsen cell and hence different deposition rates.

The microbalance was water cooled during every adsorption, because changes in the temperature of the microbalance, caused by hot 6P vapor, can influence the frequency as well. If the microbalance is not cooled, the hot vapor heats the device and thus the frequency change would not correlate with the adsorbed amount of 6P. Figure 3.4 shows TD-spectra of 6P, deposited by using three different temperatures of the Knudsen cell (255, 269, 265-271 $°C$). The fact that all spectra look similar indicates that the same amount of 6P was adsorbed. Thus, a higher or fluctuating temperature of the 6P vapor has no effects on the frequency of the microbalance as long as it is water cooled.

3.2.2 The adsorption procedure

To ensure reproducible results of the TD-spectra, one must be able to control the amount of adsorbed 6P very precisely. Thus, the following procedure for the adsorption of 6P was implemented:

- Turn on the water to cool the microbalance
- Turn on the microbalance and wait till the frequency is stable
- Choose the shutter position that only enables an evaporation on the microbalance
- Fast heating of the Knudsen cell ($I = 1\ A$) till $T = 230\ °C$
- Change the heating current to $I = 0.7 - 0.8\ A$ to adjust the temperature of the Knudsen cell (The higher the temperature the higher the evaporation rate)
- Open the shutter to start the adsorption
- Measure the frequency change and close the shutter when the desired amount is adsorbed

3.2.3 Adsorption of 6P on mica

The wetting layer is the first layer of 6P molecules; it is bonded directly to the mica surface and is called monolayer. The needles are on top of the wetting layer and form the multilayer. At first it should be confirmed that indeed such a wetting layer exists. Hence 15 $\mathring{A}$ of 6P were adsorbed on the cleaved mica surface. After the adsorption the sample was heated up to 1000 K and a TD-spectrum was recorded. Due to the fact that 6P from the monolayer has a higher desorption energy than 6P from the multilayer [5], the multilayer of 6P desorbs at lower temperatures than the monolayer of 6P. Thus, the TD-spectrum should consist of two peaks, one from the multilayer and the other from the monolayer.

The results of the 15 $\mathring{A}$ thick 6P film desorbing from the surface can be seen in figure 3.5. The TD-spectrum consists of three peaks instead of the expected two. The first peak at $T = 480\ K$ belongs to the tantalum clamps of the sample holder. This

peak is used for the temperature correction, which is explained in chapter A.1. All the TD-spectra of 6P shown in this thesis were corrected with this method, which shifts the measured temperatures to the true values of the mica surface. The second peak at $T = 730\ K$ has a corrected surface temperature of 480 K at the peak maximum and belongs to the multilayer of 6P. The third peak at around 850 K belongs to 6P from the wetting layer and has a corrected temperature of $T = 560\ K$. The areas underneath the monolayer and multilayer peaks of 6P were calculated. The ratio of multilayer to monolayer is about 4.4, indicating that the wetting layer of 6P has a mean film thickness of 3.4 $\mathring{A}$. This film thickness is in good agreement with the VdW thickness of a 6P molecule (0.35 nm) [28].

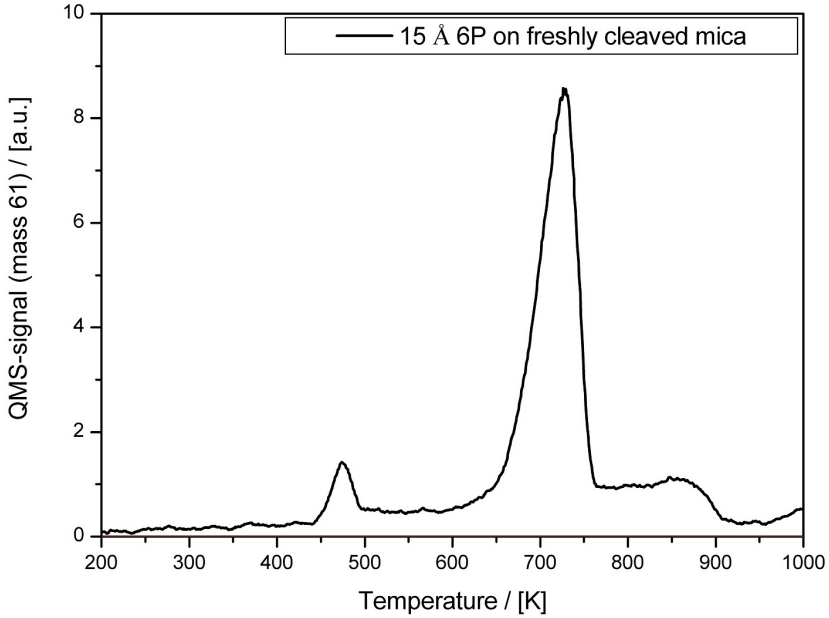

Figure 3.5: TD-spectrum of 15 $\mathring{A}$ 6P adsorbed on freshly cleaved mica. The spectrum consists of three peaks at $T = 480\ K$, $T = 730\ K$ and $T = 850\ K$. The surface temperature during the deposition was $T_{ad} = 110\ K$

The recorded TD-spectrum indeed shows the monolayer/multilayer behaviour of 6P on freshly cleaved mica. The measured spectrum was compared to the results of the thesis by Frank [25]. The comparison showed that the shapes of the spectra are similar and that the temperatures of the peak maxima are approximately the same.

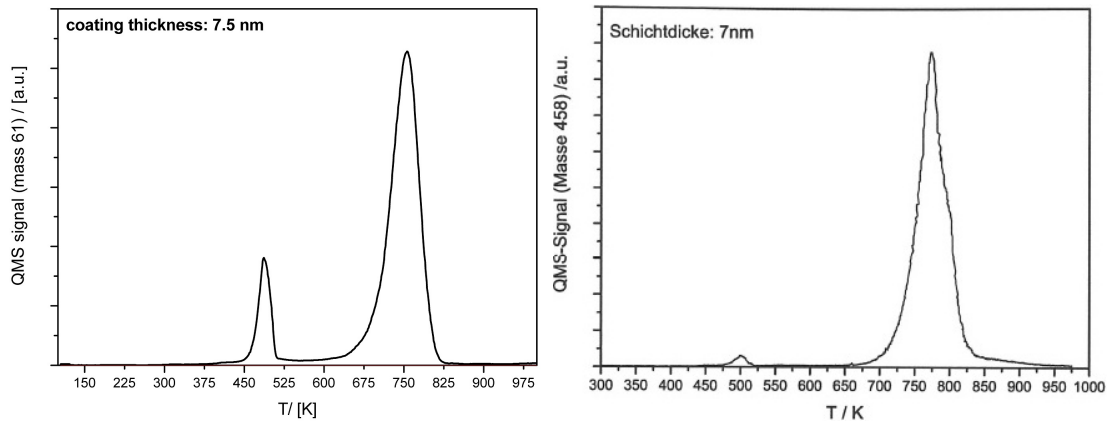

Figure 3.6: Comparison of two TD-spectra. The left shows a TD-spectrum of 7.5 nm 6P as measured in this thesis. The right images shows a TD-spectrum of 7 nm 6P measured by Frank [25].

The TD-spectra in figure 3.6 show 6P molecules desorbing from thicker film. Note that the adsorption of 6P in the thesis by Frank was done at room temperature. Therefore the starting temperature of the TD spectrum was at 300 K. In our measurements 6P was always adsorbed at low temperatures and thus the starting temperature of the TD-spectrum was 110 K. The heating curve of the mica sample is expected to be linear, but with a smaller slope than the heating curve of the sample holder, because mica is a thermal insulator. Thus, the peaks of 6P from the tantalum clamps and the mica sample in the measured TD-spectrum should be further apart as in the TD-spectrum of Frank. Figure 3.6 reveals that this is not the case. This indicates that the temperature correction has a high uncertainty. Nevertheless, this temperature correction is the best and only way to at least have an estimation of the true surface temperature.

3.2.4 Order of desorption kinetics

As already explained in chapter 1 the TD-spectra can be used to determine the order of desorption kinetics n. To evaluate this order, TD-spectra of different coverages of 6P on mica must be recorded. Five different TD-spectra from 5 to 25 $\mathring{A}$ thick 6P films were measured. After each adsorption step at 110 K the sample was heated up to 1000 K and the according TD-spectrum was recorded and plotted in figure 3.7 to

evaluate the order of kinetics from the shape of the peaks. From this comparison of the TD-spectra it is difficult to determine the order of desorption. Figure 3.7 indicates that the 6P from the multilayer follows a fractional order of desorption, because the peaks don't increase along the same leading edge, as expected for zero order. In the case of fractional order of desorption, the 6P molecules desorb from the edges of the needles.

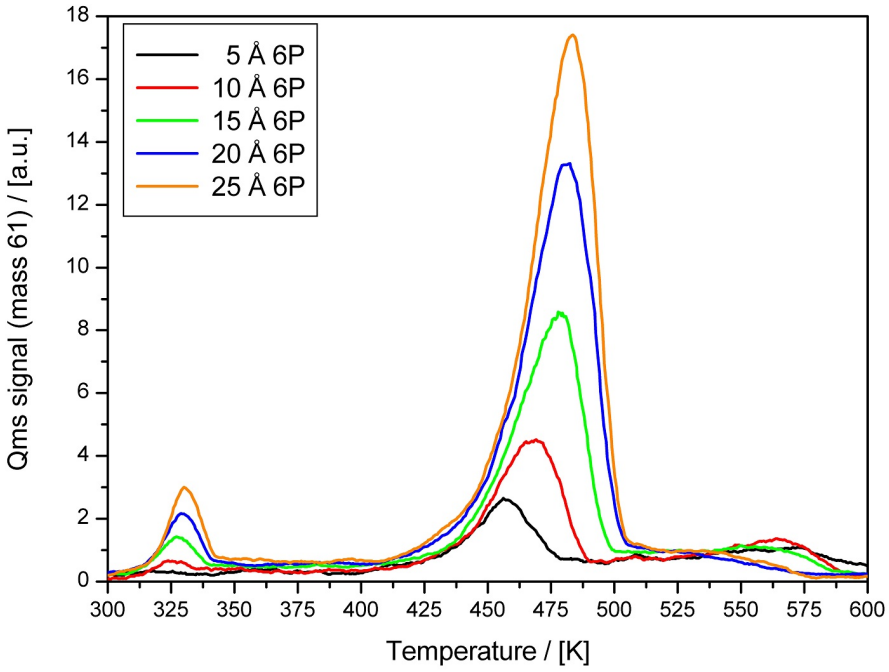

Figure 3.7: TD-spectra of 5, 10, 15, 20 and 25 $\mathring{A}$ 6P adsorbed on freshly cleaved mica. The shape of the peaks indicates a fractional order desorption for the multilayer. $T_{ad} = 110\ K$

A second approach to determine the order of kinetics is explained in chapter A.2. The method is based on the paper by Parker et al. [14]. It utilizes the fact that the desorption follows the Polanyi-Wigner rate expression (equation 1.7). Basically it is a variation of the Arrhenius plot, which enables a plot of the $[ln(r_{des}) - n \cdot ln(\Theta)]$ versus $(1/T)$ for the different orders of kinetics ($n = 0, \frac{1}{2}, 1$). This method was applied on the TD-spectra of 20 and 25 $\mathring{A}$ thick 6P films to evaluate the order of desorption. Figure 3.8 shows the three Arrhenius plots of the two TD-spectra for the zero, half, and first

order of kinetics. The curve that shows the best linear behaviour is the one with correct order of kinetics.

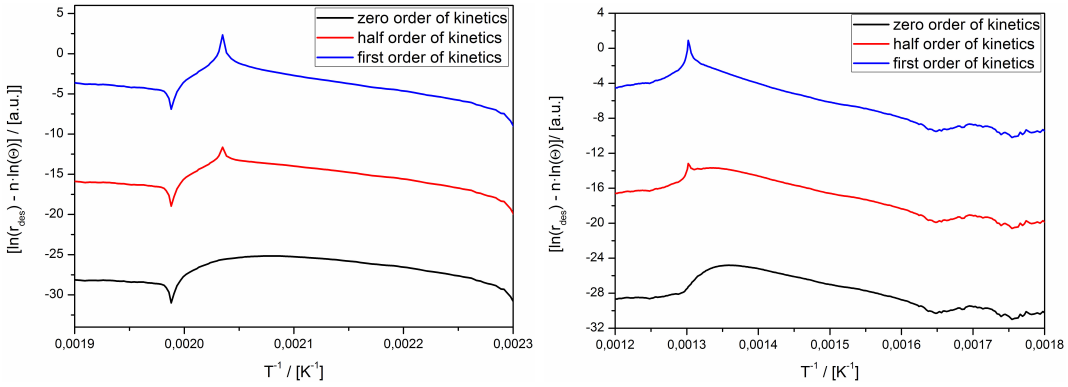

Figure 3.8: The left figure shows an image of the Arrhenius plots of a 20 $\mathring{A}$ thick 6P film in the case of zero, half and first order of kinetics. The image on the right shows the same for a 25 $\mathring{A}$ thick 6P film.

For the leading edge of the TD-spectra the Arrhenius plots yield straight lines. In both cases it is impossible to exactly determine which line shows the correct order of desorption kinetics (in the case of the multilayer), but figure 3.8 indicates that the multilayer desorption of 6P belongs rather to the $\frac{1}{2}$ order kinetics. Nevertheless, some precise and more detailed studies of 6P on freshly cleaved mica would be necessary to exactly determine the correct order of desorption.

The desorption energy of the multilayer desorption can be calculated for the case of zero, half and first order kinetics by measuring the slope in the Arrhenius plot. As one can see in figure 3.8, the slopes of the straight lines are approximately the same for all three kinetics. Thus, it is more convenient to just calculate the desorption energy for the zero order case.

3.2.5 The desorption energies

Monolayer

In figure 3.7 the wetting layer desorbs at a corrected temperature of $T = 560K$ for all different coverages. The desorption energy of the monolayer can be determined by the Redhead formula (eq.1.11). The calculation cannot be done without knowing the pre-exponential factor ν_1. In the case of atoms this factor has a value of $\nu_1 = 10^{13}s^{-1}$ [6]. For atoms this is a good value for the pre-exponential factor, but for molecules it is inappropriate because they are much bigger than single atoms. Generally the pre-exponential factor of the first order desorption, ν_1, is coverage dependent. For the present approximation this can be neglected and ν_1 is approximated by the coverage independent pre-exponential factor of zero-order desorption, ν_0 [28].

In this calculation the pre-exponential factor of zero order desorption determined by Frank was used to evaluate the desorption energy of the monolayer $\nu_0 = 3.7 \cdot 10^{25}\ s^{-1}$ [25]. According to figure 3.7 the temperature of the peak maximum is at $T_m = 560K$. Since the temperature measurement has a high uncertainty, an experimental error of $\pm 50\ K$ was assumed. This leads to the following value for the desorption energy, according to equation 1.11:

$$T_m \approx 560 \pm 50\ K \Rightarrow E_{des} = 69 \pm 6\ kcal/mol = 3.0 \pm 0.3\ eV$$

The result shows that the desorption energy calculated in this thesis is in good agreement with the results of other works [15, 25]. The desorption energy can be calculated in both units by using the Redhead formula. If the gas constant R is used for the calculation, the results have the unit $kcal/mol$. When the Boltzmann constant k_B is used instead the results have the unit eV. The results can also be easily converted into each other by the following formula:

$$E_{des}\left[\frac{kcal}{mol}\right] \cdot 4.3 \cdot 10^{-2}\left[\frac{mol \cdot eV}{kcal}\right] = E_{des}[eV]$$

Multilayer

The desorption energy of the multilayer can be determined with the Arrhenius plot, assuming a zero order desorption. This method is briefly discussed in chapter 1.3.1. To

evaluate the desorption energy, the logarithm of the desorption rate $ln(r_{des})$ is plotted as a function of $1/T$. Thus, the exponential part of the TD-spectrum becomes linear and by measuring the slope, the desorption energy can be determined. To evaluate the pre-exponential factor, it is necessary to calculate the intercept of the straight line with the y-axis. Note that for this calculation the desorption rate r_{des} has to be in the dimensions of $molecules/cm^2s$. The conversion of the y-axis was done as described in the dissertation of Müllegger [28].

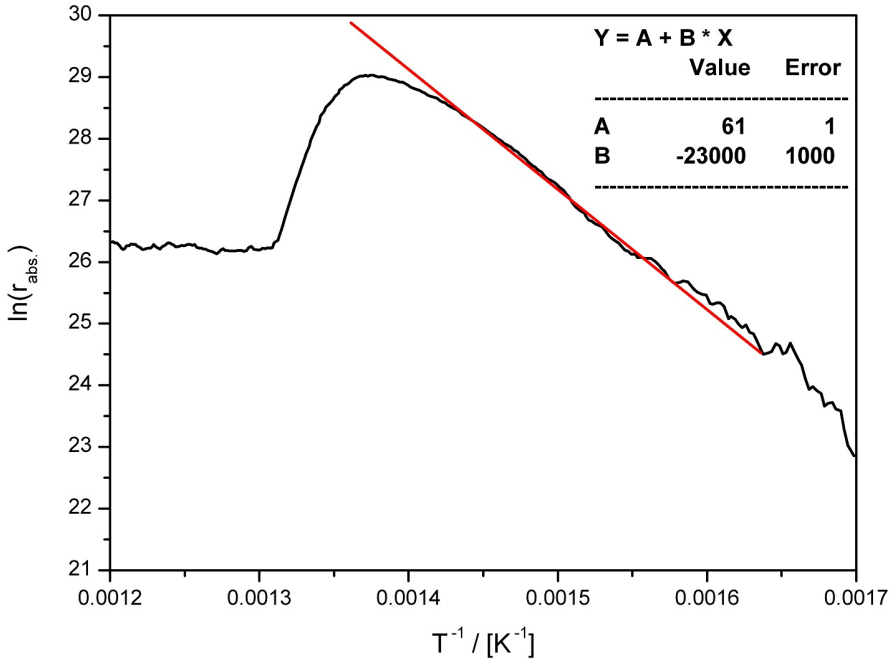

Figure 3.9: The Arrhenius plot of the TD-spectrum of 15$\AA$ 6P adsorbed on freshly cleaved mica. The linear fit is used to calculate the desorption energy and the pre-exponential factor from the slope and the intercept.

The TD-spectra of different 6P films on freshly cleaved mica (fig.3.7) were used to calculate the desorption energy and the pre-exponential factor. The Arrhenius plots for these calculations can be seen at the end of this section (fig.3.10 and fig.3.11). A detailed description of the calculation is given for the case of the 15 $\AA$ thick 6P film. Figure 3.9 shows an Arrhenius plot of this TD-spectrum. The linear fit can be described with a linear equation ($y = A + Bx$), where $B = -23000 \pm 1000$ is the slope of the line

and $A = 61 \pm 1$ is the intercept with the y-axis. Note that the errors given here are just the ones caused by the linear fit and that a higher uncertainty is caused by the temperature measurement. The slope was used to determine the desorption energy:

$$B = -23000 = -\frac{E_{des}}{R} \Rightarrow E_{des} = 46\ kcal/mol = 2.0\ eV/molecule$$

As already mentioned, the desorption rate must be rewritten in absolute values in order to determine the correct intercept A for the pre-exponential factor. The parameter A from the linear fit was used to calculate the pre-exponential factor ν:

$$A = 61 = ln(\nu) \Rightarrow \nu = e^{61} \approx 3.1 \cdot 10^{26}\ molecules/cm^2 s$$

Note that the dimension of the pre-exponential factor ν is $molecules/cm^2 s$. In order to calculate the factor, ν_0, that has the dimension of s^{-1}, the coverage Θ_0 of the 6P bulk surface must be taken into account [25, 28]:

$$r_{des} = \nu \cdot exp(-\frac{E_{des}}{kT}) = \nu_0 \Theta_0 \cdot exp(-\frac{E_{des}}{kT})$$

The absolute value of the coverage Θ_0 can be calculated from the well known 6P bulk crystal structure. One needs to know the numbers of 6P molecules on the substrate. To evaluate this number for the one cm^2 sample the number of unit cells on this surface must be determined. The corresponding surface unit cell has an area of $3.7nm^2$ and comprises two 6P molecules [28]. The total number of unit cells on the sample surface is $2.7 \cdot 10^{13}$ and thus the coverage Θ_0 for 6P is $5.4 \cdot 10^{13}\ molecules/cm^2$. This leads to the following pre-exponential factor in the correct dimension:

$$\nu_0 = \frac{\nu}{\Theta_0} = 6 \cdot 10^{12}\ s^{-1}$$

The results for the desorption energy and the pre-exponential factor in the case of the 5, 10, 20, and 25 $\mathring{A}$ thick 6P films are given here:

- $E_{des} = 32\ kcal/mol = 1.4\ eV$ $\nu_0 = 1 \cdot 10^8\ s^{-1}$ (5 $\mathring{A}$ of 6P)
- $E_{des} = 40\ kcal/mol = 1.7\ eV$ $\nu_0 = 4 \cdot 10^{10}\ s^{-1}$ (10 $\mathring{A}$ of 6P)
- $E_{des} = 38\ kcal/mol = 1.6\ eV$ $\nu_0 = 4 \cdot 10^{10}\ s^{-1}$ (20 $\mathring{A}$ of 6P)

- $E_{des} = 42\ kcal/mol = 1.8\ eV\ \ \nu_0 = 2 \cdot 10^{12}\ s^{-1}$ (25 $\mathring{A}$ of 6P)

The values calculated for the desorption energy and the pre-exponential factor of the zero order desorption, are lower than described in the literature [15, 25, 28]. Especially the pre-exponential factor is much too low for a molecule and even lower than the typical values for atoms. This has to be traced back to the high uncertainty of the temperature measurement. The calculations of the pre-exponential factor were done with and without the temperature correction. Both cases lead to too low values of the pre-exponential factor. The calculations displayed here are the ones without a temperature correction. To overcome this problem, a 50 $\mathring{A}$ thick 6P film was adsorbed directly on the steel plate of the sample holder. Therefore the true surface temperature was known at all times. The experiment is explicitly explained in the next section, here only the results are presented:

Multilayer of steel plate: $E_{des} = 51.2\ kcal/mol = 2.2\ eV$ with $\nu_0 = 2 \cdot 10^{22}\ s^{-1}$

These results are in good agreement with according literature [28]. The value of the multilayer desorption energy of 6P on a gold sample is $E_{des} = 2.4\ eV$ and the calculated frequency factor has a value of $\nu_0 = 5.6 \cdot 10^{25}\ s^{-1}$. In the previous section the desorption energy of the wetting layer (first order desorption) was calculated by using the pre-exponential factor of zero order desorption, ν_0, calculated by Frank. Using now the pre-exponential factor calculated above leads to the following monolayer desorption energy:

Monolayer: $E_{des} = 61\ kcal/mol = 2.6\ eV$ with $\nu_0 = 2 \cdot 10^{22}\ s^{-1}$

Note that even big differences in the pre-exponential factor only lead to small changes in the calculation of the monolayer desorption energy. A pre-exponential factor that is 10^3 times lower than the value determined by Frank, leads only to a 0.4 eV lower desorption energy.

The TD-spectrum of the 50 $\mathring{A}$ thick 6P film on the steel plate was used as a reference to know the correct temperature of the 6P multilayer desorption from mica. It also

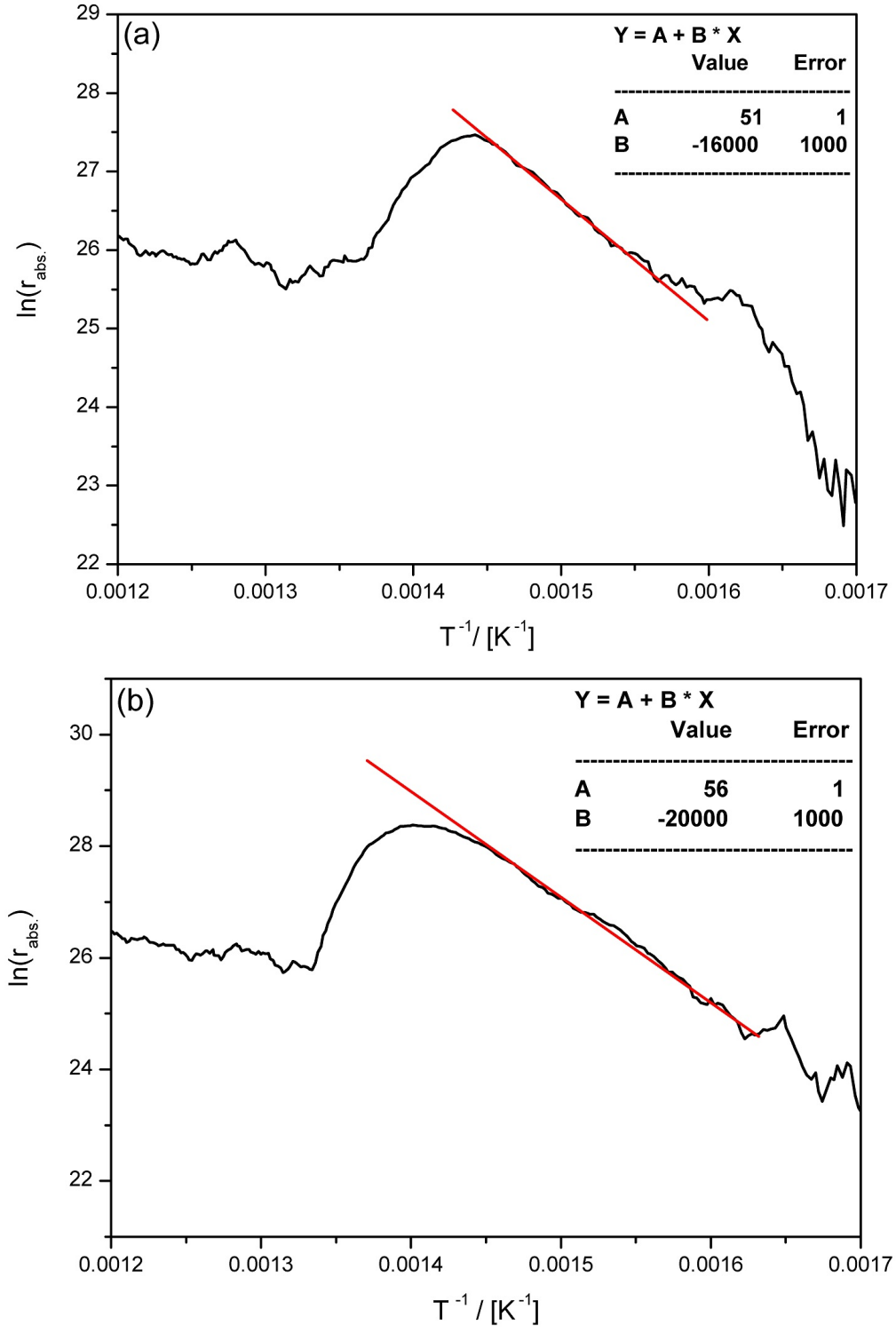

Figure 3.10: The Arrhenius plot of different amounts of 6P on freshly cleaved mica. (a) 5 $\AA$ of 6P (b) 10 $\AA$ of 6P. The slope B can be used to calculate the desorption energy and the intercept A can be used to get the frequency factor.

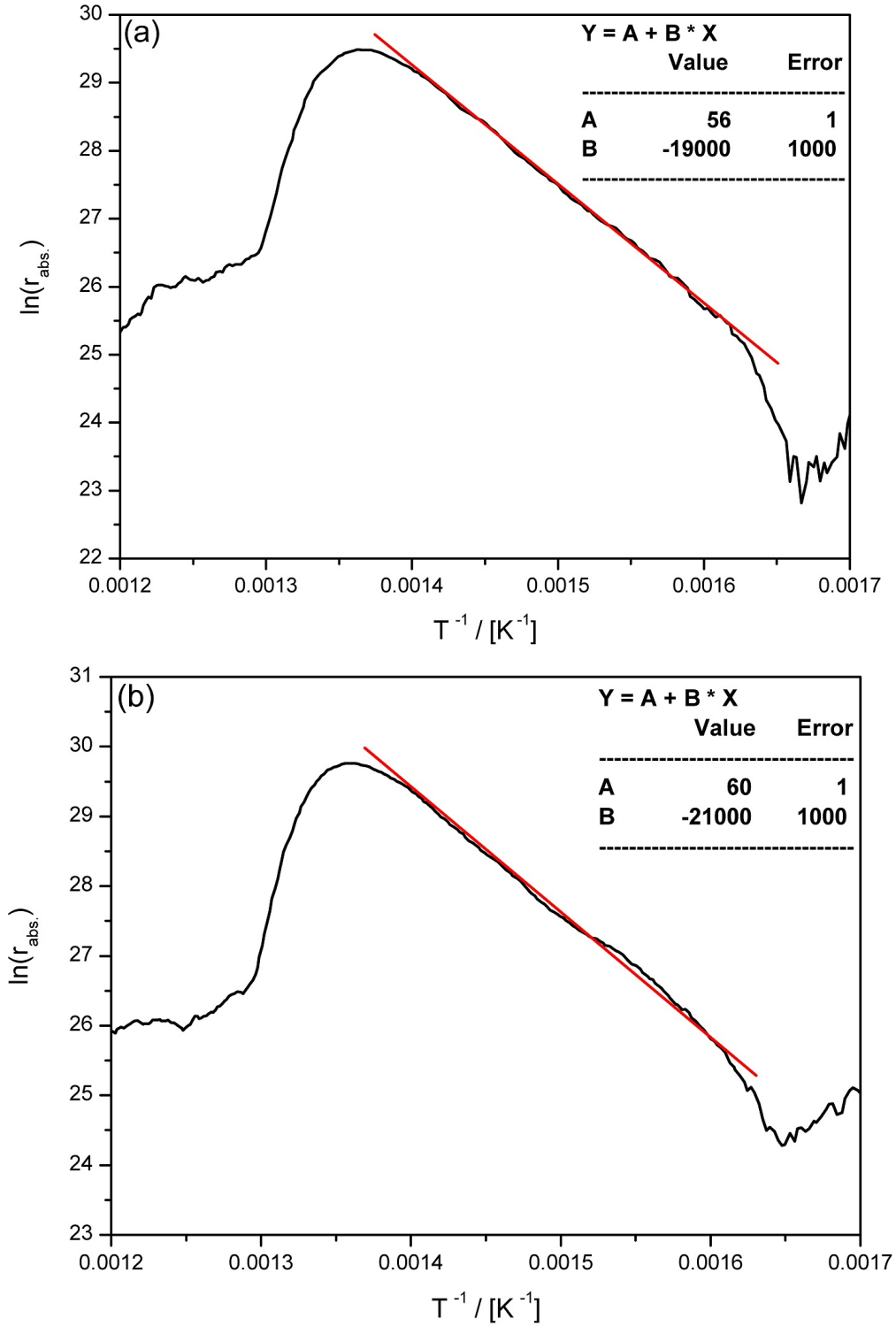

Figure 3.11: The Arrhenius plot of different amounts of 6P on freshly cleaved mica. (a) 20 $\AA$ of 6P (b) 25 $\AA$ of 6P. The slope B can be used to calculate the desorption energy and the intercept A can be used to get the frequency factor.

showed that the temperature measurement has a big influence on the calculation of the frequency factor and explains the much too low values of the frequency factor.

3.2.6 6P adsorbed on the stainless steel plate

In the previous section it was already mentioned that 6P was directly adsorbed on the steel plate of the sample holder. The main reason for this experiment was the temperature measurement. Since mica is a thermal insulator the true surface temperature was not known during the heating process and thus the analyses of the TD-spectra were difficult. A temperature correction was implemented to calculate the true surface temperature, but it turned out that it has a high uncertainty. In order to overcome these problems, 6P was adsorbed on the steel plate. Thus the true surface temperature was known at all times and it was possible to determine the multilayer desorption energy, the pre-exponential factor and the temperature of the multilayer desorption.

In the experiment a 50 $\AA$ thick 6P film was adsorbed on the steel plate at a temperature of 110 K. To assure a low interaction with the residual gas a bake-out was applied, which enabled a pressure of $5 \cdot 10^{-10}$ $Torr$. In order to clean the surface, it was sputtered for 15 minute with Ar^+ ions with an energy of 1.5 keV at a pressure of $4 \cdot 10^{-6}$ $Torr$. Then the steel plate was heated up to 700 K and kept at this temperature for 5 minutes. When the sample cooled down again, one of the tantalum clamps and the steel plate itself were investigated with AES in order to define the initial surface composition. Afterwards the thick 6P film was adsorbed on the steel plate and the tantalum clamps. The 6P covered steel plate and the tantalum clamp were reinvestigated with AES. It was expected that in these spectra only a big carbon peak or at least a high amount of carbon was detected. The sample holder was placed in front of the QMS and heated from 110 to 1000 K in order to record a TD-spectrum of the desorbing 6P molecules. In the end of the experiment two last AE-spectra of the tantalum clamp and the steel plate were made, which should prove that the whole 6P film desorbed during the heating process. In figure 3.12 all three AE-spectra of the tantalum clamp and the steel plate are plotted together. The TD-spectrum of the desorbed 6P film can be seen in figure 3.13.

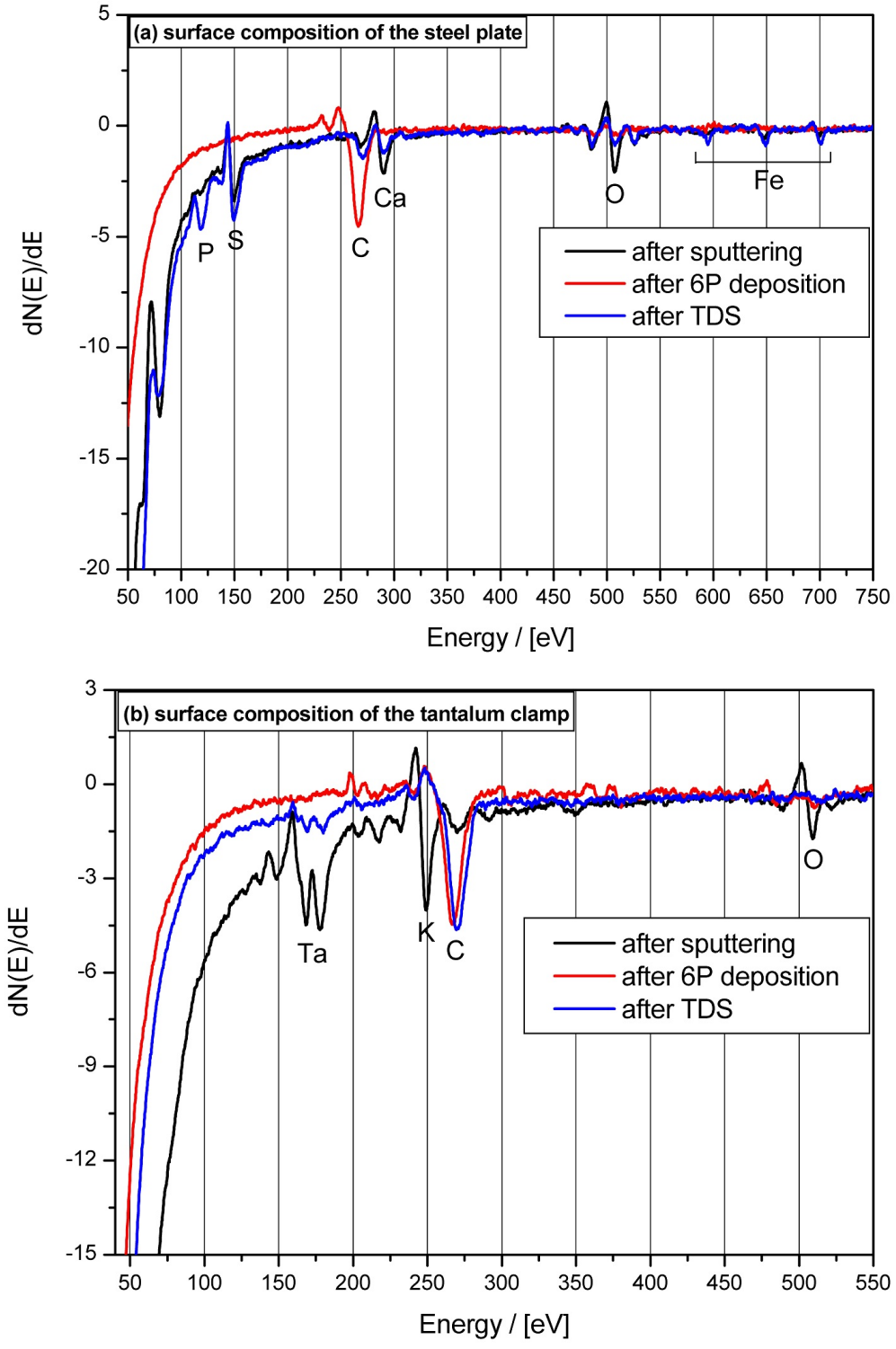

Figure 3.12: The two figures show AE-spectra of (a) the steel plate and (b) the tantalum clamp before (black curve) and after (red curve) the 6P deposition and the heating process (blue curve)

The AE-spectra in figure 3.12(a,b) show the surface composition before (black curve) and after (red curve) the 6P deposition on the tantalum clamp and the steel plate. The blue curves in these figures are the AE-spectra of the tantalum clamp and the steel plate after the heating process.

The AE-spectrum of the steel plate (black curve) shows the typical initial surface composition of iron. One can see the Auger peaks for iron (Fe), calcium (Ca), oxygen (O) and sulphur(S). As expected, the AE-spectrum after the 6P deposition only shows a big carbon peak. The carbon peak is completely gone in the AE-spectrum after the heating process, therefore we can assume that the whole 6P film desorbed. In the last spectrum (blue curve) a new peak at 120 eV was detected, which could be identified as phosphorus that segregated to the surface.

The AE-spectrum of the clamp (black curve) shows the typical peaks for tantalum at 171 and 179 eV and additionally an oxygen and a potassium peak. The potassium peak stems from former measurements with potassium adsorption. The comparison of the AE-spectrum after the 6P deposition (red curve) with the spectrum after the heating process (blue curve) revealed that most of the 6P adsorbed on the clamp also remained there. In principle this would contravene with the assumption that the first peak in the TD-spectra from 6P on mica stems from the tantalum clamps (fig.3.5). Nevertheless the first peak in these spectra definitely belongs to 6P desorbing somewhere from the sample holder and it is most likely that it desorbs from clamps.

Figure 3.13 shows the TD-spectrum that was used for the calculation of the multilayer desorption energy and the pre-exponential factor. Since 6P was directly adsorbed on the sample holder the measured temperature and the true surface temperature are the same. The multilayer desorption of 6P has its peak maximum at $T = 485\ K$, which is approximately the same temperature as for the first peak in figure 3.7. Thus the first peak in the TD-spectrum of 6P on mica stems from the sample holder. An Arrhenius plot of the TD-spectrum of the steel plate was used to calculate the multilayer desorption energy and the pre-exponential factor for the case of the zero order desorption. The method was briefly explained in the previous section and therefore only the results of these calculations are shown, which are in good agreement with literature [28]:

$$A = 83 = ln(\nu) \Rightarrow \nu = 1 \cdot 10^{36}\ molecules/cm^2 s \Rightarrow \nu_0 = 2 \cdot 10^{22}\ s^{-1}$$

$$B = -25600 = -\frac{E_{des}}{R} \Rightarrow E_{des} = 51.2\ kcal/mol = 2.2\ eV$$

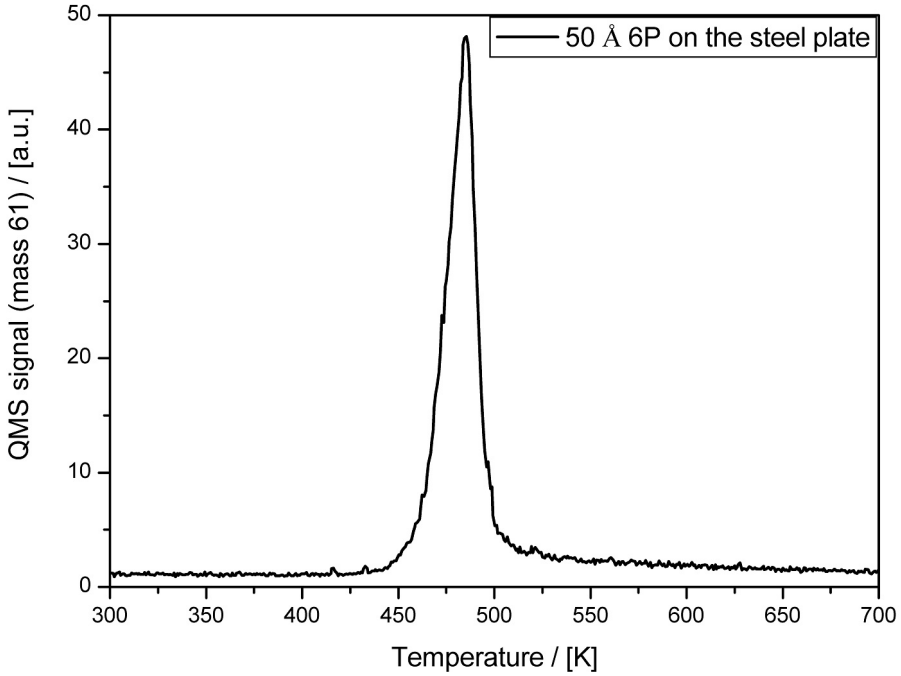

Figure 3.13: TD-spectrum of 50 $\mathring{A}$ 6P desorbed from the steel plate of the sample holder. The measured temperature is the true surface temperature and the temperature of the 6P multilayer desorption has its maximum at $T = 485\ K$. The 6P film was adsorbed at $T = 110\ K$

3.2.7 Sticking coefficient of 6P on freshly cleaved mica

As already explained in chapter 1, the sticking coefficient describes the probability that an impinging particle also adsorbs on the surface. When the probability is unity all particles that hit the surface will be adsorbed as well. In experiments, where different amounts of 6P were deposited, it is important to know if the amount measured by the microbalance correlates with the amount adsorbed on the mica sample. In figure 3.14 the desorbed amount of 6P from the mica sample was plotted as a function of the film

thickness measured with the microbalance. The linear behaviour shown in this figure indicates that all molecules impinging the surface will be adsorbed. Thus the sticking coefficient is approximately one.

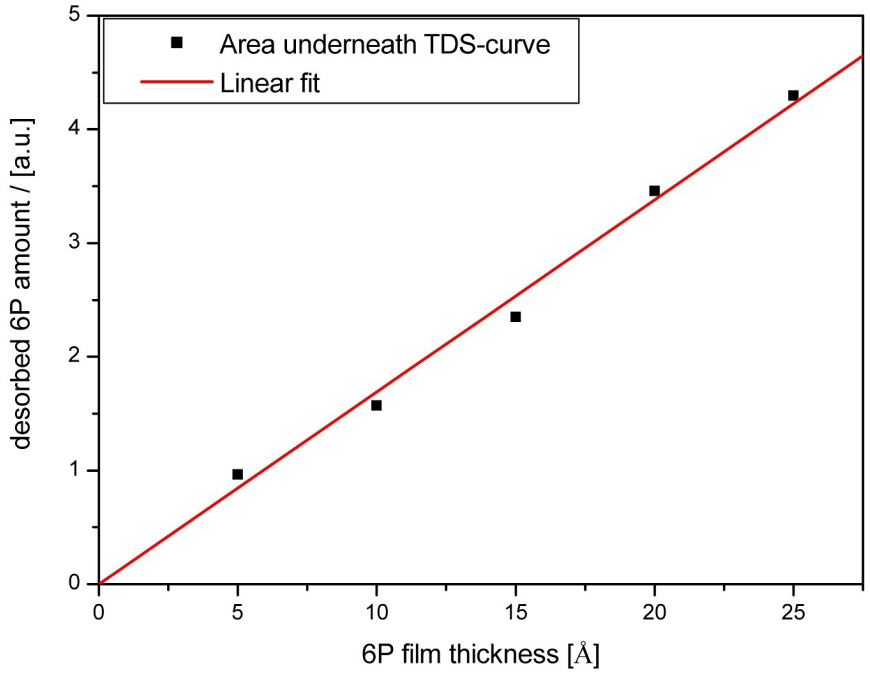

Figure 3.14: Shows the amount of desorbed 6P as a function of the film thickness as obtained by the microbalance. The linear behaviour indicates that all impinging 6P molecules also adsorb.

3.2.8 Preparing a monolayer of 6P on freshly cleaved mica

In the previous sections the 6P adsorption was studied in the multilayer regime. Now only a monolayer of 6P should be adsorbed on the freshly cleaved mica surface. This measurement will be needed later on to compare it with a potassium covered surface (see chapter 3.4). Figure 3.7 shows TD-spectra of 6P films down to a thickness of 5 $\AA$. All of these spectra show desorption of 6P from a multilayer regime, therefore the monolayer regime has a film thickness that is lower than 5 $\AA$. A monolayer consists of flat lying 6P molecules and the Van der Waals dimensions (nm^3) of such a molecule are 2.85x0.35x0.67. This indicates that a layer of flat lying molecules should have a

thickness of about 3 $\AA$.

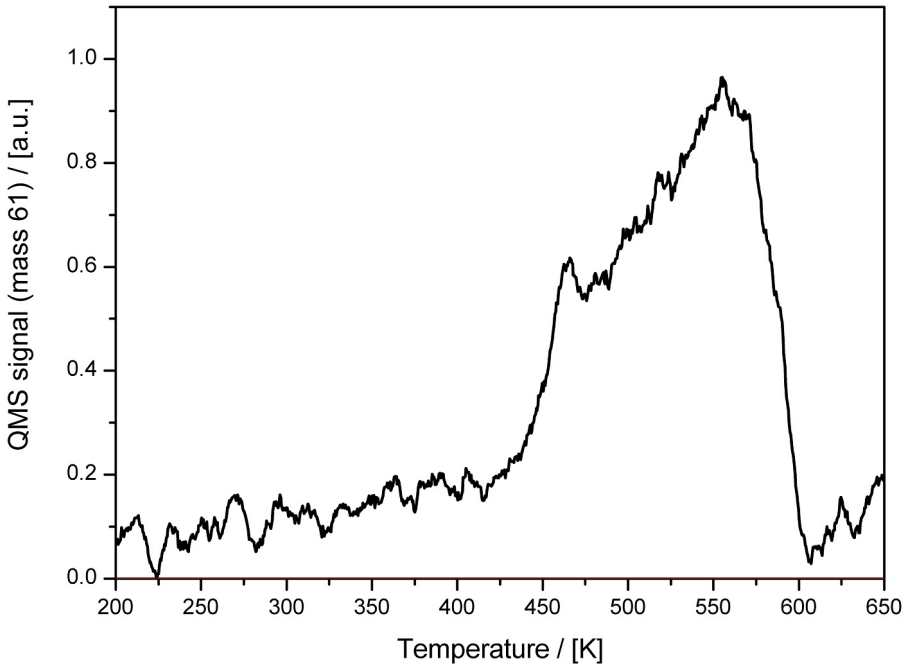

Figure 3.15: Shows the TD-spectrum of a 3 $\AA$ thick 6P film of flat lying 6P molecules. The TD spectrum only consists of one desorption peak at $T = 555\ K$. This peak belongs to 6P desorbing from the monolayer.

In the experiment the mica sample was cooled down to 110 K. Afterwards a 3 $\AA$ thick film was adsorbed on the surface in order to prepare the monolayer. The mica sample was placed in front of the QMS and heated up from 110 K to 1000 K, while the according TD-spectrum was recorded. Figure 3.15 shows this TD-spectrum, which only consists of one peak at a corrected temperature of about $T = 555\ K$. This is the temperature of the monolayer desorption. There is an indication for a multilayer peak at 450 K, which is negligible for our measurements. It turned out that a 3 $\AA$ thick 6P film is approximately one monolayer of lying 6P molecules.

3.3 Adsorption of potassium

The last measurements were only devoted to the adsorption of 6P on freshly cleaved mica. In this section the thin film layer growth of potassium on freshly cleaved mica should be studied. To understand the effects of potassium on the thin film layer growth of 6P, it is necessary to understand the behaviour of adsorbed potassium on a freshly cleaved mica surface. Therefore different amounts of potassium should be deposited on the surface. During the whole experiments pressures in the UHV-region were required, to keep the interactions between potassium and the residual gas low and to guarantee the deposition. Potassium adsorption was always performed at low temperatures (110 K), because the material has a rather low heat of evaporation (19 $kcal/mol$ or 0.8 eV) [33]. Therefore low temperatures were necessary for the preparation of a multilayer.

3.3.1 The SAES Getter deposition source

It is common to use a SAES Getter as an evaporation source for alkali metals. In our case a new holder for the evaporation source was constructed. To keep the construction simple no microbalance and thermo-couple were attached to the SAES Getter. Therefore it was difficult to control the adsorption in terms of constant evaporation rates of the source and amounts of adsorbed material on the surface. Nevertheless, it is necessary to control the adsorption in order to deposit specific amounts of potassium. The QMS, that is placed in an angle of 75° relative to the potassium source, can be used to achieve constant evaporation rates. During each potassium adsorption the QMS is set on the mass of potassium (mass 39) in order to measure the changes of the isotropic concentration of potassium in the chamber (see figure 3.16). This value is proportional to the evaporation rate of potassium. Keeping the signal in-between 1.6 and $1.8 \cdot 10^{-10}$ A guarantees that the evaporation rate is constant.

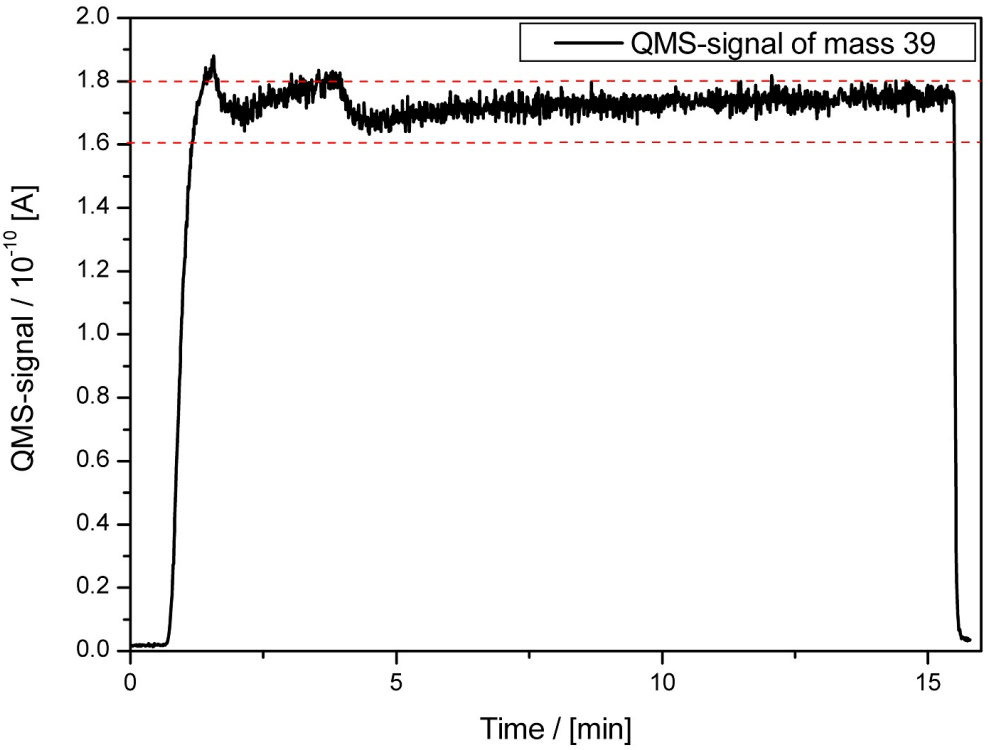

Figure 3.16: Shows the isotropic concentration of potassium when the deposition source is turned on. During the potassium deposition this value is not constant, therefore the heating current must be changed in a way that the QMS-signal remains in between 1.6 and $1.8 \cdot 10^{-10}$ A. This guarantees a constant evaporation rate and reproducible results.

When the deposition source is heated with a certain current (in this case 8 A), potassium starts to evaporate from the source. This can be seen in figure 3.16. The isotropic concentration of potassium in the chamber immediately increases when the source starts to evaporate. At the point where the deposition source is turned off, the isotropic concentration immediately drops down to the initial value. Figure 3.16 shows that the QMS-signal is slightly increasing during a potassium deposition. Therefore the heating current has to be varied during the deposition to keep the QMS-signal constant and to guarantee reproducible results. The changes of the heating current are only in the range of 0.2 A.

The TD-spectra of potassium desorbing from a surface can be used to estimate the

amount of deposited material. In order to get reproducible results the heating current I_{hc} and the QMS-signal I_{QMS} have constant values. The adsorption time t_{ad} is varied to deposit different amounts of potassium. For a high amount of potassium, deposited on a surface, one expects to see a mono- and a multilayer peak in the TD-spectrum. The goal would be to decrease t_{ad}, in order to adsorb only a full monolayer of potassium. Since the number of atoms for one monolayer of potassium on a one square centimetre mica sample is known, this number can be linked to the area underneath the monolayer peak in the TD-spectrum. This could be used as a reference to know the number of desorbing potassium atoms in every TD-spectrum. Unfortunately, there is no sign of a monolayer peak of potassium on mica in any TD-spectrum (see chapter 3.3.5), thus a nickel surface was used as a reference, where it is known that a clear distinctive behaviour for the monolayer and multilayer can be seen [29]. A detailed description of the potassium calibration can be found in chapter A.4.

The adsorption procedure

The only two parameters that can be changed during the deposition are the adsorption time and the heating current. The QMS-signal measures the isotropic concentration of potassium in the chamber and can be varied with the heating current of the SAES Getter. During the deposition the QMS-signal must be constant. For the potassium deposition the following adsorption procedure was implemented:

- The potassium source has no shutter; therefore the sample must be turned away from the source
- Record the QMS-signal (mass 39) of potassium to ensure reproducible results
- Heat up the potassium source by applying an heating current of I_{hc} =6 A (Sometimes a heating current of 8 A was necessary)
- Wait till the QMS-signal reaches a value in-between $I_{QMS} \approx 1.6 - 1.8 \cdot 10^{-10}$ A, by adjusting the heating current properly.
- Turn the sample in front of the potassium source and start taking time
- During the adsorption always keep an eye on the QMS-signal and change the heating current if necessary. (Changes will be in the range of 0.2 A)

- Turn the sample away from the potassium source and turn off the power supply for the potassium source, when the desired adsorption time t_{ad} is reached.

3.3.2 Adsorption of large potassium amounts on mica

As explained before, the adsorption of potassium in the multilayer regime requires low surface temperatures of the mica sample. Therefore the sample holder was cooled down with liquid nitrogen to temperatures of 110 K. Additionally, the adsorption of potassium requires pressures in the low UHV region (see chapter 3.3.7). In the experiments, presented here, a base pressure of $p = 3 \cdot 10^{-10}$ $Torr$ was achieved. For the investigations of the potassium films TD-spectra were recorded. We also tried to record an AE-spectrum of potassium covered mica, but it was impossible due to electric charging of the surface.

At first potassium was adsorbed for 20 minutes with a heating current of 8 A and a QMS-signal in-between $1.6 - 1.8 \cdot 10^{-10}$ A. The heating current of 8 A was necessary, because the source was nearly empty and required higher current for the adsorption. A 2.8 nm thick film of potassium was adsorbed on the mica sample. Afterwards the sample holder was heated up from 110 K to 700 K and the according TD-spectrum was recorded (fig.3.17). The TD-spectrum of a thick potassium film on mica shows two desorption peaks, the first one at 350 K and the second one at 450 K. Since potassium has a low heat of evaporation, the deposited material desorbs close to room temperature. One explanation for the double-peak could be, that potassium desorbs from a multilayer and monolayer. If this would be true, then the first peak at low temperatures belongs to potassium from the multilayer and the second peak at higher temperatures belongs to the monolayer. If the first peak represents the multilayer, it should increase with higher coverages of potassium, whereas the second peak should remain at the same height, because it is already a full monolayer of potassium on the mica sample. In order to understand the two desorption peaks and therefore the behaviour of potassium on the mica sample, bigger and smaller amounts of potassium must be adsorbed on the surface.

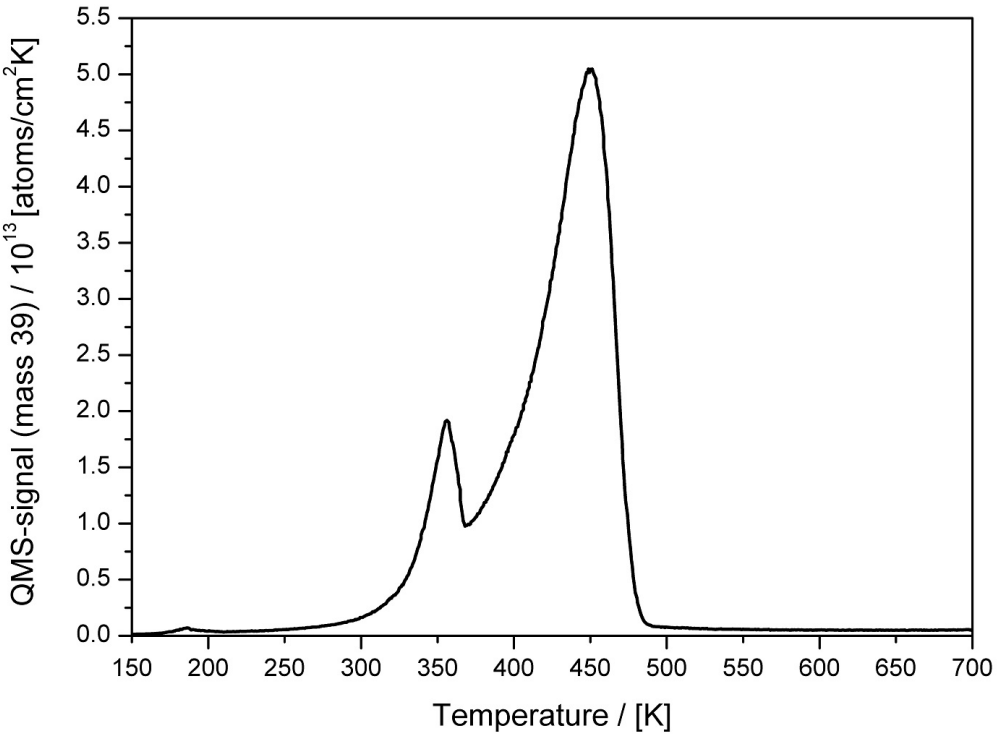

Figure 3.17: A TD-spectrum of a 2.8 nm thick potassium film desorbing from the mica surface. The spectrum shows a double peak, which cannot be explained without further investigations.

In the following experiment potassium was adsorbed for t_{ad} =2, 4, 8, 10, 15 and 30 minutes with a heating current $I_{hc} = 8\ A$ and a QMS-signal in-between $I_{QMS} = 1.6-1.8\cdot10^{-10}\ A$. The prepared potassium films had a thickness of about 0.3 to 3.7 nm. After each deposition the mica sample was placed in front of the QMS and heated up to a temperature of 700 K. The according TD-spectra were recorded and the results of these measurements were plotted together in figure 3.18. These measurements clearly show that the two desorption peaks of potassium do not represent desorption from the multi- and monolayer. Both peaks increase linearly along their leading edge and the peak maximum shifts to higher temperatures for higher coverages. This indicates that both peaks have the behaviour of a zero order desorption and therefore represent potassium desorbing from the multilayer. A monolayer peak cannot be seen in these TD-spectra.

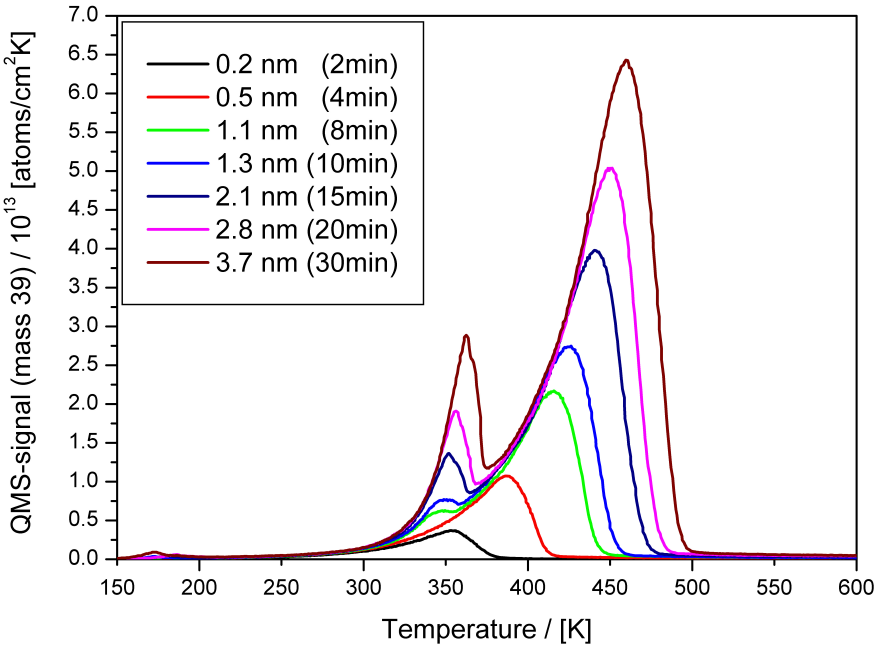

Figure 3.18: The TD-spectra of different amounts of potassium desorbing from the mica sample are plotted together. The spectra clearly show that the double peak does not stem from a mono- and multilayer.

The measurements above clearly show, that the double peak stems from potassium desorbing from the multilayer. The peak at 350 K appears after an adsorption of a 1.1 nm thick potassium film and is always only about 10 percent of the second peak. One explanation for this behaviour can be, that one peak stems from potassium desorbing from the tantalum clamps and the other one from the mica sample itself. This makes sense if one keeps in mind that mica is a thermal insulator. Thus the first peak at 350 K belongs to potassium desorbing from the tantalum clamps, because the clamps are in good thermal conduction with the sample holder and therefore the surface temperature matches the measured temperature. The area of the clamps is much smaller than the area of the mica sample. This explains why the first peak is always smaller than the second peak and only appears above a certain coverage. When the temperature of the sample holder is already at 450 K, the surface temperature of the mica sample has

only reached 350 K and therefore the second peak represents the multilayer desorption from the mica surface. To prove this assumption, potassium was adsorbed directly on the sample holder.

3.3.3 Adsorption of potassium on the sample holder

In order to run this experiment, the sample holder was installed without a mica sample. Therefore potassium was directly adsorbed on the steel plate. A bake-out was performed before the actual measurements to reach the required pressure of $3 \cdot 10^{-10}$ $Torr$. The deposition source was changed as well and therefore only a heating current of 6 A was necessary. The QMS-signal during the adsorption was kept at the usual value. In the experiment the sample holder was again cooled down to 110 K. The expected result is a TD-spectrum of potassium that only shows a single peak with a maximum at $T = 350$ K (fig. 3.19).

Before potassium was deposited on the sample holder, the steel plate and the tantalum clamps were cleaned with the sputter gun. The surface was bombarded with Ar^+ ions with an energy of 1.5 keV at a pressure of $7 \cdot 10^{-6}$ $Torr$. Subsequently the sample holder was heated up to 700 K and kept at this temperature for 5 minutes. To characterise the initial surface composition both, the steel plate and one of the tantalum clamps were investigated with AES. The according AE-spectra can be seen in figure 3.20 (black curve). These spectra show the initial surface composition and characteristic peaks of the materials. In the case of the steel plate the Auger-peaks of phosphorus (P; 120 eV), sulphur (S; 150 eV), calcium (Ca; 290 eV), oxygen (O; 510 eV) and typical peaks for iron (Fe; 594, 650 and 701 eV) can be seen. The AE-spectrum of the clamp showed the typical peaks for tantalum (Ta; 169 and 179 eV) and a carbon-peak at 270 eV. There are small peaks at 205 and 215 eV, which indicate the presence of argon, although the sample holder was heated after the sputtering.

After the characterisation of the initial surface composition a 2.9 nm thick film of potassium was adsorbed on the steel plate and the tantalum clamps. After the deposition, the sample holder was placed in front of the AES to record spectra of the clamp and the steel plate. The according AE-spectra can also be seen in figure 3.20

(red curve) together with the initial surface composition. The AE-spectra revealed that indeed a thick film of potassium was adsorbed on the surface, because in both cases only an Auger peak for potassium (K; 248 eV) can be seen.

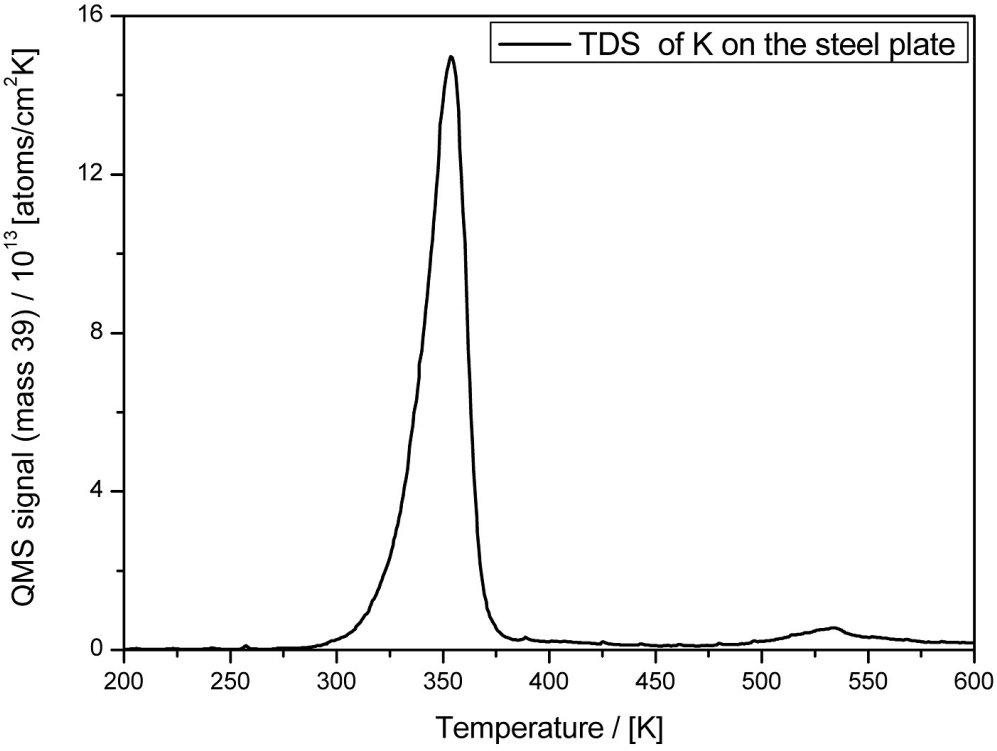

Figure 3.19: TD-spectrum of potassium adsorbed for 20 minutes onto the steel plate. The spectrum shows the multilayer peak of potassium at 350 K and a monolayer peak at 535 K. The sample was heated up to 1000 K but there is no desorption of potassium above 550 K, therefore the TD-spectrum is only displayed up to 600 K.

At the end of the experiment the sample holder was placed in front of the QMS and heated from 110 K up to 1000 K. The according TD-spectrum was recorded and can be seen in figure 3.19. As expected, the multilayer peak of potassium has its maximum at a temperature of $T = 350$ K. There is also no evidence of the double peak in this spectrum. This underpins that the second peak at 450 K in figure 3.17 stems from potassium desorbing from the mica sample and that the higher desorption temperature can be related to the fact that mica is a thermal insulator. In the TD-spectrum

in figure 3.19 a second desorption peak at $T = 535\ K$ appears. The peak represents potassium desorbing from the monolayer on the steel plate. This result corresponds with experiments, where potassium was adsorbed on an iron plate at room temperature [33]. In that case potassium only formed a monolayer on the iron surface, because the bulk potassium has a too low heat of evaporation. The temperature of the peak maximum for the monolayer desorption in these experiments was $T = 550\ K$.

After potassium was removed by heating the surface, the steel plate and the tantalum clamp were again investigated with AES. The according AE-spectra can be seen in figure 3.20 (blue curve). The investigation showed that during the heating process nearly all the potassium desorbed from both, the tantalum clamp and the steel plate. There is no evidence of a potassium peak in the AE-spectra after the heating, but the typical features for tantalum and iron can be seen again. Thus, all the potassium adsorbed on the surface, desorbs when the surface is heated up to at least 600 K.

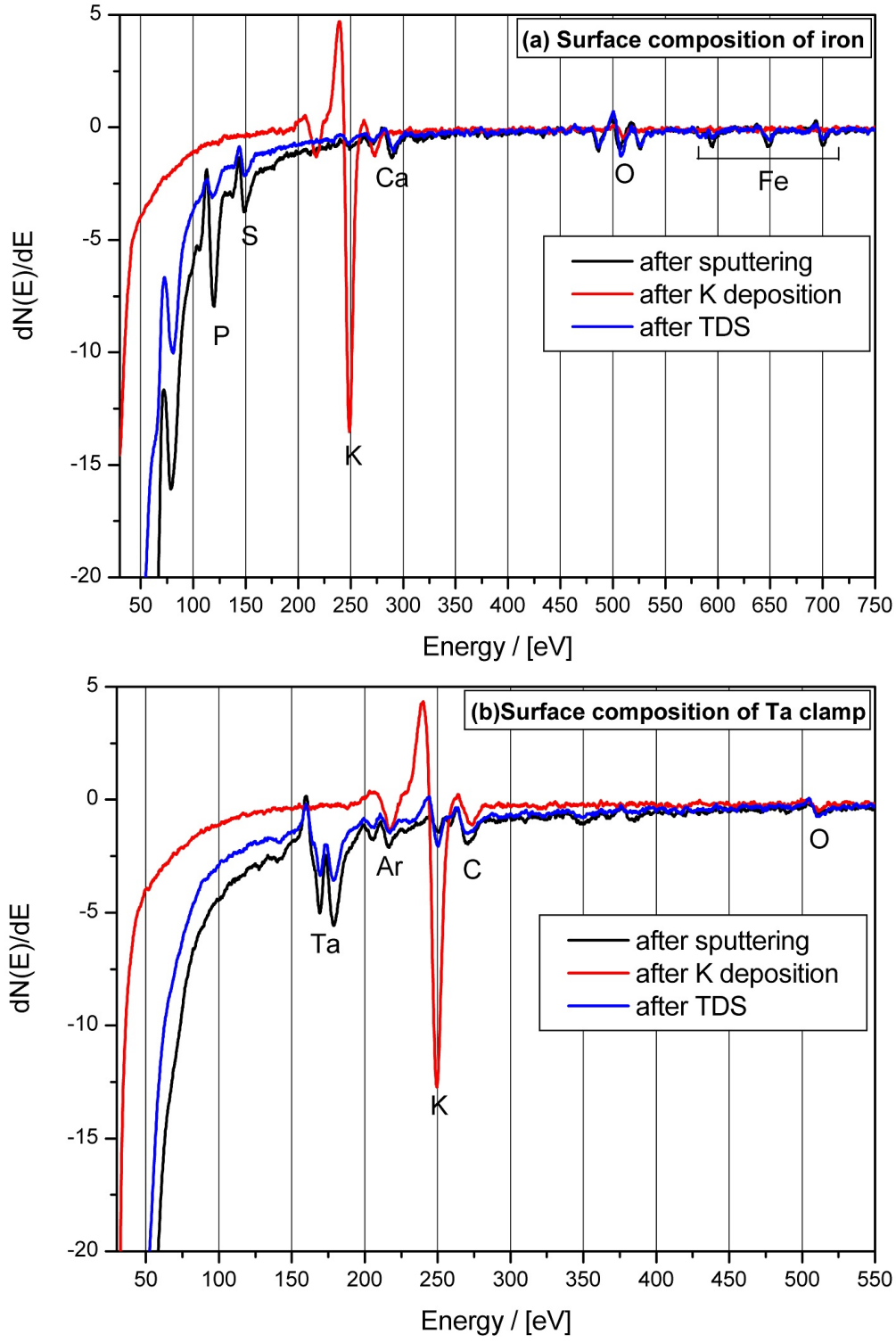

Figure 3.20: The two figures show AE-spectra of the steel plate (a) and the tantalum clamp before (black curve) and after (red curve) the potassium deposition and the heating process (blue curve)

3.3.4 Desorption energy of potassium in the multilayer

Overall, potassium formed a multilayer on three different metals, the Ta-clamps, the steel plate and the nickel surface. The TD-spectra of potassium desorbing from the mica sample show a double peak, which can be related to potassium desorbing from the clamps and the mica sample itself. In this case, only the desorption energy for tantalum was calculated. The spectra of potassium desorbing from tantalum and the steel plate can be seen in the previous sections. The TD-spectra of potassium desorbing from nickel can be seen in chapter A.4. In all three cases the multilayer desorption takes place at 350 K and belongs to a zero order of desorption. Therefore the desorption energy of the multilayer peak can be calculated with the same method that was used in the case of 6P. The Arrhenius plots with the according linear fits of all three cases can be seen in figure 3.21.

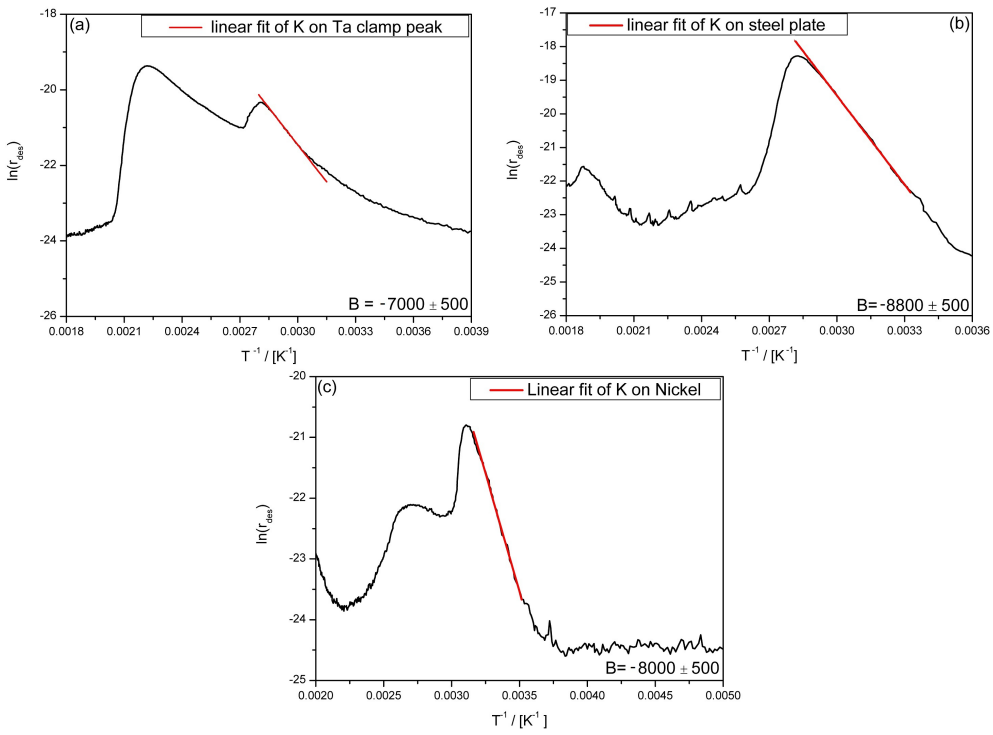

Figure 3.21: Arrhenius plots of potassium desorbing from (a) tantalum, (b) the steel plate and (c) a nickel surface. The desorption energy for the multilayer peaks were calculated by measuring the slope B of the linear fits.

The slope B of the linear fits can be used to calculate the desorption energy of the multilayer. The results of these calculations are shown here:

Multilayer desorption energy:

- Tantalum clamp: $B = -7000 \rightarrow E_{des} = 0.60 \pm 0.04\ eV$
- Nickel sample: $B = -8000 \rightarrow E_{des} = 0.69 \pm 0.04\ eV$
- Steel sample: $B = -8800 \rightarrow E_{des} = 0.76 \pm 0.04\ eV$

As already mentioned before, the heat of evaporation of potassium is about 0.8 eV. According to this value the measured desorption energies are in good agreement. The low value of 0.6 eV desorption energy of potassium on the tantalum clamps can probably be related to the fact that the peak in the TD-spectrum is an overlap of potassium desorbing from the clamps and the mica sample. The more or less best value for the desorption energy was calculated for the steel plate.

3.3.5 Adsorption of small potassium amounts on mica

In the previous section TD-spectra of potassium in the multilayer regime have been studied. In this region there was no sign of a monolayer peak. Now smaller amounts of potassium were deposited on mica, to check if one can see a monolayer desorption in these TD-spectra. In the experiment the QMS-signal was in between 1.6 and $1.8 \cdot 10^{-10}$ A, the heating current was always about 6 A and the base pressure during the experiment was at $1.3 \cdot 10^{-9}$ $Torr$. The sample was covered with different amounts of potassium, which were removed by heating the sample. Potassium was deposited for 0.5, 1, 1.5, 2, 4, 6 and 8 minutes onto the mica sample, leading to film thicknesses of 0.04 to 0.57 nm. After each adsorption the sample holder was placed in front of the QMS, heated up from 110 to 700 K and the according TD-spectrum was recorded. To have a better overview of the results, all the spectra were plotted together in figure 3.22.

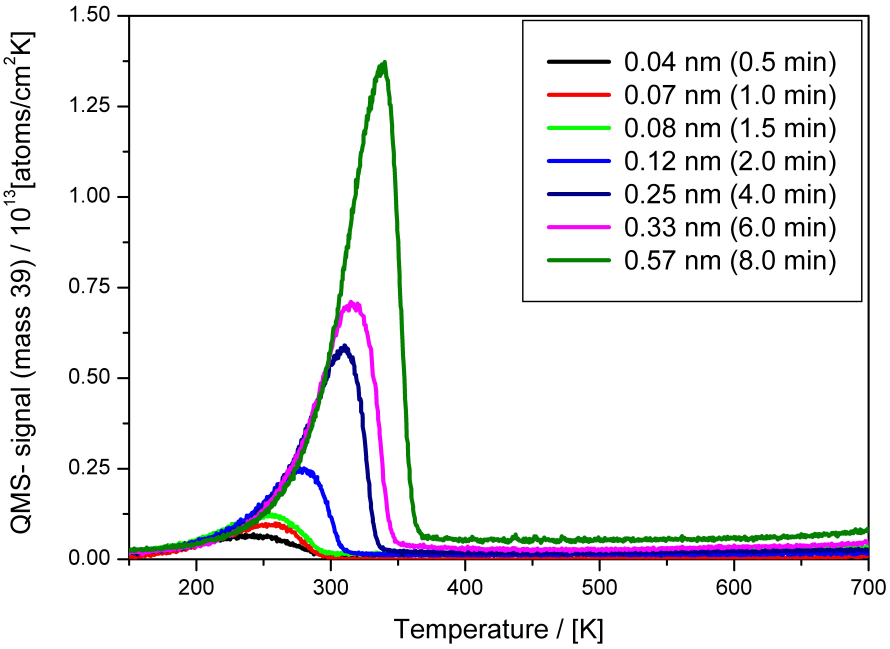

Figure 3.22: Shows the TD-spectra of potassium desorbing from the mica sample. Different films with different thicknesses have been deposited onto the sample.

All the TD-spectra in this figure only show a single peak for the multilayer desorption of potassium from mica. The absence of the double peak can be dedicated to the amount of adsorbed material. Due to the smaller amounts desorption of potassium from the tantalum clamps cannot be detected with the QMS. Although the potassium coverage was small there is no sign of a monolayer desorption in the TD-spectra. This indicates that some potassium remains on freshly cleaved mica after the heating process and forms a potassium covered surface. Thus the adsorption/desorption cycles of the very first potassium depositions on freshly cleaved mica have to be investigated in more detail.

3.3.6 Ad-/Desorption cycles of potassium on freshly cleaved mica

The latter experiments indicated that some potassium remains on the surface. Therefore the adsorption/desorption behaviour of potassium on freshly cleaved mica was studied in more detail. For this purpose a new air cleaved mica sample was installed. To guarantee low interactions with the residual gas a bake-out was applied, which enabled pressures in the range of 10^{-10} $Torr$. The initial surface composition of the freshly cleaved mica was recorded with AES.

An about 1.3 nm thick potassium film was deposited on freshly cleaved mica at a surface temperature of 110 K. The heating current of the SAES Getter was 8 A and the QMS-signal (I_{QMS}) was in-between $1.6 - 1.8 \cdot 10^{-10}$ A. Subsequent heating from 110 K to 1000 K leads to potassium desorption. The according TD-spectrum was recorded with the QMS. In addition, an AE-spectrum was recorded after the TDS. This procedure was repeated three times.

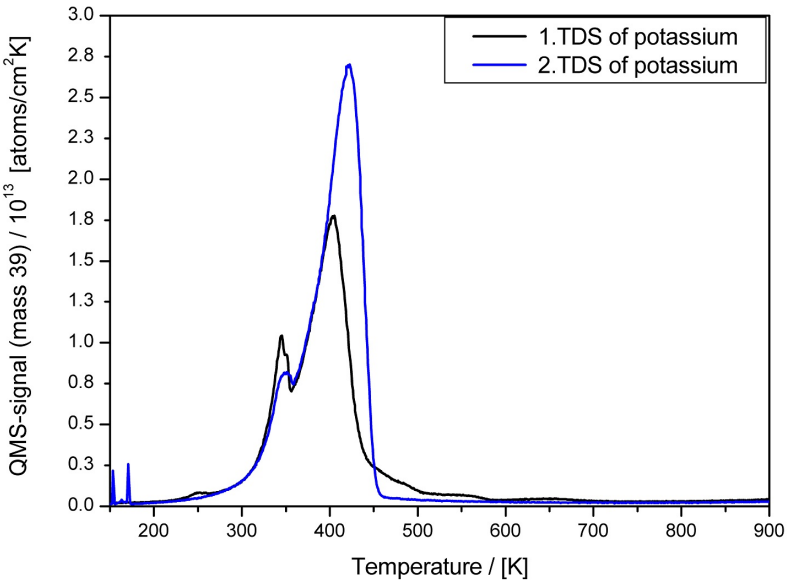

Figure 3.23: Shows the TD-spectra after the first and second potassium deposition (1.3 nm). The second TD-spectrum has a higher multilayer desorption peak which means that more potassium comes off the surface.

In figure 3.23 the TD-spectra of the first and second potassium deposition are plotted together. Both spectra show potassium desorption, however, some part of deposited potassium remains on the surface after the first adsorption/desorption cycle.

Figure 3.24 shows the TD-spectra of the second and third potassium deposition. These spectra have a similar shape, which leads to the conclusion that now the same amount of potassium desorbs from the mica surface. This indicates that for the second and third cycle, all potassium deposited also desorbs during the heating process and that the first adsorption/desorption cycle formed a saturation potassium coverage which is stable up to 1000 K.

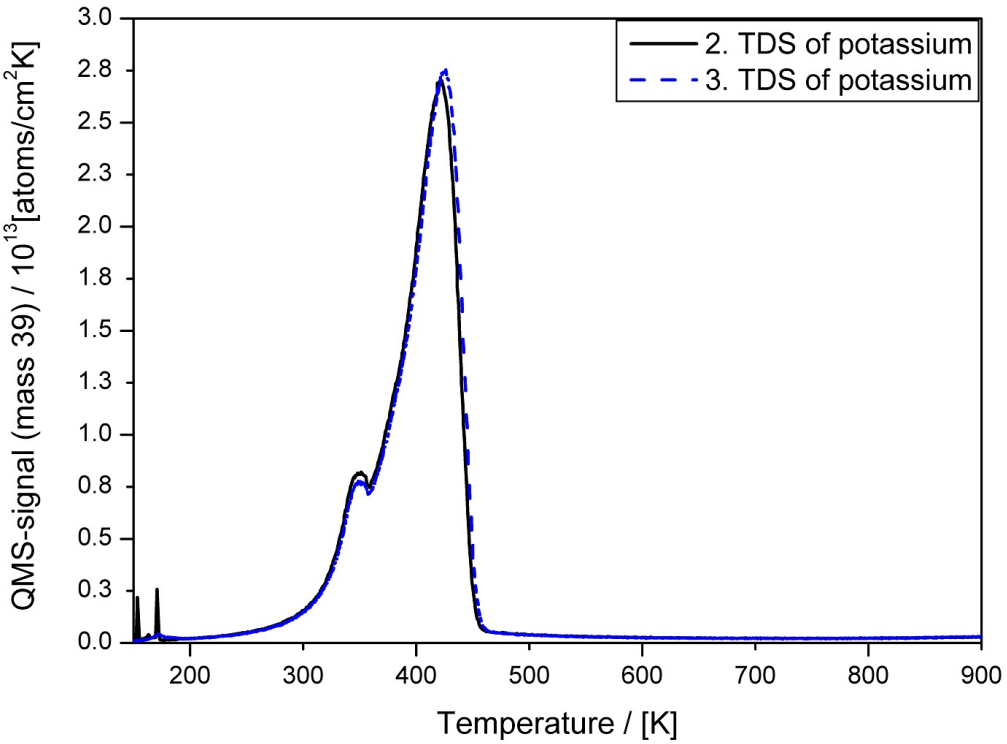

Figure 3.24: The TD-spectra of the second and third potassium deposition on the mica sample. The TD-spectra have the same shape, indicating that in both cases all potassium deposited also desorbs.

In figure 3.25 the AE-spectra after the first and third adsorption/desorption cycle

are plotted together with the AE-spectrum of freshly cleaved mica. In this figure only the Auger peak of potassium is depicted. The comparison of the potassium peak of freshly cleaved mica (half monolayer) with the Auger peak after the first cycle shows that the peak height has doubled after this procedure, indicating that indeed the saturation layer is a full layer of potassium. The Auger peak after the third cycle is similar to the peak of the second cycle. Thus the full monolayer of potassium is stable up to 1000 K and all subsequent deposited potassium desorbs during the heating process.

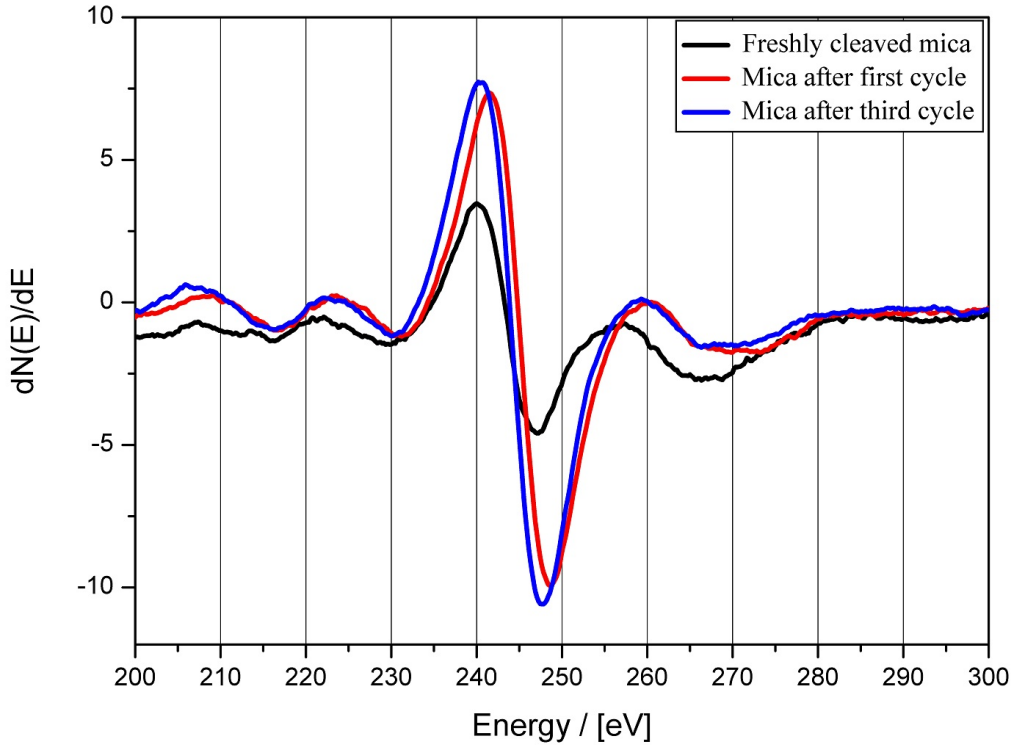

Figure 3.25: Shows the Auger peak of potassium on freshly cleaved mica and after the first and third adsorption/desorption cycle. The potassium peak after the first cycle has doubled in height and did not change anymore after the third cycle.

The experiments clearly show that the first adsorption/desorption cycle leads to the formation of one monolayer potassium on mica. Note that the formation of a saturation coverage only occurs after the first cycle if a proper amount of potassium is

deposited on freshly cleaved mica. Otherwise the formation of a saturation coverage would require more cycles. The effect of potassium remaining on the surface will be used later on to prepare a well defined potassium covered mica sample.

3.3.7 Influence of residual gas on potassium adsorption

As already mentioned before, potassium reacts with the residual gas in the chamber. To keep this interaction low a bake-out has to be performed to reach a pressure in the low UHV region. In the experiments explained before the pressure was always in between $3 \cdot 10^{-10}$ and $3 \cdot 10^{-9}$ $Torr$. A too high pressure causes reactions of potassium with the residual gas during the deposition. These reactions can affect the adsorption of potassium.

In this section the effects of a higher base pressure during the adsorption process should be studied. In order to do this, the pressure can be increased by opening a dosing valve that is conducted to air. At the beginning of the experiment the pressure was at $2 \cdot 10^{-9}$ $Torr$. At first potassium was adsorbed for 8 minutes with the usual settings for the QMS-signal and the heating current, leading to a film thickness of 0.78 nm. After the adsorption the sample was placed in front of the QMS to record a TD-spectrum. Subsequently the pressure was increased to $2 \cdot 10^{-8}$ $Torr$ and again potassium was adsorbed for 8 minutes. After the according TD-spectrum was recorded the pressure was increased to $2 \cdot 10^{-7}$ $Torr$ to adsorb potassium for another 8 minutes. When the last TD-spectrum was recorded, the dosing valve was closed and the pressure decreased to its initial value. In all three TD-spectra the mica sample was heated up from 110 to 900 K. The TD-spectra of these measurements are plotted together in figure 3.26. To be able to plot all three TD-spectra in one figure the desorption rate r_{des} is given as $ln(r_{des})$.

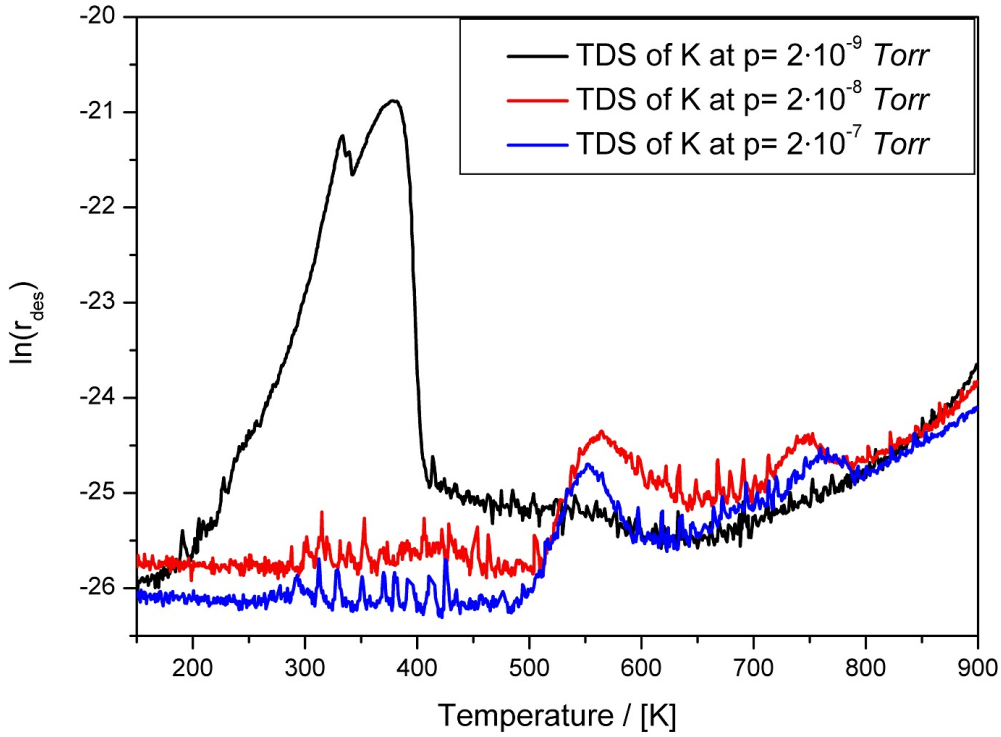

Figure 3.26: Three TD-spectra of potassium desorbing from mica ($t_{ad} = 8$ min). The three measurements were done at the pressures of $2 \cdot 10^{-9}$, $2 \cdot 10^{-8}$ and $2 \cdot 10^{-7}$ $Torr$.

Figure 3.26 shows that too high base pressures during the adsorption process have a big influence on the potassium deposition. At a pressure of 10^{-9} $Torr$ potassium forms a multilayer on the mica surface, which can be seen in the according TD-spectrum. At a pressure of 10^{-8} and 10^{-7} $Torr$ potassium that evaporates from the SAES Getter interacts with the residual gas. Therefore no metallic multilayer of potassium is formed on the surface, but there are some potassium compounds (KO_x, KOH) that are bonded strongly to the surface and desorb at higher temperatures. It has to be mentioned, that there are some measurements at pressures of 10^{-8} $Torr$, where it was possible to construct a multilayer but this pressure range should be avoided because the residual gas clearly affects the adsorption of potassium. The results underpin that UHV conditions are necessary for the potassium deposition.

The residual gas affects the firm potassium coverage

As mentioned above, the potassium adsorption was always performed under UHV conditions. The pressure was usually in between $3 \cdot 10^{-10}$ and $3 \cdot 10^{-9}$ $Torr$, but it turned out that already a pressure in the range of 10^{-9} $Torr$ has effects on the formation of the firm potassium layer. At a pressure in the range of 10^{-10} $Torr$ the half monolayer of potassium on freshly cleaved mica is filled up to a full monolayer, that cannot be removed during the heating process. Therefore after the first adsorption/desorption-cycle the potassium peak in the AE-spectrum is twice as high as in the AE-spectrum of freshly cleaved mica. When the deposition is performed at a base pressure in the range of 10^{-9} $Torr$, more potassium remains on the surface after the heating process. In this case the potassium peak in the AE-spectrum of potassium covered mica is five times as high as in the AE-spectrum of freshly cleaved mica.

Table 3.1: Sample number Nr, base pressure p, potassium peak height of freshly cleaved mica K_1, potassium peak height of potassium covered mica K_2 and oxygen peak height of the freshly cleaved mica O_1

Nr	$p/Torr$	$K_1/a.u.$	$K_2/a.u.$	$O_1/a.u.$	$\frac{K_1}{O_1}$	$\frac{K_2}{K_1}$
1	10^{-10}	8.1	17.2	8.6	0.94	2.1
2	10^{-10}	5.9	16.1	6.3	0.94	2.7
3	10^{-9}	4.6	23	4.3	1.07	5.0
4	10^{-9}	5.7	25.4	4.9	1.16	4.5
5	10^{-8}	2.3	11.1	2.3	1.00	4.8

Table 3.1 compares the AE-spectra of five different freshly cleaved mica samples with the AE-spectra of the according potassium covered mica samples. In the case of two mica samples the base pressure during the potassium deposition was in the range of 10^{-10} $Torr$, for two other samples the base pressure was in the range 10^{-9} $Torr$ and for one sample the base pressure was in the range of 10^{-8} $Torr$. The AE-spectra were compared in terms of the ratio of potassium peak heights on freshly cleaved and potassium covered mica. The ratio of the potassium and oxygen peaks were determined for all freshly cleaved mica samples.

The value of the K_1/O_1 ratio of freshly cleaved mica is always about 1.1 ± 0.1. Thus, the initial surface composition for all five mica samples is the same. Each freshly cleaved mica sample has a half monolayer of potassium on its surface. When the potassium deposition is performed in a good vacuum (10^{-10} $Torr$), the interaction of potassium with the residual gas is negligible. The potassium layer of mica is filled up to a full layer and the K_2/K_1 ratio has a value of 2.1 to 2.7. If, however, the base pressure during the deposition is in the range of 10^{-9} $Torr$ or higher, then the interaction of potassium and the residual gas comes into play and more potassium remains on the surface. The K_2/K_1 ratio has then a value of 4.5 to 5. Nevertheless, both potassium films are strongly bonded to the surface and cannot be removed during the heating process, but all potassium above this layer will desorb during the heating process.

Figure 3.27 shows the AE-spectra of two of these mica samples. In figure 3.27(a) one can see the AE-spectra of the freshly cleaved and potassium covered mica surface, where the deposition was performed at a pressure in the range of 10^{-10} $Torr$. In this case the potassium peak has increased and is twice as high as the initial peak. One can also see that the oxygen peak of the potassium covered mica surface has decreased, because now a layer of potassium is on top of the surface. In figure 3.27(b) one can see the AE-spectra of the freshly cleaved and potassium covered mica surface, where the deposition was performed at a pressure in the range of 10^{-9} $Torr$. This time the potassium peak is 4.5 times higher than the initial peak, but the oxygen peak can still be seen and has not decreased. This can be related to the fact that potassium has reacted with the residual gas and formed potassium compounds, like KO_x or KOH, that are strongly bonded to the surface.

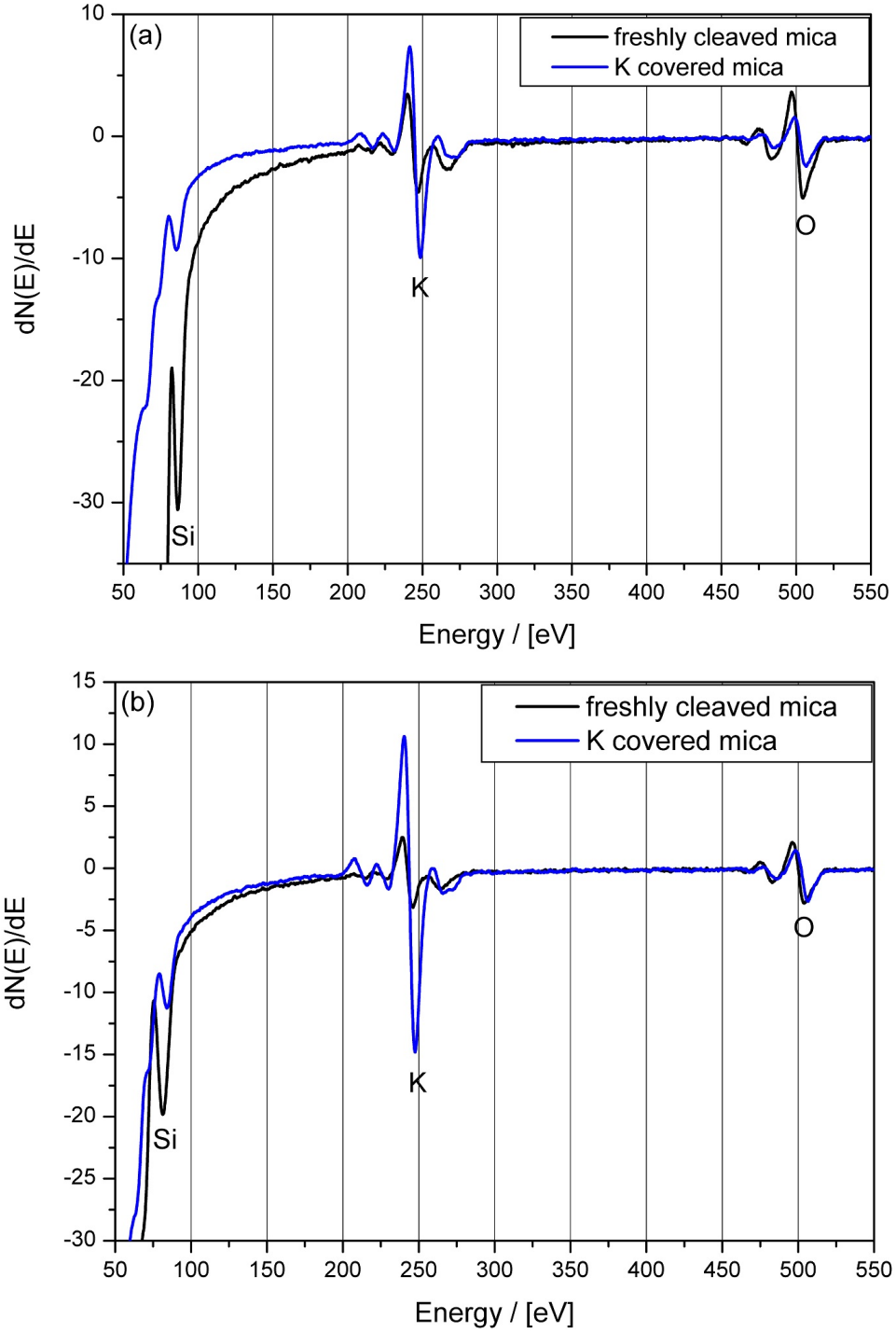

Figure 3.27: Shows the AE-spectra of freshly cleaved and potassium covered mica samples. The potassium deposition was performed at a pressure of (a) 10^{-10} $Torr$ and (b) 10^{-9} $Torr$. The higher pressure causes reactions of potassium with the residual gas that leads to the formation potassium compounds, like KO_x or KOH.

3.4 Adsorption of 6P on potassium covered mica

Up to this point only the single adsorption of 6P or potassium on freshly cleaved mica has been studied. The results of these investigations are now being used to study the effects of pre-adsorbed potassium on the thin film layer growth of 6P on a mica sample. On freshly cleaved mica 6P forms a wetting layer of lying 6P molecules with needle-like islands composed of lying 6P molecules on the top. The measurements presented in this section shall show that a pre-adsorbed potassium layer leads to changes in the layer growth of 6P, like dewetting and the formation of dendritic islands of standing 6P molecules.

3.4.1 Adsorption of potassium and 6P

In order to study the effects of potassium on the layer growth of 6P, a new freshly cleaved mica sample was installed. The measurements in chapter 3.3.7 showed that pressures lower or in the range of 10^{-9} $Torr$ are necessary for the potassium deposition. Therefore a bake-out was performed before the actual measurements, where a base pressure of $2 \cdot 10^{-9}$ $Torr$ was achieved. A pressure in this range causes already some interactions of potassium with the residual gas that have effects on the formation of the firm potassium layer (see chapter 3.3.7). Nevertheless, this pressure range was used in the experiments, because it is enough to guarantee a potassium film on top of the mica surface that cannot be removed during a heating process.

At first, an AE-spectrum of the freshly cleaved mica surface was recorded, which can be seen in figure 3.28. One can see a usual AE-spectrum of a mica sample, which consists of silicon (Si, 90 eV), potassium (K, 249 eV), carbon (C, 272 eV) and oxygen (O, 510 eV). The aluminum peak at 60 eV was not detected in this spectrum. The potassium to oxygen ratio is about 1.2. This is an indication that always about the same amount, i.e. half a potassium layer, remains on the surface of freshly cleaved mica. The AE-spectrum guarantees that the mica sample is in the usual state at the beginning of the experiment

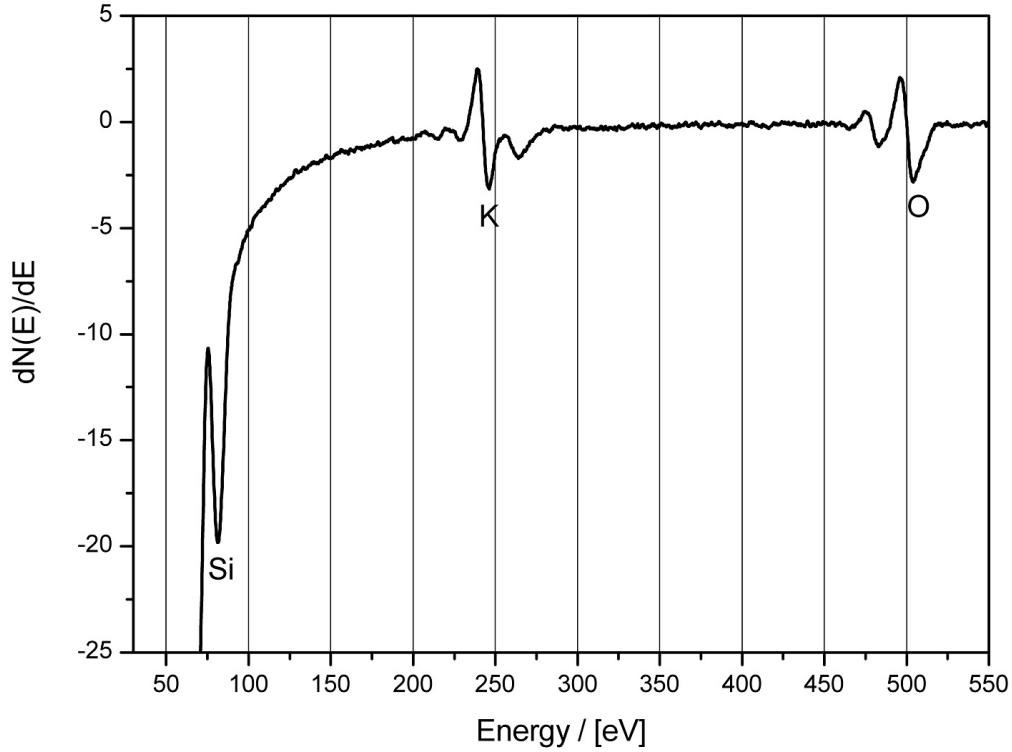

Figure 3.28: An AE-spectrum of the freshly cleaved mica sample. The surface consists of silicon, potassium, carbon and oxygen.

Before the actual experiment was started, a TD-spectrum of a full monolayer 6P on freshly cleaved mica was recorded, because later on it will be used as a reference. In order to prepare this monolayer of 6P, a 3 $\AA$ thick 6P film was adsorbed on freshly cleaved mica (see chapter 3.2.8). Afterwards the sample was placed in front of the QMS and heated up from 110 K to 1000 K. The according TD-spectrum can be seen in figure 3.29. In the spectrum one can see the monolayer peak of 6P at a corrected temperature of 570 K, as well as an indication of the multilayer peak at around 485 K.

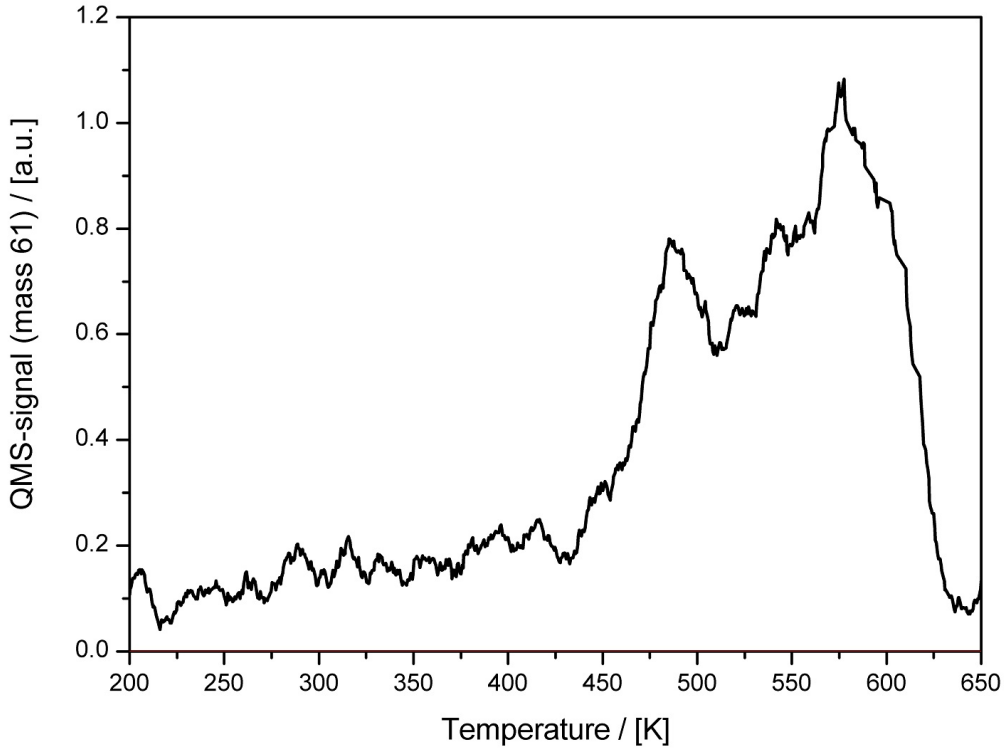

Figure 3.29: The TD-spectrum of 3 $\AA$ 6P desorbing from freshly cleaved mica. 6P was adsorbed at a surface temperature of 110 K. The TD-spectrum is only displayed from 200-650 K, because there are no features outside this region.

This TD-spectrum will be used as a reference to compare it with a TD-spectrum of 3 $\AA$ 6P desorbing from a potassium covered mica surface. The pre-adsorbed potassium is expected to lead to dewetting and the formation of islands of standing 6P molecules. When this happens, one expects a TD-spectrum (for 3 $\AA$ 6P) that consist of one desorption peak at lower temperature, than the monolayer peak of 6P on freshly cleaved mica. There also should be no sign of a monolayer peak at $T = 570$ K, because this would represent the existence the wetting layer on the potassium covered mica.

Potassium deposition

The fact that potassium remains on the surface and forms a firm potassium layer that cannot be removed by heating can be used to prepare potassium covered mica (see chapter 3.3.5). Although, as it was already pointed out, the experiments require UHV conditions these experiments have been done in the range of 10^{-9} $Torr$, due to experimental reasons. In this case still a non negligible interaction between the evaporated potassium and the residual gas (see chapter 3.3.7) takes place, leading to more than the half monolayer of potassium. This is due to some potassium compounds (KO_x, KOH) bonded to the surface.

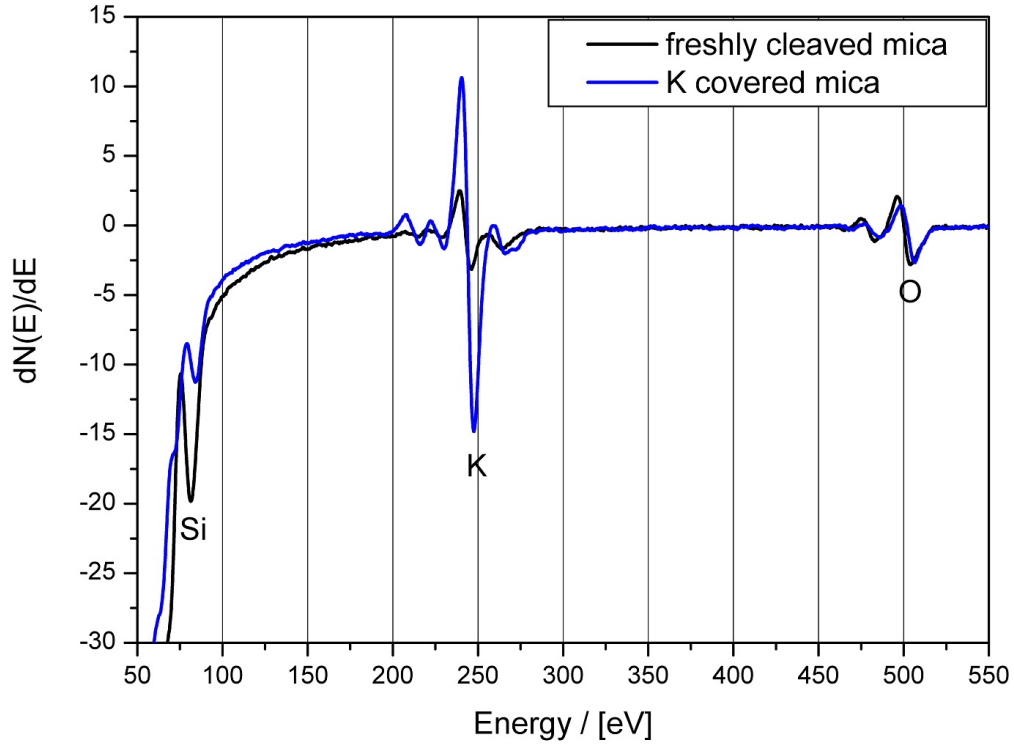

Figure 3.30: AE-spectrum of a freshly cleaved (black curve) and a potassium covered (blue curve) mica sample

The mica sample was cooled down with liquid nitrogen to a temperature of 110 K. A 3.5 nm thick potassium film was deposited on the sample. After adsorption the mica sample was heated up from 110 to 1000 K. This first ad- and desorption

cycle already leads to a saturation potassium coverage that is stable up to 1000 K. An AE-spectrum of this potassium covered surface was recorded and plotted together with the AE-spectrum of freshly cleaved mica. In figure 3.30 one can see that after the first ad- and desorption the amount of potassium on the surface has increased. The potassium peak is now about five times higher than the initial peak.

The 6P deposition

The stable potassium covered mica sample can now be used to study the thin film layer growth of 6P. The sample was cooled down with liquid nitrogen to a temperature of 110 K. The base pressure of $2 \cdot 10^{-9}$ $Torr$ guarantees low interactions with the residual gas. Thus, the conditions during the deposition were the same as for the reference spectrum. A 3 $\mathring{A}$ thick 6P film was adsorbed onto the potassium covered surface. After the deposition the sample was placed in front of the QMS and heated up from 110 K to 1000 K. The according TD-spectrum was recorded and can be seen in figure 3.31. To have a better overview, the spectrum is already plotted together with the TD-spectrum of 3 $\mathring{A}$ 6P on freshly cleaved mica. The red curve represents 6P desorbing from the potassium covered surface, whereas the black curve represents 6P coming from the freshly cleaved mica.

In figure 3.31 one can clearly see that the TD-spectrum of 6P desorbing from potassium covered mica has changed compared to the one of freshly cleaved mica. In the case of 6P on potassium covered mica, the desorption peak is now sharper and appears, as expected, at a lower temperature. This could be related to a formation of islands of standing 6P molecules, but further investigations with AFM are necessary to prove this assumption. The desorption energy of 6P from the standing islands on potassium covered mica is similar to that from the needle-like islands on freshly cleaved mica, because the desorption peaks have similar shapes. Note that the temperature in figure 3.31 is in fact the corrected temperature. The area underneath the peaks represents the amount of 6P desorbing from the surface. The area of the TDS from potassium covered mica is $0.9 \cdot 10^{-10}$ AK, whereas the area of the TDS from freshly cleaved mica has a value of $1.2 \cdot 10^{-10}$ AK. The deviation between these two values is about 25 percent and can be related to an experimental error. Therefore, the same amount of

6P on potassium covered mica forms islands of standing molecules whereas on freshly cleaved mica a wetting layer of lying 6P molecules is formed. The measurement clearly shows the influence of potassium on the thin film layer growth of 6P.

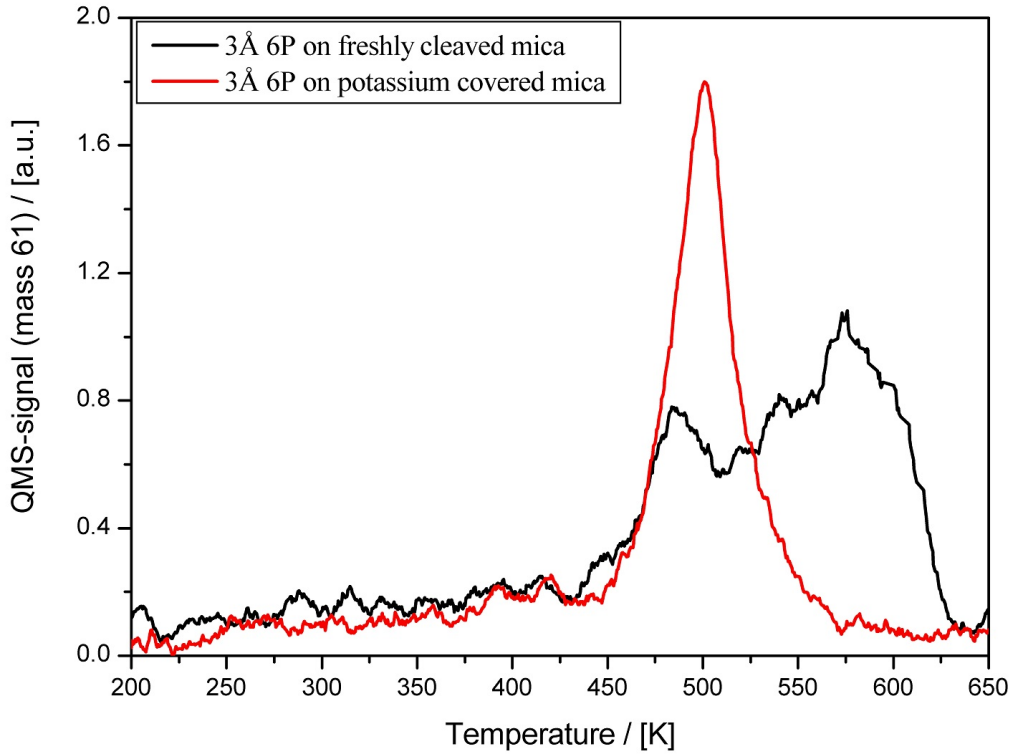

Figure 3.31: The TD-spectra of 6P desorbing from freshly cleaved mica (black curve) and potassium covered mica (red curve). In both cases the adsorption temperature was 110 K and the base pressure was at 10^{-9} $Torr$. The potassium layer causes a shift of the 6P desorption peak on potassium covered mica.

The latter experiment was performed during one day. The next day it was repeated in order to see if the results are reproducible. Therefore another 3 $\AA$ 6P were adsorbed on the sample. This time we passed on adsorbing potassium, because the potassium coverage is stable up to 1000 K. After the 6P deposition the sample was heated up from 110 K to 1000 K and the according TD-spectrum was recorded.

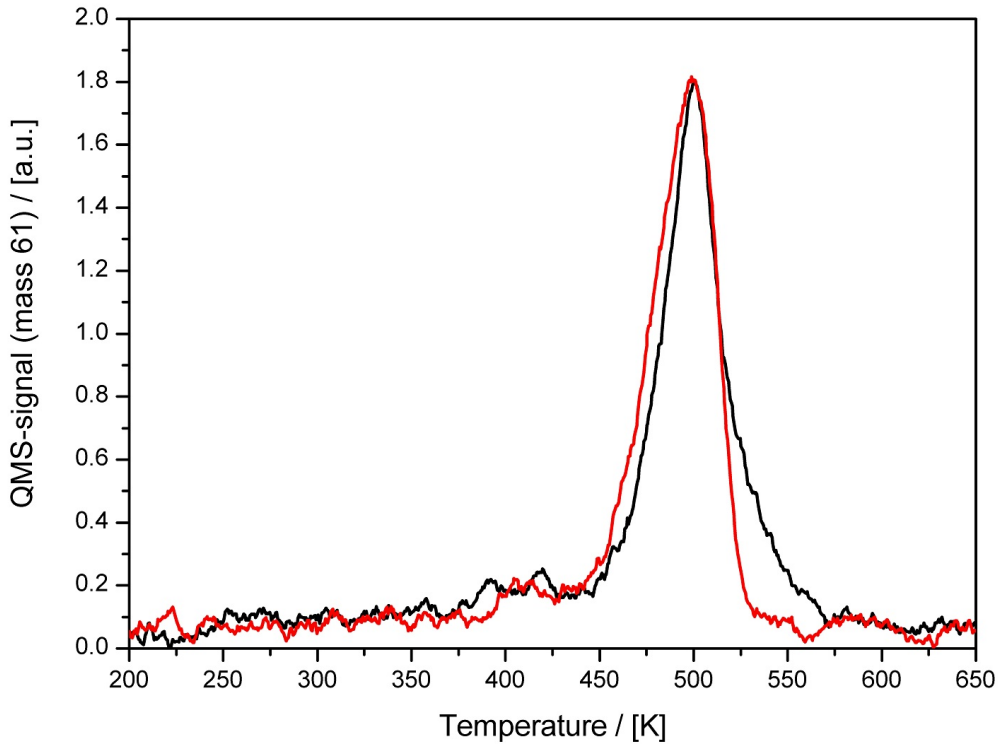

Figure 3.32: Shows the TD-spectra of the first (black curve) and second (red curve) 6P deposition on potassium covered mica.

The TD-spectrum can be seen in figure 3.32, together with the TD-spectrum of the first 6P deposition on potassium covered mica. The black curve represents the first 6P deposition, whereas the red curve shows the TD-spectrum of the second 6P adsorption. As one can see, the two spectra are similar, which means that the results are reproducible even a day after the preparation of the potassium layer.

After the last 6P deposition and subsequent desorption, an AE-spectrum of the potassium covered mica sample was recorded. The spectrum can be seen in figure 3.33, together with the already recorded spectrum of the potassium covered mica. In this figure there is no sign of a change in the surface composition, after 6P was deposited and removed. This means on the one hand that all the deposited 6P desorbed during the heating process and on the other hand that the potassium layer remains unchanged during the whole procedure.

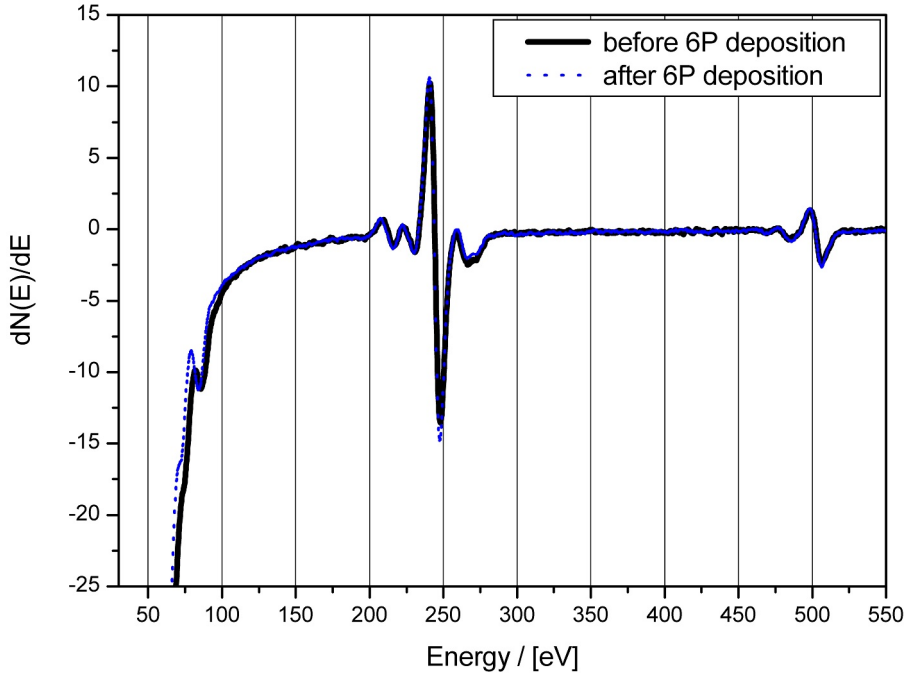

Figure 3.33: Shows two AE-spectra of the potassium covered mica surface. The AE-spectrum before (black curve) and after (blue curve) 6P ad- and desorption look identical.

3.4.2 The TD-spectra of different 6P films on potassium covered and freshly cleaved mica

In chapter 3.2.4 different amounts of 6P were adsorbed on freshly cleaved mica. Subsequently 5, 10 and 15 $\AA$ thick 6P films were deposited on freshly cleaved mica and desorbed by heating the sample. The according TD-spectra all showed a monolayer and a multilayer peak of lying 6P molecules. In order to compare the potassium covered with freshly cleaved mica, the same amounts of 6P were deposited on the potassium covered sample. Thus, 5, 10 and 15 $\AA$ thick 6P films were adsorbed on potassium covered mica. After each deposition the sample was placed in front of the QMS and heated up from 110 K to 1000 K and the according TD-spectrum was recorded. All spectra and the spectrum of 3 $\AA$ 6P are plotted together in figure 3.34(a). Note that all these spectra represent 6P desorbing from islands of standing 6P molecules. Therefore all

shown spectra are still in the sub-monolayer regime, because a monolayer of standing 6P molecules is about 25 $\mathring{A}$ [15].

Figure 3.34(b) shows the same 6P films on freshly cleaved mica. The comparison with the TD-spectra of figure 3.34(a) shows, that the monolayer peak in the TD-spectra of freshly cleaved mica disappears in the TD-spectra of potassium covered mica. This can be related to a dewetting of the 6P molecules. Due to the pre-adsorbed potassium, 6P stops forming a wetting layer of lying 6P molecules and instead grows in form of islands of standing molecules. Therefore, one can see a difference between the peak heights of 6P on potassium covered and freshly cleaved mica. In both cases (freshly cleaved and potassium covered) the same amount of 6P is adsorbed on the surface. In the case of freshly cleaved mica 6P desorbs in form of a multilayer and monolayer peak (needle-like islands and a wetting layer). On potassium covered mica all the 6P desorbs from islands of standing molecules, which results in one higher desorption peak in the TD-spectrum. This can be underpinned by the comparison of the areas underneath the desorption peaks, which can be seen in table 3.2

Table 3.2: 6P film thickness d, areas of desorption peaks for freshly cleaved mica A_1, areas of desorption peaks for potassium covered mica A_2

$d/\mathring{A}$	$A_1/10^{-10}\ AK$	$A_2/10^{-10}\ AK$
3	0.9	1.2
5	1.9	1.4
10	2.6	2.9
15	4.1	4.7

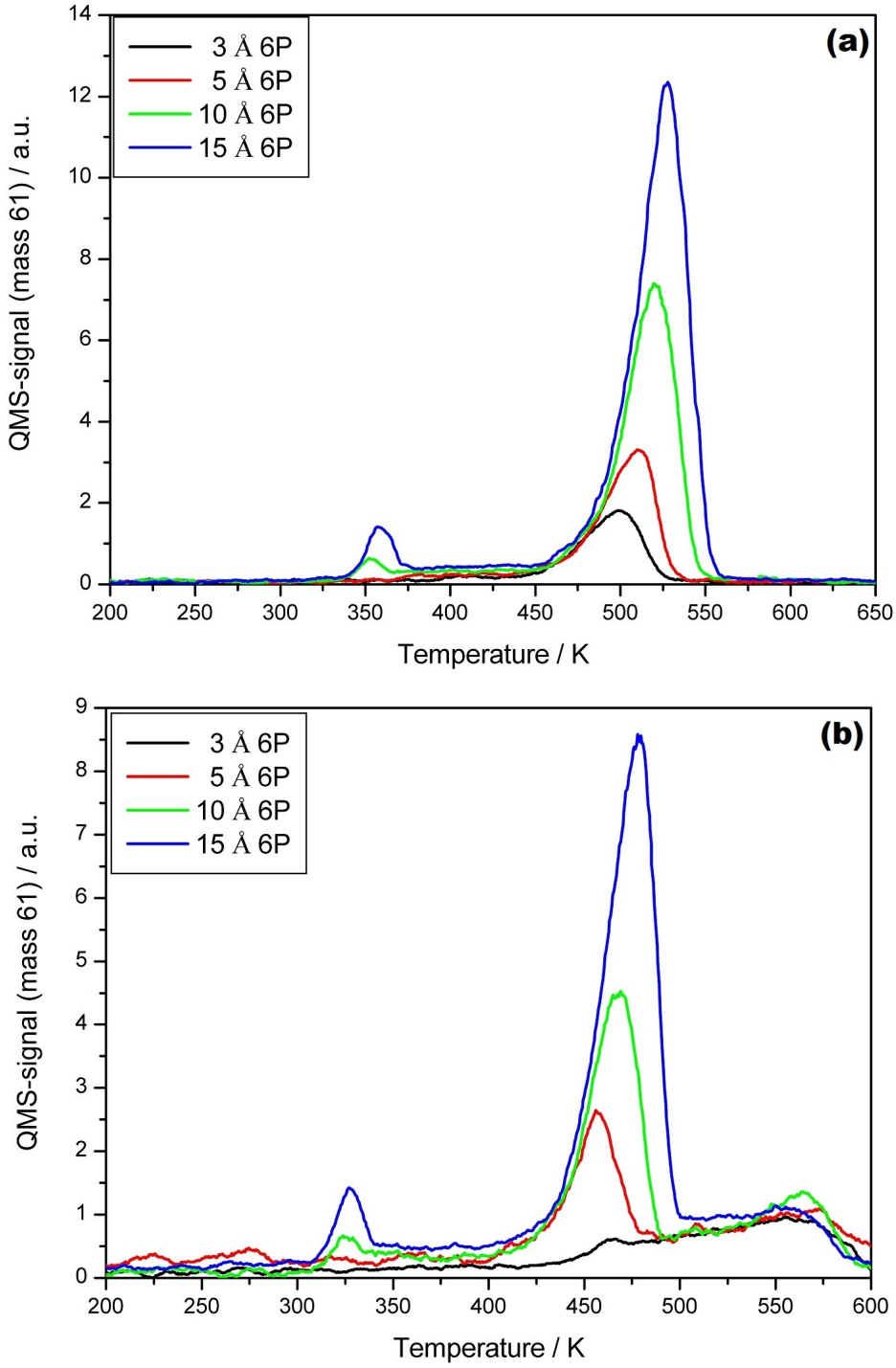

Figure 3.34: TD-spectra of 6P desorbing from (a) potassium covered and (b) freshly cleaved mica. The comparison reveals the effects of pre-adsorbed potassium on the 6P layer growth.

The AFM pictures of 6P on potassium covered and freshly cleaved mica

In the previous section it was already mentioned that further investigations with AFM are necessary. It was assumed that due to the pre-adsorption of potassium, dewetting and a formation of islands of standing molecules occur in the thin film layer growth of 6P. The TD-spectra are a good indication that this assumption is true and all effects seen in the TD-spectra can be related to this new formation, but nevertheless AFM measurements are necessary to prove the assumption.

Since atomic force microscopy (AFM) is an ex-situ method, the mica sample must be demounted. Before the sample was removed from the chamber a 3 $\AA$ thick 6P film was adsorbed on the potassium covered surface. After the deposition the chamber was vented and the sample was removed from the chamber. The 6P covered sample was placed underneath the AFM to measure the topography of the surface. In figure 3.35(a) the AFM image of this surface can be seen.

The image of the potassium covered surface with the 3 $\AA$ thick 6P film is plotted together with an AFM image of a thick 6P film on freshly cleaved mica (fig. 3.35). The image of 6P on freshly cleaved mica was recorded by Tümbek and is shown here to compare the different 6P film formations on potassium covered and freshly cleaved mica. In figure 3.35(b) one can clearly see the needle-like islands on top of the wetting layer. The wetting layer itself cannot be seen in the AFM, because the AFM cannot depict full layers. The image in figure 3.35(a) shows that 6P starts to form small dendritic islands on potassium covered mica. The islands have a diameter of 200 to 400 nm. Additionally, one can see some small rounded islands, that are much higher than the 6P-islands (about 20 nm). These islands could be formed by the potassium compounds (KO_x, KOH) but it is not possible to determine this with the methods used here.

In order to be sure that the dendritic islands are in fact islands of standing 6P molecules the height of these islands was measured. Thus, a cross section over three islands in the AFM picture was taken. The cross section measurements can be seen in figure 3.36 and the bars in figure 3.35 mark the regions of these cross sections.

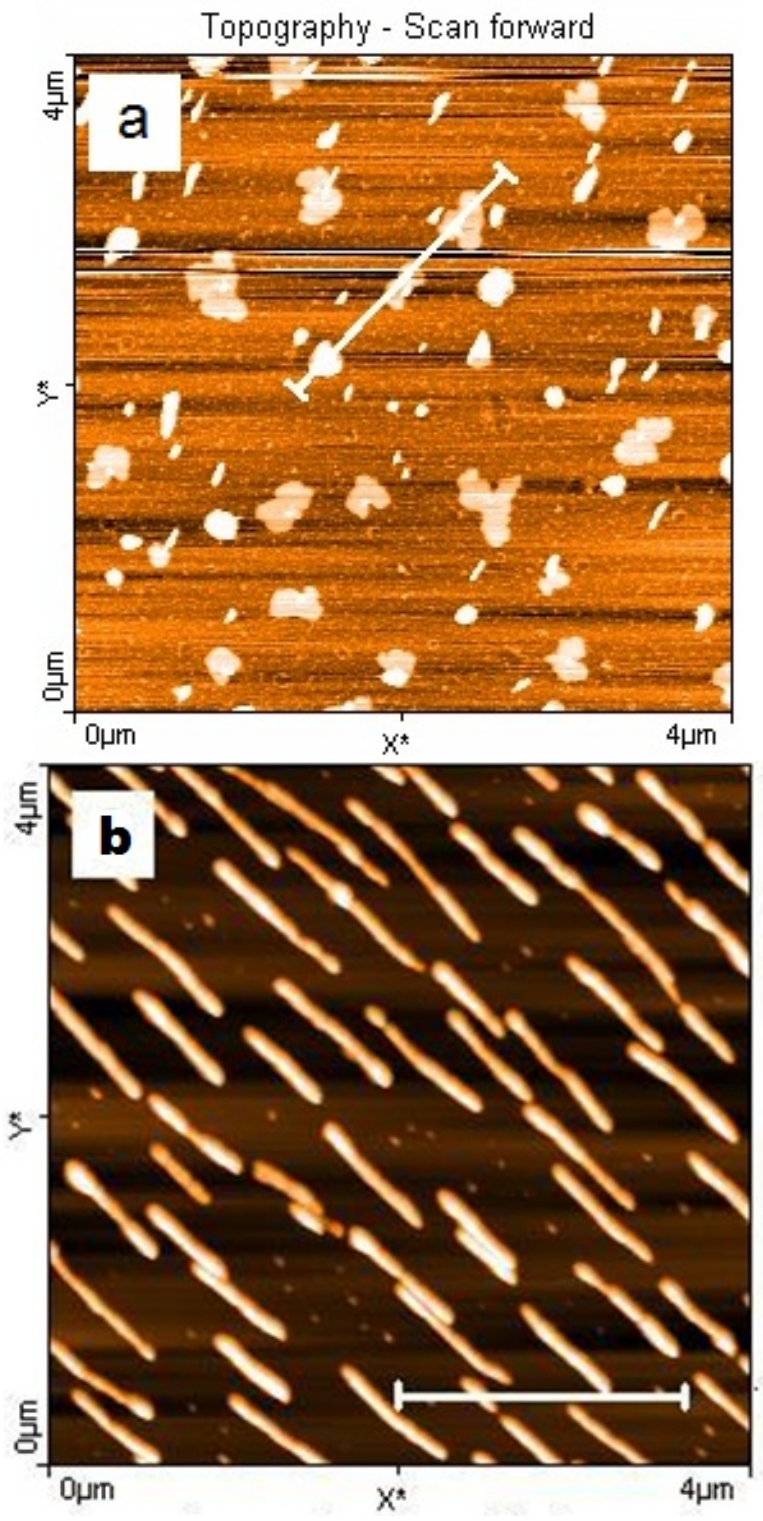

Figure 3.35: AFM images of (a) 6P on potassium covered and (b) 6P on freshly cleaved mica. The bars in the images represent the areas of the cross section.

The heights of the dendritic islands (left image) are in the range of 2.6 to 2.9 nm, which is in good agreement with the VdW-length (2.85 nm [28]) of the 6P molecule. Hence, the dendritic islands really consist of standing 6P molecules. The right image shows a cross section of the needle-like islands. These islands are much higher than the dendritic islands, because they consist of lying 6P molecules stacked together to needles.

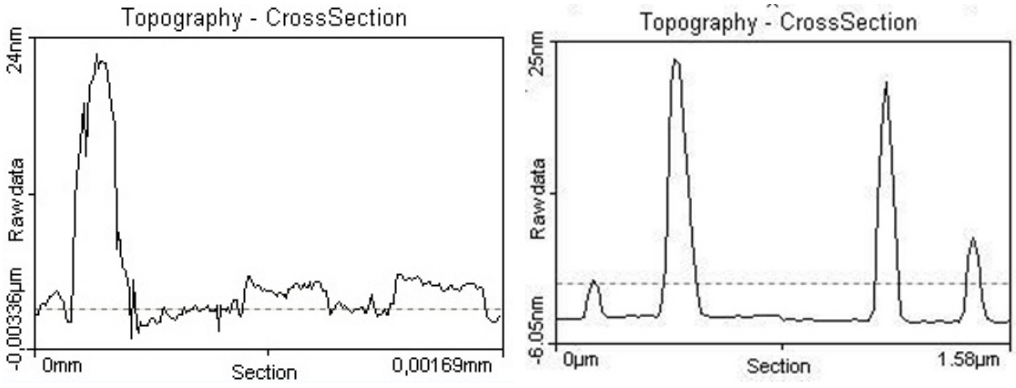

Figure 3.36: Cross section of freshly cleaved mica (right) and potassium covered mica (left).

Chapter 4

Summary and Conclusion

This work was focused on the adsorption of potassium on freshly cleaved mica and its effects on the subsequent thin film layer growth of 6P. Thermal desorption spectroscopy (TDS, in-situ) and atomic force microscopy (AFM, ex-situ) were the main analytical methods to describe the effects of potassium on the layer growth of 6P molecules. Auger electron spectroscopy (AES) was applied for chemical analysis of the mica sample before and after the potassium deposition. The pre-adsorption of potassium leads to a change of the layer growth of 6P from needle-like islands on top of a wetting layer on freshly cleaved mica to islands of standing 6P molecules without a wetting layer on potassium covered mica. Furthermore AES and TDS measurements revealed that proper potassium ad- and desorption cycles lead to a saturation potassium coverage on the mica sample, that is stable up to 1000 K.

Deposition of 6P on freshly cleaved mica

All samples were cooled down with liquid nitrogen to a temperature of 110 K during the adsorption. The TD-spectra of 6P consisted of the two expected desorption peaks (fig. 3.5). The first and second peak represent the multilayer and monolayer desorption of 6P from freshly cleaved mica. Mica has a rather low heat conductivity normal to the (001) plane [26], which is why the surface temperature on mica always lags behind the measured temperature. A temperature correction, that was implemented, corrects the measured temperatures to the true surface temperatures of the mica substrate. Although a comparison with results of Frank [25] revealed a high uncertainty of this

correction (fig. 3.6), it is still the best and only way to at least estimate the true surface temperature. The multilayer desorption peak of 6P is at a temperature of 485 K, whereas the monolayer desorption peak has its maximum at a temperature of 560 K (corrected temperatures). The comparison of the TD-spectra of different 6P films (fig. 3.7) indicates half order desorption for the multilayer peak and first order desorption for the monolayer peak.

- Monolayer desorption energy of 6P: $E_{des} = 3.0 \pm 0.3\ eV$
- Multilayer desorption energy of 6P: $E_{des} = 2.2 \pm 0.2\ eV$

Deposition of potassium on freshly cleaved mica

The aim was to study the adsorption behaviour of potassium on mica. The adsorption in the multilayer regime required temperatures of 110 K, because potassium has a rather low heat of evaporation (19 $kcal/mol$). Additionally, UHV conditions were necessary to guarantee low interactions with the residual gas. It turned out that pressures lower than or in the 10^{-9} $Torr$ region were needed to deposit a metallic multilayer of potassium on the surface. The appearance of two desorption peaks (350 K and 450 K) of potassium in the TD-spectra (multilayer regime, fig. 3.18) is an experimental artefact and can be related to the bad heat conductivity of mica normal to the (001) plane [26]. The temperature of the mica surface lags behind the steel plate. Thus, the first peak stems from the tantalum clamps, whereas the second larger peak represents desorption from mica. We have checked this behaviour by thermal desorption spectroscopy of K multilayers, which were directly adsorbed onto the steel plate (fig. 3.19). The absence of a monolayer peak in all TD-spectra of potassium on mica can be explained by the fact that some of the deposited potassium remains on the mica surface after the first adsorption/desorption cycle. The TD-spectra (fig. 3.23 and 3.24) of the first three potassium depositions (always 1.3 nm) on a freshly cleaved mica sample, pointed out that already the first cycle leads to the formation of a saturation potassium coverage, which is stable up to 1000 K. However, the amount of this saturation coverage depends on the base pressure during adsorption. A pressure in the range of 10^{-10} $Torr$ leads to 1 monolayer of potassium. AE-spectra of freshly cleaved and potassium covered mica (fig. 3.27) showed that the potassium peak is indeed twice as high as the initial peak. Non negligible interactions with the residual

gas at a pressure $> 10^{-9}$ $Torr$ lead to a five times higher potassium peak in the AE-spectrum. This leads to the assumption, that some potassium compounds like KO_x and KOH are strongly bonded to the surface.

- Multilayer desorption energy of potassium: $E_{des} = 0.76 \pm 0.04$ eV

Deposition of potassium and 6P on mica

All samples were air cleaved and immediately put in the UHV-chamber. The AE-spectra of these freshly cleaved mica samples showed that the amount of potassium on the surface is quite reproducible. The K/O ratio in these spectra was always about 1.1 ± 0.1, which indicates that indeed a half monolayer of potassium remains on each face after the cleaving. At a pressure of 10^{-9} $Torr$ a potassium covered mica surface was prepared (fig. 3.30). Subsequent TD-spectra of different 6P films (fig. 3.34) showed that 6P has indeed a different adsorption behaviour. The spectra indicate that the layer growth has changed from needle-like islands, composed of lying molecules, to islands of standing molecules. The absence of the monolayer desorption peak in the TD-spectra of potassium covered mica can be attributed to dewetting. AFM-images of a potassium covered surface with a 3 $\AA$ thick 6P film proved the formation of islands composed of standing molecules. The height of these islands is in-between 2.6 to 2.9 nm, which is in good agreement with the VdW-length of a 6P molecule (2.85 nm).

It is assumed that the reason for the formation of a wetting layer and the needle-like islands are electric fields existing on the surface of freshly cleaved mica, caused by electric dipoles generated after cleavage. The change of the thin film layer growth of 6P on potassium covered mica can be related to a destruction of the lateral dipoles due to the surface modification. Thus, the attractive forces between the 6P molecules and the substrate become weaker, which results in dewetting and the formation of dendritic islands.

Appendix A

Supplements

A.1 Temperature correction

The mica samples were always mounted onto a sample holder, where four tantalum clamps press the mica against the steel plate (fig. 2.2(b)). The temperature is measured with a thermocouple on the back of the steel plate. The mica sample has a bad thermal conductivity normal to the (001) plane, therefore the true surface temperature of mica always lags behind the measured temperature. A result of this behaviour are desorption peaks of 6P from the tantalum clamps at 500 K and the mica surface at 800 K. Since the tantalum clamps have the same temperature as the steel plate, we know that 6P desorbs at 500 K. Therefore mica reaches a surface temperature of 500 K when a temperature of 800 K is measured. In order to correct the measured temperature to the true surface temperature the following temperature correction was implemented:

$$T_{mica} = T_{init} + k_\beta \cdot (T_{tc} - T_{init})$$

T_{init} ... The steel plate and mica have the same starting temperature, typically 110 K
T_{tc} ... Temperature measured by the thermocouple on the back of the steel plate

The slope k_β can be derived from the position of the multilayer desorption peaks of the tantalum clamps (T_{Ta}) and the mica sample (T_{mica}) in the uncorrected TD-spectrum:

$$k_\beta = \frac{T_{Ta} - T_{init}}{T_{mica} - T_{init}}$$

A.2 Order of kinetics

Thermal desorption spectroscopy (TDS) is a powerful technique to determine the desorption kinetics of molecules from the surface. There are several techniques for the analysis of a TD-spectrum. The method presented here is a variation of the Arrhenius plot and can be used to determine the desorption energy, E_{des}, and the order of kinetics, n, including fractional orders [14]. The Arrhenius plot, as explained in chapter 1, only works for the zero order desorption, with $n = 0$. The modified Arrhenius plot allows different values for the order of kinetics and is based on the following form of the Polanyi-Wigner equation:

$$r_{des} = \frac{\nu_n \Theta^n}{\beta} \cdot exp\left(-\frac{E_{des}}{k_B T}\right)$$

Taking the logarithm and rearranging this equation, leads to the following expression for the modified Arrhenius plot:

$$ln(r_{des}) - n \cdot ln(\Theta) = ln(\frac{\nu_n}{\beta}) - \frac{E_{des}}{k_B T}$$

Where r_{des} is the desorption rate, n the order of kinetics, Θ the coverage, ν_n the pre-exponential factor, β the heating rate (typically 1 K/s), E_{des} the desorption energy, k_B the Boltzmann constant and T the temperature.

The latter equation is linear with respect to $(1/T)$. Plotting the left-hand side of this expression $[ln(r_{des}) - n \cdot ln(\Theta)]$ versus $(1/T)$ yields a line with the slope $(-E/k_B)$ and the intercept $ln(\nu_n/\beta)$. If an incorrect value of n is used in constructing the plots, the expression will retain a term containing Θ and the plot will not be linear with respect to $(1/T)$ [14]. In our case different values for the order of kinetics ($n = 0,\ 1/2,\ 1$) where chosen to construct the modified Arrhenius plots. The Arrhenius plot with the best linear behaviour has the correct order of desorption. The pre-exponential factor and the desorption energy can be determined from the correct Arrhenius plot.

A.3 Quartz microbalance

The deposited amount of 6P was measured with the microbalance. A XTM/2 Deposition Monitor from the company INFICON was used to measure the frequency change of the microbalance. The accuracy of the measurement is $\pm 0.1\ Hz$. To reach such an accuracy the microbalance is water cooled.

In order to deposit 6P on the mica sample and measure the frequency change of the microbalance at the same time, the microbalance is placed in an angle of about 45° relative to the Knudsen cell. To calculate the mass change per unit area on the microbalance, Δm_1, one can use the following equation [34]:

$$\Delta m_1 = S^{-1} \cdot \Delta\tau = S^{-1} \cdot \frac{\Delta f_1}{f_1^2} \ \Rightarrow\ \Delta m_1\ [\mu g/cm^2] = 0.0123 \cdot \Delta f\ [Hz]$$

$S \ldots$ the sensitivity factor of the crystal ($S = 2.26 \cdot 10^{-6}\ cm^2 s/g$)
$f_1 \ldots$ frequency ($f_1 = 6\ MHz$)
$\tau \ldots$ periodic time

A.3.1 Calibration of the quartz microbalance

If the microbalance is placed at the position of the sample, one can show that a frequency change of $1Hz$ on the microbalance correlates with a 1 $\mathring{A}$ thick 6P film deposited on mica [34]:

$$\Delta d = \frac{\Delta m_1}{\rho} = \frac{\Delta f_1}{\rho \cdot S \cdot f_1^2} \qquad with\ \rho = 1.3\ g/cm^3$$

$$\Delta d[nm] = 0.1 \cdot \Delta f_1\ [Hz]$$

Nevertheless, the microbalance is placed in an angle of 45° relative to the Knudsen cell, to measure the frequency change during the adsorption. Since the evaporation rate is angular dependent, the amount of deposited material on the microbalance would be different to the sample. The microbalance is placed closer to the Knudsen cell (r_2) than the sample (r_1). Thus, the angular dependence is compensated and the evaporation rates at the microbalance (I_1) and the sample (I_2) are equal (see fig. A.1). The

distances r_1 and r_2 must be chosen so that the following equations are fulfilled:

$$I_0 = \frac{A}{r_1^2},\ I_1 = \frac{A \cdot cos^2(\Theta)}{r_2^2},\ I_0 \stackrel{!}{=} I_1$$

$$\Rightarrow \frac{r_2}{r_1} = cos(\Theta) = 0.7075 \quad with\ \Theta = 45^\circ$$

Where A is the Area of the sample. In our construction the distance r_1 is 60 mm, which leads to a value of 42.45 mm for the distance of the microbalance.

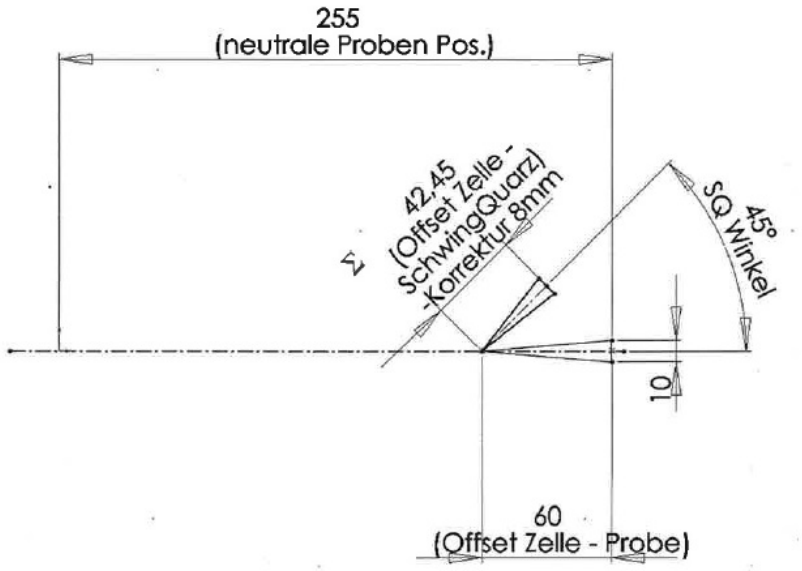

Figure A.1: Schematic of the position of the microbalance and the sample relative to the 6P evaporation source.

A.4 Potassium on a nickel surface

The TD-spectra of potassium on mica show no sign of a monolayer peak. Therefore one monolayer of potassium was deposited on a poly-crystalline nickel surface, because the number of potassium $[atoms/cm^2]$ of such a layer is well known for the nickel surface. According to Pölzl [29] a full Ni(111) layer has $1.86 \cdot 10^{15} atoms/cm^2$. The saturation

coverage of potassium on Nickel is about 0.25 ML, which leads to a value of:

$$N_{ads} = 4.65 \cdot 10^{14}\ atoms/cm^2$$

potassium atoms on the nickel surface. This value can be used to calibrate the TD-spectra and rewrite the y- axis in absolute values. The area underneath a desorption peak corresponds to the number of atoms desorbed per unit area ($atoms/cm^2$). This relation is given by the following equation [29]:

$$N_{ads} = c \cdot \int IdT$$

Where c is the proportionality factor, $\int IdT$ is the area underneath the desorption peak, β is the heating rate ($\beta = 1\ K/s$) and A is the sample area ($A = 1cm^2$). To determine the proportionality factor the area underneath the desorption peaks of the TD-spectrum in figure A.2 was calculated.

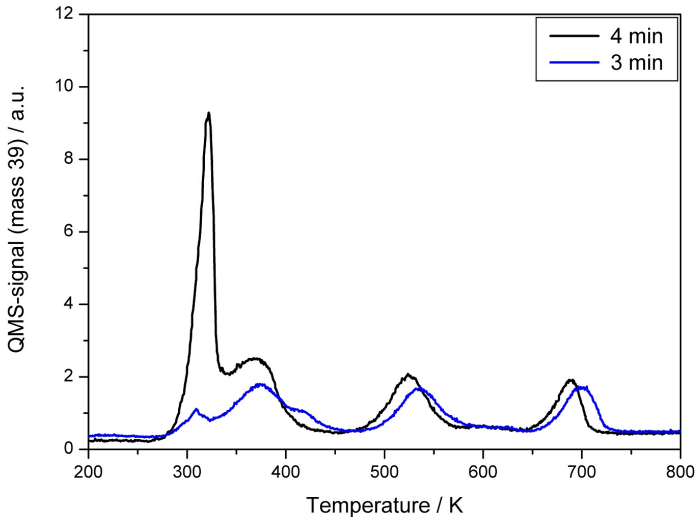

Figure A.2: TD-spectra of potassium desorbing from a Ni-surface. Potassium in the multilayer regime (black curve), one monolayer of potassium (blue curve). $T_{ad} = 110K$

The area underneath the desorption peaks (blue curve) amounts to $\int IdT = 3.7 \cdot$

10^{-8} AK. The proportionality factor can then be calculated:

$$c = 1.3 \cdot 10^{22} \ \frac{(atoms/cm^2)}{K \cdot A}$$

A.4.1 Film thickness of the potassium multilayer

The proportionality factor can not only be used to calibrate the TD-spectra, it is also possible to estimate the mean film thickness of metallic multilayers of potassium on mica. In the TD-spectrum of a mica sample one can only see a multilayer desorption. To calculate the approximate thickness of the desorbed multilayer, d, it is necessary to multiply the area underneath the peak ($\int IdT$) with the proportionality factor (c). This gives us the number of atoms per unit area. If the mass of one potassium atom ($m_{1K} = 6.5 \cdot 10^{-23}$ g) and the density of potassium ($\rho = 0.86$ g/cm^3) [29] is known, the film thickness of the multilayer can be calculated with the following equation:

$$d[cm] = \frac{m_{1K}}{\rho} \cdot c \cdot \int IdT$$

Bibliography

[1] S.R. Forrest and M.E. Thompson. Introduction: Organic electronics and optoelectronics. *Chemical Reviews,* 107:923-925, 2007

[2] F. Balzer and H.-G. Rubahn. Chain-length dependent *para*-phenylene film- and needle-growth on dielectrics. *Surface Science,* 548:170-182, 2004

[3] K. Müller and C.C. Chang. Electric dipoles on clean mica surfaces. *Surface Science,* 14:39-51, 1969

[4] K. Müller and C.C. Chang. Low energy electron diffraction observations of electric dipoles on mica surfaces. *Surface Science,* 8:455-458, 1968

[5] P. Frank, G. Hlawacek, O. Lengyel, A. Satka, C. Teichert, R. Resel and A. Winkler. Influence of surface temperature and surface modifications on the initial layer growth of para-hexaphenyl on mica (001). *Surface Science,* 601:2152-2160, 2007

[6] K. Oura, V.G. Lifshits, A.A. Saranin, A.V. Zotov and M. Katayama. Surface science an Introduction. *Springer,* 2003

[7] H. Ibach. Physics of surfaces and interfaces. *Springer,* 2006

[8] R.I. Masel. Principles of adsorption and reaction on solid surfaces. *John Wiley & Sons, Inc.,* 1996

[9] A. Zangwill. Physics at surfaces. *Cambridge University Press,* 1988

[10] A. Tamtögl. Adsorption and desorption processes on clean and Zn-modified Pd(111). *Diploma thesis, Tu Graz,* 2008

[11] H.G. Rubahn, H. Sitter, G. Horowitz and K. Al-Shamery. Interface controlled organic thin films. *Springer,*, 2009

[12] M. Vollmer and F. Träger. Analysis of fractional order thermal desorption. *Surface Science,* 187:445-462, 1987

[13] A.J. Slavin and D.P.B. Young. A new kinetic theory for thermal desorption of two-dimensinal islands. *Journal of Vacuum Science and Technology A,* 8:2463-2467, 1990

[14] D.H. Parker, M.E. Jones and B.E. Koel. Determination of the reaction and activation energy for desorption kinetics using TPD spectra: Application to D_2 desorption from Ag(111). *Surface Science,* 233:65-74, 1990

[15] T. Potocar. Nucleation and layer growth of para-hexaphenyl on sputtered mica(001). *Master thesis, TU Graz, 2010*

[16] C.M. Chan, R. Aris and W.H. Weinberg. An analysis of thermal desorption mass spectra. I. *Applications of Surface Science,* 1:360-376, 1978

[17] C.M. Chan and W.H. Weinberg. An analysis of thermal desorption mass spectra. II. *Applications of Surface Science,* 1:377-387, 1978

[18] P.A. Redhead. Thermal desorption of gases. *Vacuum,* 12:203-211, 1962

[19] D.J. O'Connor, B.A. Sexton and R.St.C. Smart. Surface analysis methods in materials science. *Springer,* 2003

[20] H. Bubert and H. Jenett. Surface and thin film analysis. *Wiley-VCH,* 2002

[21] P.W. Palmberg, G.E. Riach, R.E.Weber, and N.C. MacDonald. Handbook of Auger electron spectroscopy. *Physical Electronics Industries, Inc.,* 1972

[22] P. Frank. Thin film growth of rod-like and disc-shaped organic molecules on insulator and noble metal surfaces. *PhD thesis, TU Graz,* 2009

[23] Nanosurf. Operating instructions, easyScan 2 AFM. 2005.

[24] Nanosurf. Software reference, easyScan 2. 2005.

[25] P. Frank. Adsorption, Schichtwachstum und Desorption von p-Hexaphenyl auf Glimmer-Oberflächen. *Diplomarbeit, TU Graz,* 2006

[26] A.S. Gray and C. Usher. Thermal conductivity of mica at low temperatures. *Journal of Materials Science,* 12:959-965, 1977

[27] R. Resel. Surface induced crystallographic order in sexiphenyl thin films. *Journal of Physics: Condensed Matter,* 20, 2008

[28] S. Müllegger. Adsorption and thin film growth of oligo-phenylenes on gold surfaces. *PhD thesis, TU Graz,* 2005

[29] H. Pölzl. Absolutbestimmung der Kaliumbedeckung auf Metalleinkristalloberflächen. *Diplomarbeit, TU Graz,* 1996

[30] http://www.webelements.com/potassium/crystal_structure.html

[31] F. Balzer, M. Schiek, H.G. Rubahn, K. Al-Shamery and A. Lützen. Surface bound organic nanowires. *Journal of Vacuum and Techonology B,* 26:1619-1623, 2008

[32] A. Andreev, G. Matt, C.J. Brabec; H. Sitter, D. Badt, H. Seyinger and N. S. Sariciftci. Highly anisotropically self-assembled structures of *para*-sexiphenyl grown by hot-wall epitaxy. *Advanced Materials,* 12:629-633, 2000

[33] S.B. Lee, M. Weiss and G. Ertl. Adsorption of potassium on iron. *Surface Science,* 108:357-367, 1981

[34] O. Stráník. Adsorption und Schichtwachstum von p-Quaterphenyl auf Goldoberflächen. *Diplomarbeit, TU Graz,* 2002